TABLE OF CONTENTS

Page

XII

LIST OF TABLES

LIST OF FIGURES

Page

.

LIST OF SYMBOLS AND ACRONYMS

b	Length of slice base
c'	Effective cohesion
$c_{reduced}$	Reduced cohesion value
E	Inter-slice normal force
F	Factor of safety
g'	Rate of gravity increase
g_{limit}	Limiting gravity acceleration at moment of failure
g_{actual}	Actual gravity acceleration
L	Length of sliding mass
GIM	Gravity increase method
LFS	Local factor of safety
N	Normal force
R	Radius of circular plane
S	Available shear strength
SRF	Strength reduction factor
SRM	Strength reduction method
S_a	Shear force
S_r	Resisting shear strength stress
S_m	Mobilized shear stress
t_{limit}	Time function (largest time that verifies the equilibrium state)
u	Pore water pressure
W	Weight of the sliding mass
w	Horizontal width of slice base
X	Inter-slice shear force
$\phi_{reduced}$	Reduced friction angle value
σ'	Effective normal stress
ϕ'	Effective friction angle
α	Inclination of sliding mass
λ	The ratio between inter-slices shear-to-normal values along slip surface

$f(x)$	Function describing the direction of inter-slice forces
σ_x	Horizontal stress
σ_y	Vertical stress
τ_{xy}	Tangent stress
τ^*	Shear stress at the failure state
σ_n	Normal stress
τ_n	Shear stress

INTRODUCTION

Several factors can have an impact on slope stability such as slope geometry, shear resistance of soils, and external loads such as loads resulting from constructions, earthquakes or rainfall. These variables should be considered when studying slope stability. The concept of safety factor in slope stability analysis is based on the ratio of soil shear strength to the shear stress required for equilibrium (Duncan, 1996). Whenever this ratio is more than 1, the slope is deemed to be stable. This means that the forces available to make the slope stable are greater than the forces that cause failure.

Recent papers have tried to include more complex phenomena in slope stability analysis. For example, the influence of rainfall on subsurface flow and slope stability was studied by Shao et al. (2014; 2015) for both saturated and unsaturated conditions. They used a coupled numerical model to simulate the influence of dual-permeability and rainfall events on subsurface flow and slope stability. These complex analyses cannot always be conducted with the specialized finite element codes used in geotechnical engineering. On the other hand, these complex problems can be studied with more general finite element codes, such as COMSOL Multiphysics. However, these general finite element engines often lack some of the basic tools that are needed to assess the stability of soil slopes.

The main object of this study was to program a slope stability tool for COMSOL. With this tool, COMSOL uses a finite element analysis to calculate the stresses in the slope. A MATLAB code was programmed to determine the factor of safety for different slip surfaces based on the finite element stresses imported from COMSOL. COMSOL and MATLAB are integrated via the MATLAB LiveLink tool in order to expand the capability of COMSOL (Ozana et al., 2016). A stress-based limit equilibrium method based on Krahn (2003) was followed. With this approach, normal and shear stresses along the plane of failure are calculated based on finite element stresses. The factor of safety is a ratio of the shear strength calculated from the normal stress and Mohr-Coulomb parameters, and the mobilized shear stress calculated from the finite element shear stress. The code presented in this thesis is the

first to allow COMSOL to be used for geotechnical applications where slope stability must be evaluated.

Two finite element computer programs were used in this study: SIGMA/W and COMSOL. SIGMA/W (GEO-SLOPE International Ltd, 2007) can be integrated with SLOPE/W to evaluate the stability of slopes with different geometries and layers. SLOPE/W is a slope stability module that includes a limit equilibrium method based on finite element stress (GEO-SLOPE International Ltd, 2012). Results from SLOPE/W were used to verify the results obtained from MATALB and COMSOL. SLOPE/W and SIGMA/W were used in this study because the stress-based method was developed by Krahn (2003) for SLOPE/W.

The thesis is organized in four chapters. Chapter 1 includes a presentation of the main types of slope stability methods, such as limit equilibrium and force reduction methods. It reviews the three computer programs that were used in this study for slope stability analyses (GEO-SLOPE, COMSOL, and MATLAB). Chapter 1 also reviews a previous attempt at slope stability calculations with COMSOL. Chapter 2 describes the MATLAB script that was programmed to calculate safety factors for COMSOL models and its verification with the GEO-SLOPE software package. Chapter 3 presents modelling results and verification of the MATLAB script based on comparisons of COMSOL and GEO-SLOPE safety factors for different slopes. Chapter 4 presents a conclusion, some suggestions for future applications for the script and modifications that would allow more complex slope geometries and soil profiles to be studied.

CHAPTER 1

LITERATURE REVIEW

Slope stability analyses are an important aspect of geotechnical engineering. Slope stability calculations require the study and interpretation of the different forces acting on the soil or rock mass. Different methods have been proposed for this purpose based on slope geometry, failure mechanisms, assumptions regarding forces and stresses distributions. Two main groups of methods are presented in this chapter. The first group includes limit equilibrium methods, such as the Swedish, Bishop simplified, and Morgenstern and Price methods. The second group includes procedures based on the finite element and finite difference methods. These methods include an analysis of stress and strain in the factor of safety calculations.

1.1 Limit equilibrium methods

Limit equilibrium methods form the most common family of methods for slope stability calculations. Most limit equilibrium methods divide the mass inside a circular failure surface into a series of vertical slices in order to analyze the forces inside the slope. These methods are based on the concept of moment or force equilibrium in the soil or rock mass. The factor of safety is derived from the moment or force equilibrium equations, or sometimes from both. Limit equilibrium methods differ based on shape of failure surface (circular versus non-circular) and assumptions regarding inter-slice forces. Limit equilibrium methods have shown great success in assessing slope stability in different conditions (Fredlund et al., 1981).

Three well-known methods are presented in the following sections. The first approach to limit equilibrium analysis was introduced by Fellenius (1936). He proposed the Ordinary method (Swedish method) of slices. This method neglects all inter-slice forces. Force equilibrium is assumed at failure. This method was improved by Janbu (1954) and Bishop

(1955). For instance, Bishop's Simplified method (1955) considers normal inter-slice forces (Fredlund et al., 1999).

With the Morgenstern & Price (1965) method, both force and moment equilibrium conditions are satisfied. The method also assumes that the inclination of the inter-slice force is known. The solution for this method needs an arbitrary assumption regarding the direction of the resulting inter-slice shear and normal forces (Abramson, 2002). The three methods that are presented below are available in the SLOPE/W software from GEO-SLOPE International (2016).

1.1.1   Principles of limit equilibrium methods

Limit equilibrium methods (LEM) use a Mohr-Coulomb criterion to define shear strength along the slip surface. The differences between the main LEM methods are centred on the equations used to verify equilibrium (force, moment or both) and the inter-slice forces that are considered (normal or shear inter-slice forces, or both).

The available shear strength S can be computed from the effective normal stress σ_n' and the effective Mohr-Coulomb parameters, cohesion c' and friction angle ϕ':

$$S = c' + \sigma'_n \tan\phi' \tag{1.1}$$

Mobilized shear stress is defined as the shear stress τ acting on the slip surface. According to Janbu (1973) and Nash (1987), the slip surface is exposed to a maximum mobilized shear stress at failure. According to Janbu (1954), the factor of safety F can be expressed as a ratio of available maximum shear strength S at failure to mobilized shear stress τ at the limit equilibrium state:

$$F = \frac{c' + \sigma'_n \tan\phi'}{\tau} = \frac{S}{\tau} \tag{1.2}$$

It is essential to understand the concept of factor of safety to determine whether slopes are stable or not. The factor of safety can be explained in two ways based on the limit equilibrium method considered: force and moment equilibrium (Cheng & Lau, 2014).

Figure 1.1 illustrates a definition for the factor of safety based on force equilibrium assuming that there is no pore pressure. Normal N and shear S_a forces act on the failure plane. Force equilibrium considers the weight W of the sliding mass, and the failure surface inclination α and length L. The factor of safety based on force equilibrium can thus be defined as:

$$F = \frac{Sum\ of\ resisting\ forces}{Sum\ of\ driving\ forces} = \frac{S_a}{W\sin\alpha} = \frac{c'L + N\tan\phi'}{W\sin\alpha} \tag{1.3}$$
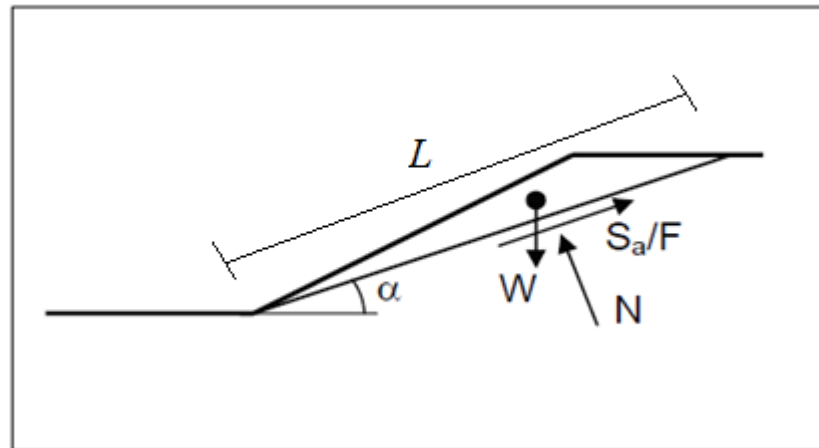
Figure 1.1 Concept of factor of safety based on force equilibrium analysis
Adapted from Abramson (2002)

Figure 1.2 illustrates a definition for the factor of safety based on moment equilibrium assuming there is no pore pressure. The resisting shear force acting on the failure surface generates a counter clockwise moment around the center of rotation O with a lever arm equal to the radius of the failure surface R. The weight of the sliding mass generates a clockwise moment with a lever arm equal to x. The factor of safety in terms of moment equilibrium analysis is determined as the ratio of the sum of resisting moments to the sum of driving moments. The resistance moments are computed by integrating on the failure surface the

product of the shear strength and the radius. Equation 1.4 gives the factor of safety based on moment equilibrium for the example presented on Figure 1.2:

$$F = \frac{Sum\ of\ resisting\ moments}{Sum\ of\ driving\ moments} = \frac{R \int_0^L S\ dl}{W.x} \tag{1.4}$$
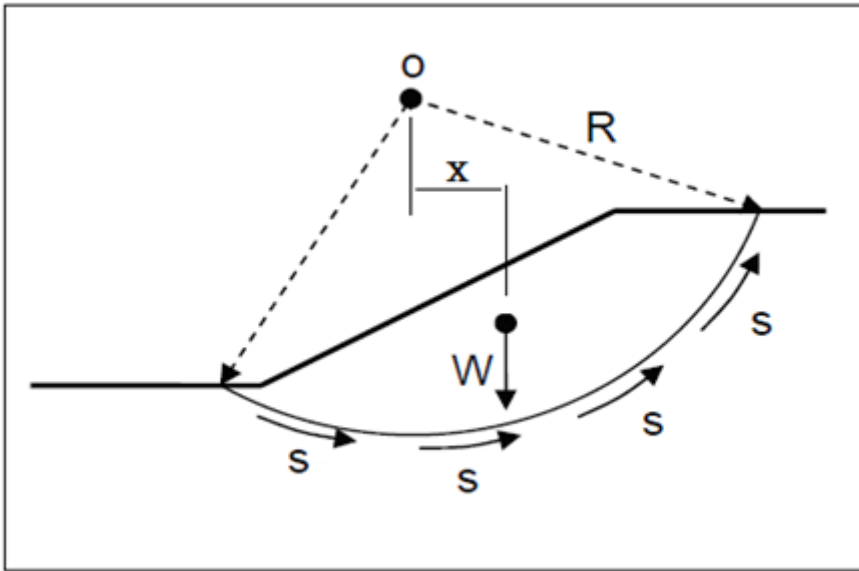
Figure 1.2 Concept of factor of safety based on moment equilibrium analysis
Adapted from Abramson (2002)

1.1.2   Main limit equilibrium methods

1.1.2.1   Swedish method

The first method of slices was developed by Fellenius (1936). It divides the length of the sliding mass into several slices. The Swedish method ignores both the normal and shear inter-slice forces (Figure 1.3). The effective normal force N' at the base of the slice is determined by subtracting the force due to pore pressure (ul, where l is the slice base length) from the component of the weight perpendicular to the slice base ($Wcos(\alpha)$):

$$N' = (W\cos\alpha - ul) \tag{1.5}$$

The method takes into account moment equilibrium. The factor of safety in the ordinary method is expressed as follows:

$$F = \frac{\sum[c'l + N'\tan\phi']}{\sum[W\sin\alpha]} \tag{1.6}$$
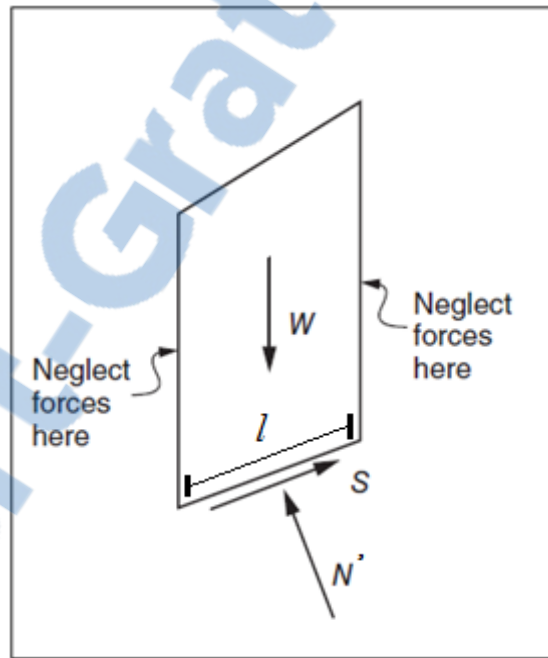
Figure 1.3 Slice with forces considered in the Swedish method of slices
Adapted from Duncan & Wright (2005)

1.1.2.2 Bishop method

The Bishop method considers inter-slice normal forces and ignores inter-slice shear forces (Abramson, 2002). The forces on both sides of each slice (E_i and E_{i+1}) are assumed to be horizontal (Figure 1.4). The normal N and tangent T forces on each slice are calculated by

verifying the equilibrium of their vertical component with the weight of the soil in the slice (*W*):

$$N \cos\alpha + S \sin\alpha - W = 0 \qquad (1.7)$$
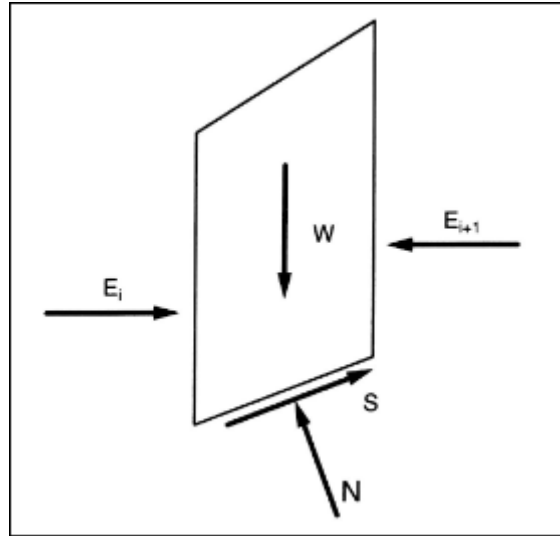
Figure 1.4 Slice with forces for Simplified Bishop procedure
Adapted from Duncan & Wright (2005)

The mobilized shear stress is calculated as the ratio of the shear strength calculated from the effective normal force *N'* and the Mohr-Coulomb parameters, and the factor of safety. The overall factor of safety is obtained by dividing the sum of moments due to the shear strength by the sum of moments due to the soil weight. The factor of safety value is present on both sides of equation 1.8.

$$F = \frac{\sum \left[\dfrac{c'\Delta x + (W - u\Delta x)\tan\phi'}{\cos\alpha + \sin\alpha \, \tan\phi'/F} \right]}{\sum W \sin\alpha} \qquad (1.8)$$

Therefore, the factor of safety must be obtained by an iterative procedure. In order to calculate the factor of safety by the Bishop Method, a guess value of *F* must be assumed and used to compute a new *F* value with Equation 1.8. This process is repeated until convergence

is reached (GEO-SLOPE International). The simplified Bishop's method is recommended for the analysis of circular failure surfaces (Abramson, 2002).

1.1.2.3   Morgenstern and Price method

Both the Swedish and Bishop methods are based on moment equilibrium alone. The Morgenstern & Price (1965) method allows both the force and moment equilibrium conditions to be verified. It also assumes inclined inter-slice forces for both sides (Figure 1.5). A function *f(x)* needs to be assumed to describe the direction of inter-slice normal force *E* and inter-slice shear force *X* with respect to the x direction. The various shear-to-normal ratios along the slip surface are the values of λ at each slice (Abramson, 2002). Equation 1.9 is proposed by the authers based on assumed function and ratio between inter-slices normal and shear forces to assess stability of slopes. The Morgenstern & Price method allows specifying different types of inter-slice force functions such as constant and half-sine functions. Factor of safety is calculated for both force and moment equilibrium.

$$X = E \lambda f(x) \tag{1.9}$$
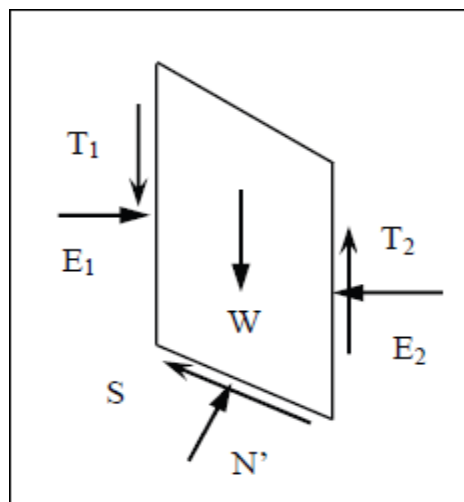
Figure 1.5 Distribution of slice forces for the Morgenstern-Price method
Adapted from Duncan & Wright (2005)

1.2   Finite element and finite difference methods

A soil mass is exposed to different loads such as the soil weight and external loads. These loads result in stresses and strains in the soil mass that increase the probability of slope instability. The stress distribution is influenced by the stress-strain properties of the different soil materials (Kondner, 1963). Assumed stress distributions for the limit equilibrium methods presented in section 1.1 vary. Slope stability methods based on finite element stress and strain analyses allow some of the hypotheses behind the limit equilibrium methods to be eliminated. Several slope stability methods based on FEM stresses were developed in the 1980s and 1990s (Matsui & San, 1992). Three main methods are presented in the following sections: the gravity method, the strength reduction method, and stress-based limit-equilibrium methods. As with the limit-equilibrium methods presented in section 1.1, finite-element and finite-difference methods also allow a factor of safety to be calculated.

The concept of finite element analysis depends on a discretization of the slope body into small elements (Figure 1.6). The slope body is assumed to represent a continuum whose mechanical behaviour (e.g. linear elastic) is described by sets of partial differential equations. Displacements, stresses, and strains at nodes in the domain are obtained with the finite element analysis. Once the displacements are obtained, deformations and stresses σ_x, σ_y, and, τ_{xy} can be calculated. Finite element and finite difference methods for slope stability calculations are based on these displacements, stresses and strains.
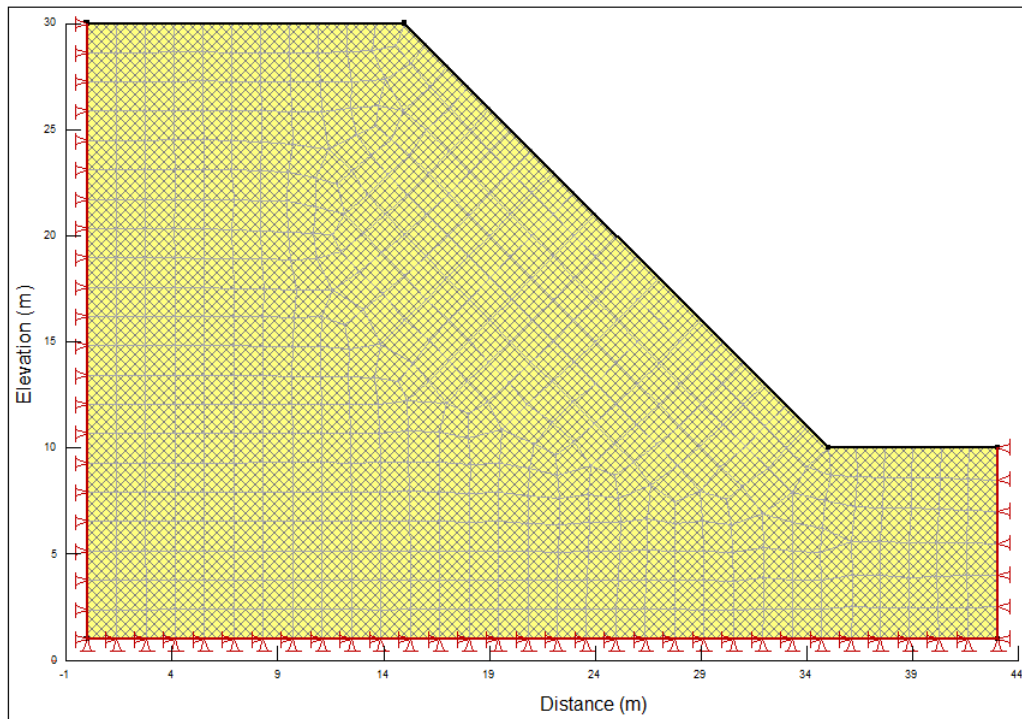
Figure 1.6 Discretization of slope into finite elements by SIGMA/W

1.2.1 Gravity increase method

The gravity increase method GIM consists in increasing the slope mass until the slope fails and an equilibrium state cannot be achieved. The critical slip surface is reached by increasing the gravity gradually with no change in material properties. The increasing gravity g_{limit} is defined as the product of the rate of gravity increase with respect to time g' and a parametric time variable t_{limit}:

$$g_{limit} = g'.t_{limit} \tag{1.10}$$

The gravity increase method defines failure as the highest time value where the loading due to the acceleration of gravity brings strength of slope to the failure merge (Swan & Seo, 1999). The failure in GIM is based on the rate of displacement and damage within the elements during the analysis of finite element. The critical slip surface is formed when the

highest gravity level is reached which causes the largest deformation before failure state (Li et al., 2009). The factor of safety can be defined as the ratio between the critical acceleration of gravity g_{limit} and the real acceleration of gravity g_{actual} equal to 9.81 m/s^2.

$$F = \frac{g_{limit}}{g_{actual}} \tag{1.11}$$

1.2.2   Shear strength reduction method

The shear strength reduction method (SRM) was first proposed by Matsui & San (1992). The method was applied by these authors in the 1980s and 1990s for embankment and excavation slopes. Their results proved that this method can be used to evaluate the stability of both types of slopes. Since then, other authors have applied this method (Donald & Giam 1988; Ugai & Leshchinsky 1995; Griffiths & Lane 1999).

With this technique, the slope's shear strength parameters, its effective cohesion and its friction angle, are progressively reduced until failure occurs. A series of strength reduction factors (SRF) are used to divide the real shear strength parameters. The factor of safety in the SRM is defined as the ratio between the real shear strength parameters to the critical shear strength parameters that lead to failure.

$$F = \frac{Real\ Strength\ parameters}{Critical\ Strength\ Parameters} \tag{1.12}$$

Failure in the shear strength reduction method is defined as the point where deformations begin to increase rapidly with increasing strength reduction factor values. Shear strength parameters are typically obtained from the Mohr-Coulomb criteria and are reduced incrementally by increasing the SRF:

$$SRF = \frac{c'}{c'_{reduced}} = \frac{tan\phi'}{tan\phi'_{reduced}} \tag{1.13}$$

where $c'_{reduced}$ is the reduced cohesion value and $\phi'_{reduced}$ is the reduced friction angle value.

Since the method is based on finite element analysis, it can be adapted to conduct probabilistic analyses of slope stability. A probabilistic analysis is based on defined random variables (cohesion and friction angle) of the slope material. The analysis uses the mean value of the probabilistic values. The conjunction between shear strength reduction method and probabilistic analyses allows SRM to use the random values for assessing slope stability. The results of the coupled analysis are probability failure values, critical strength reduction factor (mean value) and standard deviation values for the critical strength reduction factor.

The strength reduction method has several advantages:
1. An arbitrary slip surface geometry (e.g., circular slip surface) does not have to be assumed;
2. Assumptions regarding inter-slice shear forces are not required;
3. The SRM method is more suitable for complicated conditions (e.g., large-scale slopes of complex geometry);
4. This method gives information about the stress and pore pressure in the soil mass;
5. The displacement depends on strength parameters, such as the soil or rock cohesion and friction angle, but it also depends on their stress-strain properties (E, ν) (Cheng & Wei, 2007).

The SIGMA/W software can be used to compute values of the factor of safety based on SRM. Several SRF values are tested in order to get reduced values of c' and ϕ'. The new values are applied in the finite element model to calculate displacements until a critical value is reached. The SRF then gives the F value (GEO-SLOPE International Ltd, 2007).

1.2.3   Limit equilibrium methods based on finite-element stress

The limit equilibrium methods that have been presented in section 1.1 do not include a stress and strain analysis of the slope materials. According to Bishop (1952), the stresses that are

assumed for limit equilibrium analyses do not always correspond to the actual stress in the field. With limit equilibrium methods based on finite element stresses, the stress and strain in the soil mass are computed. The FE stress field is rotated to calculate the shear and normal stress components on the failure surface. The normal and shear stress components and the Mohr-Coulomb parameters allow a ratio between resisting shear forces S_r and mobilized shear forces S_m to be calculated. Figure 1.7 shows the main steps of limit equilibrium analyses based on FE stresses.
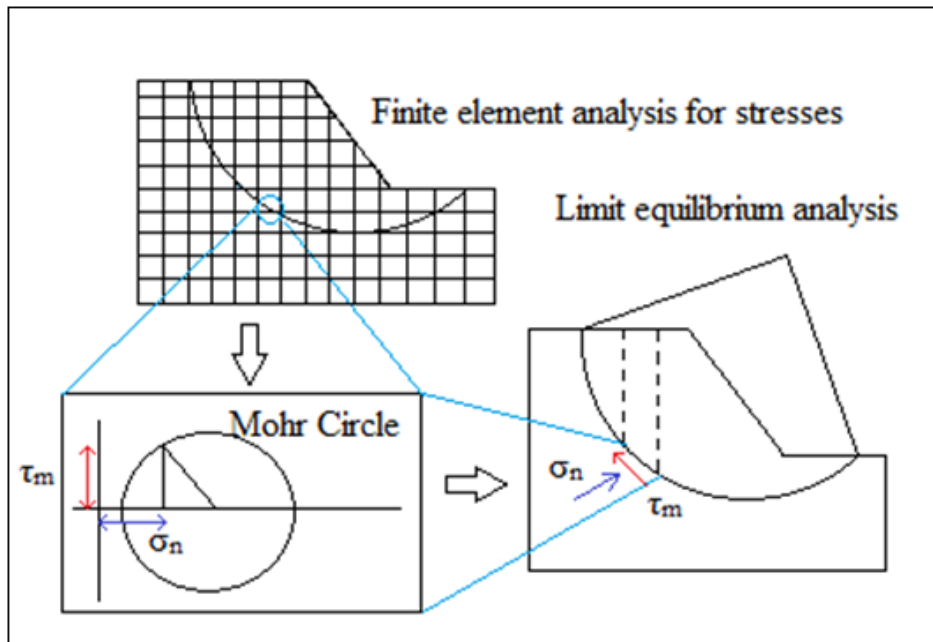
Figure 1.7 Stresses calculated by FEA and used in a limit equilibrium analysis
Adapted from Fredlund et al. (1999)

The Mohr circle and its equations are used to find the normal σ_n and shear τ_m stress components on the failure surface from σ_x, σ_y, and, τ_{xy} (Figure 1.8). The rotation angle is calculated from the slip surface inclination.

The shear strength S_r and mobilized shear stress S_m are calculated from equations 1.14 and 1.15 respectively.

$$S_r = c' + \sigma_n tan\phi' \tag{1.14}$$

$$S_m = \tau_m \tag{1.15}$$

The shear strength and mobilized shear stress must be converted to forces by multiplying the stress values with the base length of the slice. The factor of safety (F) is obtained by summing the resisting and mobilized forces and by comparing them:

$$F = \frac{\sum S_r}{\sum S_m} \tag{1.16}$$
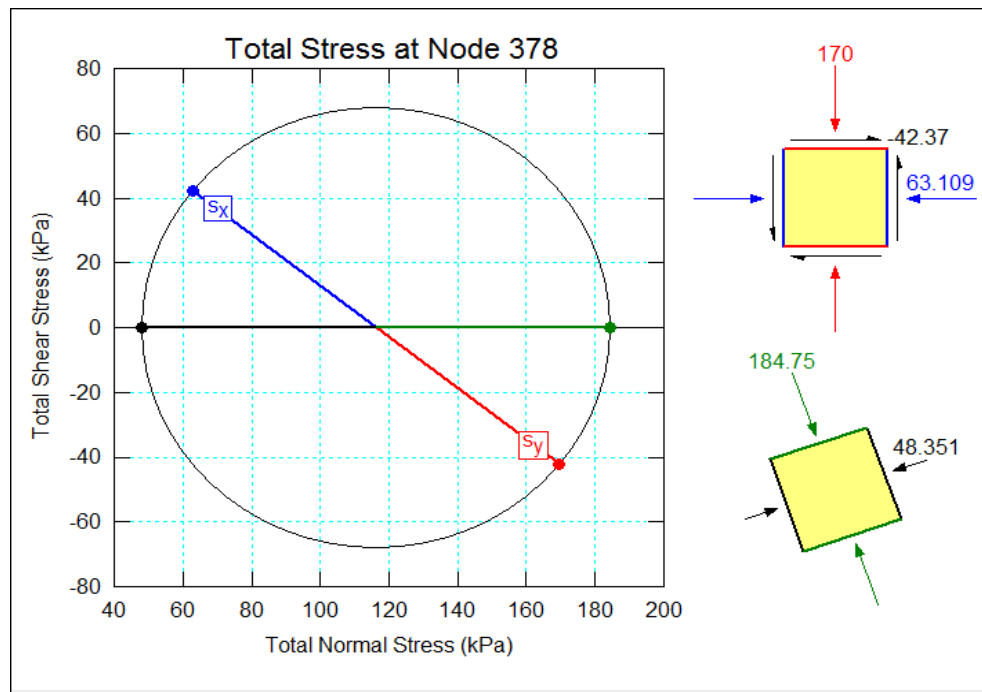
Figure 1.8 Example of Mohr circle to calculate the normal
and shear stresses in SIGMA/W

A large array of tools can be used to calculate the stress in a slope body. For instance, SIGMA/W can be used to compute ground stresses. Figure 1.9 shows an example of vertical stress values obtained with SIGMA/W. These stresses can be transferred to SLOPE/W to calculate F values for a series of slip surface.
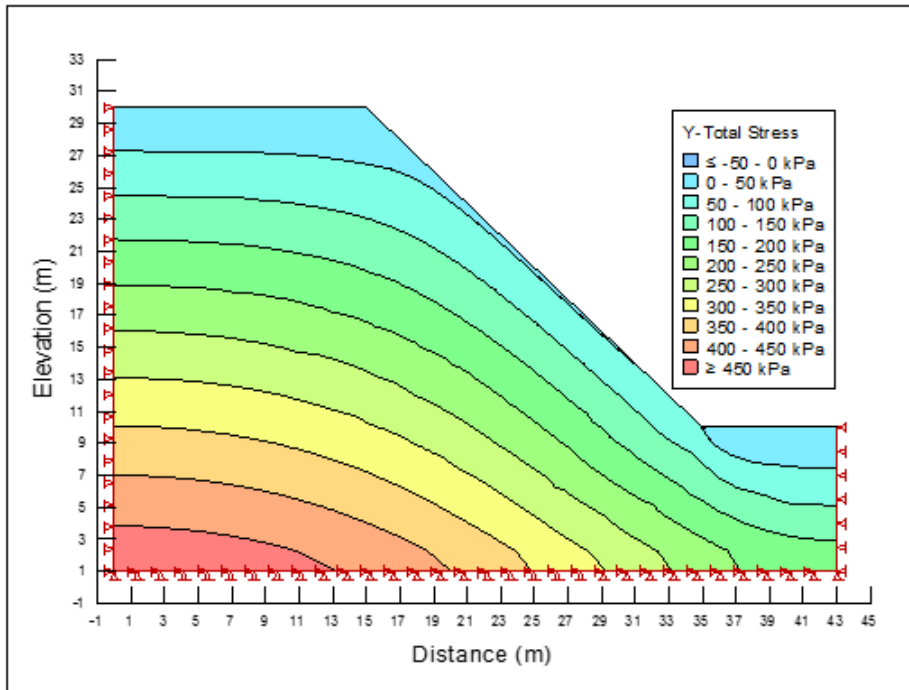
Figure 1.9 Vertical stress contours calculated by SIGMA/W

1.2.3.1 Procedure for limit equilibrium analyses based on finite-element stress

The procedure for limit equilibrium analysis based on a finite element stress analysis was presented by Krahn (2003). The main steps can be summarized as follows:

1. A FE code is used to calculate the ground stresses σ_x, σ_y, and τ_{xy} at the base of each slice;
2. The inclination of the base of each slice (α) is used to rotate the stress components. The rotation is conducted using the Mohr circle and its equations to get the normal and shear stress components at the base of each slice;
3. Equation 1.14 is used to calculate the shear strength at the base of each slice;
4. The resisting and mobilized shear forces are calculated by multiplying the mobilized shear stress and the shear strength at the base of each slice by its base-length (L) to convert stresses to forces;

5. This procedure is repeated for each slice to obtain the total available resisting force and mobilized shear force;

6. The factor of safety is obtained by dividing the total available resisting force by the total mobilized shear force (equation 1.16);

7. Steps 2 to 6 are repeated for different slip surfaces. The critical slip surface will result in the lowest factor of safety.

1.2.3.2   Advantages of using finite element stress method in limit equilibrium analysis

Using FEM stresses for limit equilibrium analyses has many advantages. One of the main challenges with limit equilibrium methods is to define the normal and shear stresses at the base of each slice. These stresses can easily be computed with a finite element analysis.

Figures 1.10 and 1.11 compare the normal stress distributions calculated from a finite-element analyses with SIGMA/W (curves labelled F.E.) with the normal stress distributions assumed with the Morgenstern-Price method (curves labelled L.E.) for two slip surfaces (Krahn, 2003). Figure 1.10 shows the stress distribution for a slip surface that goes through the slope toe. The normal stress values are similar for both methods near the slope crest. Starting from slice 7, a gap develops between the finite-element and Morgenstern-Price normal stresses. The normal stresses become approximately constant for FEM from slice 22 to slice 27. For the Morgenstern-Price method, the normal stress decreases after slice 22. Figure 1.11 shows the normal stress distribution for a deeper slip surface. In this case, the normal stress values for FEM and the Morgenstern-Price method are similar, thus indicating that classical limit-equilibrium methods can be based on adequate normal stress values for some slip surfaces.
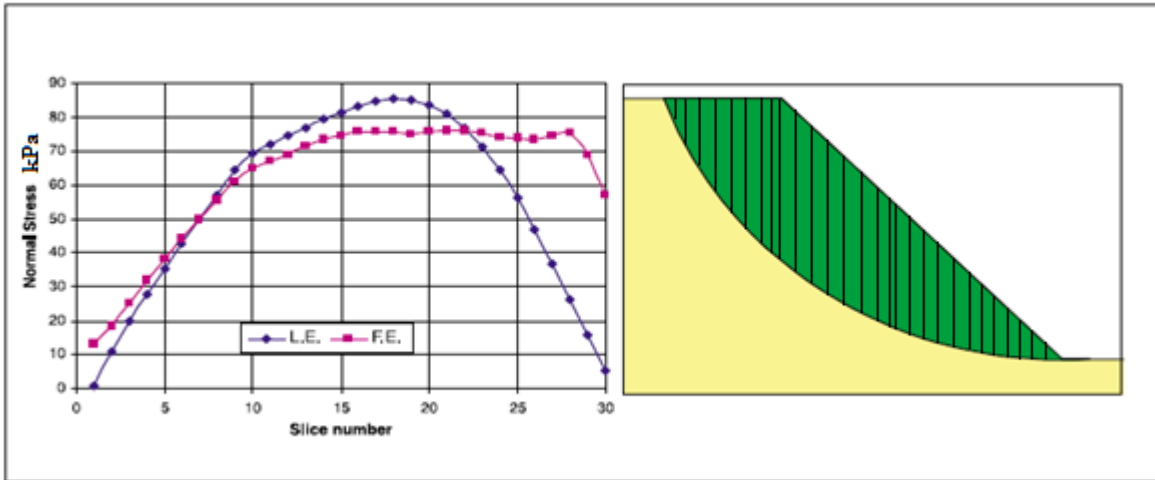
Figure 1.9 Distribution of the normal stresses along the toe slip surface
Adapted from Krahn (2003)
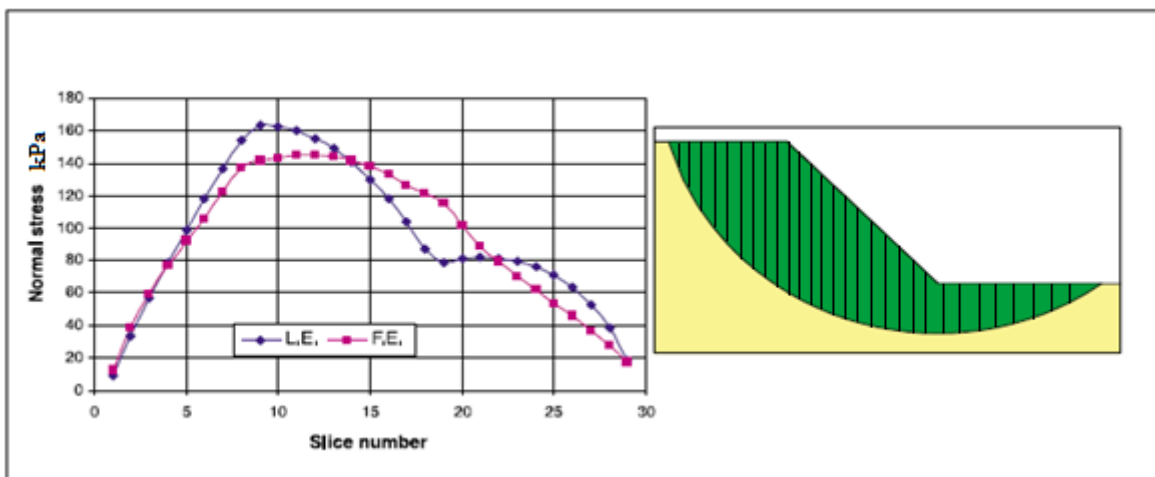
Figure 1.10 Distribution of the normal stresses along a deep slip surface
Adapted from Krahn (2003)

Limit equilibrium analyses based on finite element stresses have the following advantages:

1. FEM stresses are not based on assumed inter-slice forces;
2. The factor of safety is computed based on ground stresses that can be more representative of the real stresses in the field;
3. Dynamic stresses resulting from seismic waves can be considered in the slope stability analyses with FEM methods.

1.3   Slope stability analyses with COMSOL and MATLAB

1.3.1   COMSOL Multiphysics

COMSOL Multiphysics is a computer program based on the finite element method. Its geomechanics and subsurface flow modules allow different geotechnical problems to be studied (e.g., settlements). Unfortunately, COMSOL does not include native tools for slope stability calculations. As a consequence, the literature currently presents very few slope stability analyses based on COMSOL models.

One of the only examples of slope stability analysis based on a COMSOL model was presented by Shao et al. (2014). They used COMSOL to analyse the stability of slopes with a coupled dual-permeability. They computed local values of the factor of safety (Lu et al., 2012). The local factor of safety (*LFS*) is based on the comparison of the local Mohr-Circle in the slope body with a Mohr-Coulomb criterion. The local factor of safety is defined as a ratio between the shear stress on the failure envelope τ^* and the actual shear stress magnitude τ:

$$LFS = \frac{\tau^*}{\tau} \tag{1.17}$$

The main difference between the local factor of safety and the general factor of safety is that the LFS is computed at individual points of the studied slope but the general factor of safety is computed along a given slip surface for limit equilibrium methods (Zaruba & Mencl, 1982) or is unique for a given slope for strength reduction methods.

Shao et al. (2015) applied linear-elastic behaviour to a fine-grained slope to obtain the stresses. Their local factor of safety values were influnced by the rainfall rate and pore water-pressure. This influence was observed to depend on the soil preoperies. The instability of the slope increases with increasing pore pressures.

1.3.2   MATLAB

New tools for COMSOL can be programmed using the MATLAB LiveLink, a MATLAB programming interface for COMSOL. MATLAB is a programming language for scientific computing. MATLAB has been used separately from COMSOL for a large number of geotechnical applications, such as determining the principal stresses in rock and soil and determining the hydraulic parameters during pumping tests (Zúñiga et al., 2007). Independently from COMSOL, MATLAB was used by Zeng et al. (2009) to conduct slope stability analyses. They used an algorithm to search for the most critical slip surface for slopes.

1.4   Objectives

As previously mentioned, COMSOL does not include a slope stability module. The main objective of this project was to program and validate a limit equilibrium module for COMSOL. This module was to be based on finite-element stresses obtained with COMSOL Multiphysics. The second objective was to verify this new module with the Geo-Studio software package. To our best knowledge, this thesis presents the first example of limit equilibrium analysis with COMSOL.

CHAPTER 2

METHODOLOGY

The main objective of this thesis was to program a MATLAB script to conduct slope stability analyses for COMSOL models. COMSOL was used to define the slope geometry and to calculate the stresses in the slope body. MATLAB was used to set the failure surface parameters in COMSOL, to calculate the normal and tangent stress components with respect to the failure surface from the raw x and y stresses calculated in COMSOL, and to calculate the factor of safety for each failure surface. Figure 2.1 shows a schematic representation of the three main components of the COMSOL-MATLAB module.

The current version of the MATLAB script has some important limitations. First, it only allows circular failure surfaces to be tested. Second, it only supports materials with Mohr-Coulomb failure criteria. Third, it only allows three soil layers with different properties to be included in the geometry. The MATLAB script could however easily be modified to conduct more complex analyses.

The MATLAB script was verified using a similar stress-based method programmed in SLOPE/W. In this case, SLOPE/W performs the limit equilibrium analysis while SIGMA/W calculates the stresses and deformations in the slope body (Krahn, 2003). The SLOPE/W model was used to verify the factor of safety for identical sets of failure surfaces. SIGMA/W was used to verify the stress values calculated in COMSOL and rotated in MATLAB. Four slopes with different geometries and layering were used for the verification.

COMSOL Model

- Defines the slope geometry.

- Defines the soil properties for the stress-strain calculations (e.g. E, ν and ρ for a linear-elastic material).

- Calculates the stresses on the failure surface

COMSOL Local Server

- The server allows data to be exchanged between COMSOL and MATLAB.

MATLAB Script

- Sends the failure surface geometry to COMSOL (center and radius) for stress calculations.

- Calculates the normal and tangent stress values for each slice.

- Calculates the factor of safety.

- Defines the soil properties for Mohr-Coulomb failure criterion.

Figure 2.1 A schematic representation of the three components of the COMSOL-MATLAB slope stability module

2.1   COMSOL model

COMSOL version 5.2 was used in this study. In the COMSOL 2D model, the solid mechanics interface was used to calculate displacements, stresses and strains inside the slope model. This stress-strain analysis is based on Navier's equation. Plane strain and linear-elastic soil behaviour are assumed. The linear-elastic behaviour is based on three main parameters: Young's modulus E, Poisson's ratio v, and soil density ρ.

The COMSOL model includes only one main object (Figure 2.2): the slope body. It is based on a polygon or a series of polygons if the soil is layered.

The same boundary conditions were used in all the slope models that were tested. Free displacements were specified at the surface. Horizontal displacements are fixed at the left and right sides of the model. The bottom of the model has fixed horizontal and vertical displacements. The MATLAB code can handle different boundary conditions.

Gravity was applied to the slope body in the negative y-direction as a force per unit volume. The MATLAB code allows other forces to be added in the COMSOL model (e.g., influence of heat transfer on stress).

A COMSOL server is needed to integrate COMSOL with MATLAB. The server allows COMSOL to be integrated in MATLAB scripts or JAVA classes (e.g. Pirnia et al. 2016). When conducting slope stability analyses, both the COMSOL mph-file and MATLAB script should be in the same directory. The COMSOL server must be launched before the MATLAB script.
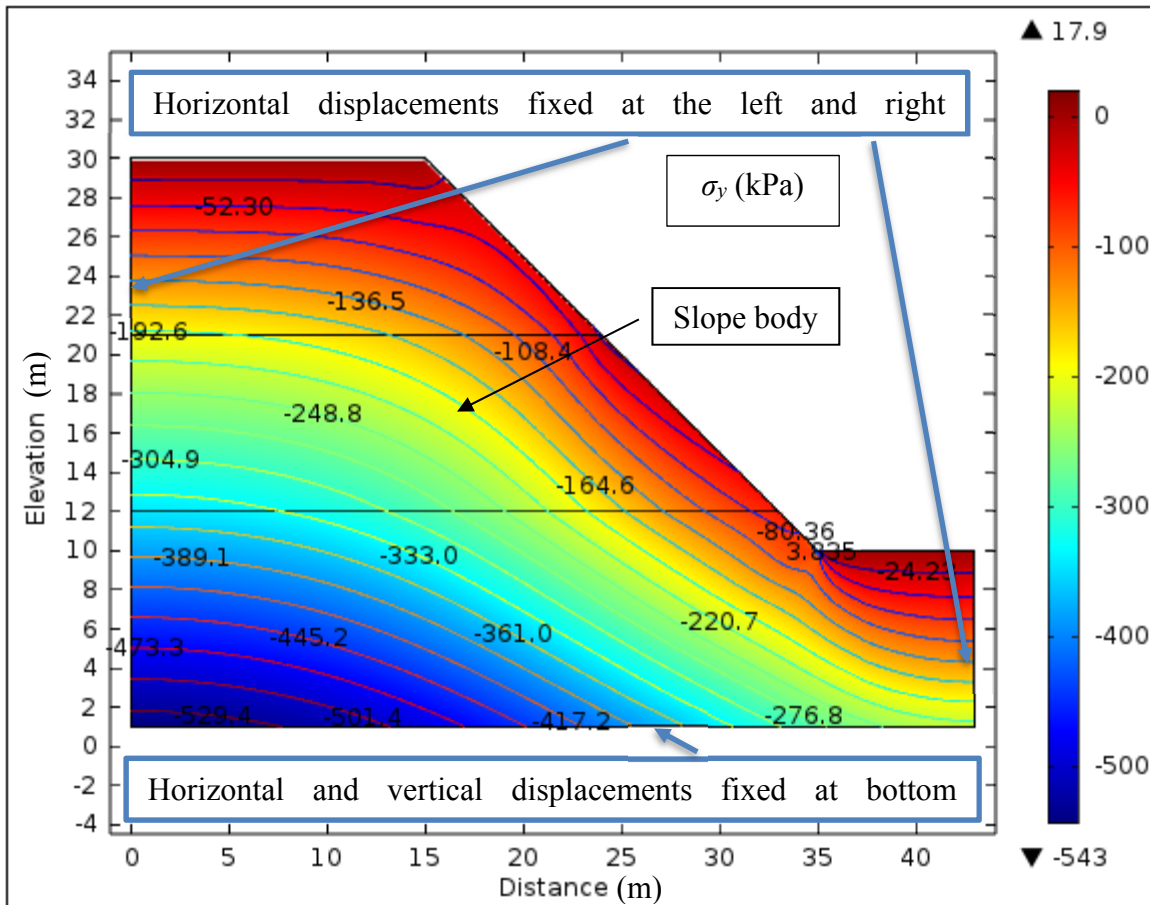
Figure 2.2 Slope geometries defined in the COMSOL model

The following steps must be followed when defining the COMSOL model. Figure 2.3 shows these steps as shown in COMSOL software.

1. The model geometry is defined. A polygon interface is used to define the slope body. The input for this interface is the x and y coordinates for all points that form the slope geometry;

2. The parameters for the physics interface of the slope are defined. Linear-elastic material properties are defined. These properties include Young's modulus, Poisson's ratio, and density. Boundary conditions and body loads are defined. In case of layered slopes, other linear-elastic materials are created;

3. A new mesh sequence is created. A user-controlled mesh is built automatically. Also the element size parameters and free quad settings are applied;

4. A default solver sequence is defined for a stationary study in order to compute the required stresses.
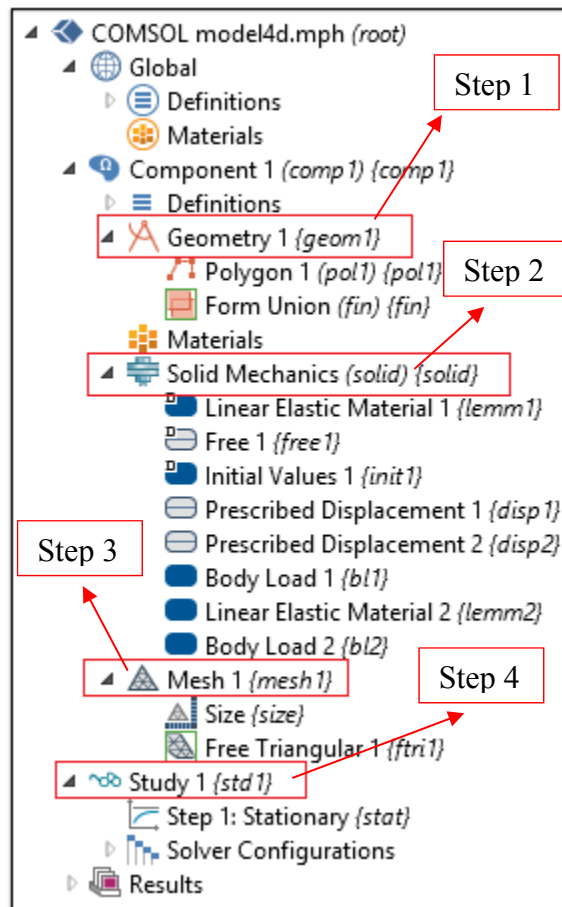
Figure 2.3 The tree structure identifying the main steps for the COMSOL model creation

2.2   MATLAB script

The MATLAB script was used to define the parameters describing the slip surfaces, to define the Mohr-Coulomb parameters of the slope material for uniform or layered slope, to define a number of slices, to define the slope geometry, to import the finite element stresses from COMSOL, to calculate the normal and shear stresses along the failure surface, to compute the shear strength and to compute values of the factor of safety. All these steps will be explained in more details in this section. The MATLAB code is presented in Appendix I.

The parameters describing the slip surfaces, Mohr-Coulomb criteria, number of slices and slope geometry are defined in the first section of the script. The slip surface in the current analysis is assumed to be circular. The x and y coordinates of the center, and the failure surface radius values are defined in three vectors. Soil properties (cohesion and friction angle) are defined in vectors. The number of slices inside the failure wedge is defined. These slices are used to integrate the stress to calculate the factor of safety. A matrix (variable *SlipCircles*) of all possible combinations of the three vectors components is built to define *n* slip surfaces for which the factor of safety will be calculated. The same matrix is used later in the script to store the factor of safety values. The geometry of the slope body is defined using the *x-y* coordinates of a polygon or a series of polygons if the soil is layered.

In the second section of the script, a COMSOL file is opened by the MATLAB script. The filename is stored in a string that can be changed by the user. The COMSOL file must be in the same directory as the MATLAB script. The code lines that follow allow points to be defined for the stress interpolation. The variables to be evaluated for these points are also defined (σ_x, σ_y, τ_{xy}). The finite element equations are then solved. They only need to be solved once per simulations. The finite element stresses for the different slip circles are interpolated from the same finite element simulation.

Section three of the script contains a loop (*for* loop) that allows the factor of safety to be calculated for all slip surfaces. Inside the loop, the coordinates of a series of points on the

failure circle are computed using the radius and the trigonometric circle parametrization. Once the slip circle is defined, the intersection points between the circle and the slope geometry are computed using the *polyxpoly* function. Normally, two intersection points are found for suitable slip circles. Incorrect circles either do not touch the slope body or have more than two intersection points (special case in benched slope). The script moves to the next for loop iteration without calculating a factor of safety for these two cases.

For correct slip surfaces, the two extreme x values of the intersection points are used to define the limit of the soil wedge inside the slip surface. The slice width is calculated from the difference between the two extreme x values. The x-coordinates of the slice bases are then calculated based on the slice width. The y-coordinates are based on x-coordinates of the slice base and the failure circle equation. Finally, mid-points x_m and y_m (red points) at the base of each slice are computed based on left and right coordinates x_b and y_b (blue points) at the base of each slice (Figure 2.3). These points are the locations where the finite element stresses should be computed.
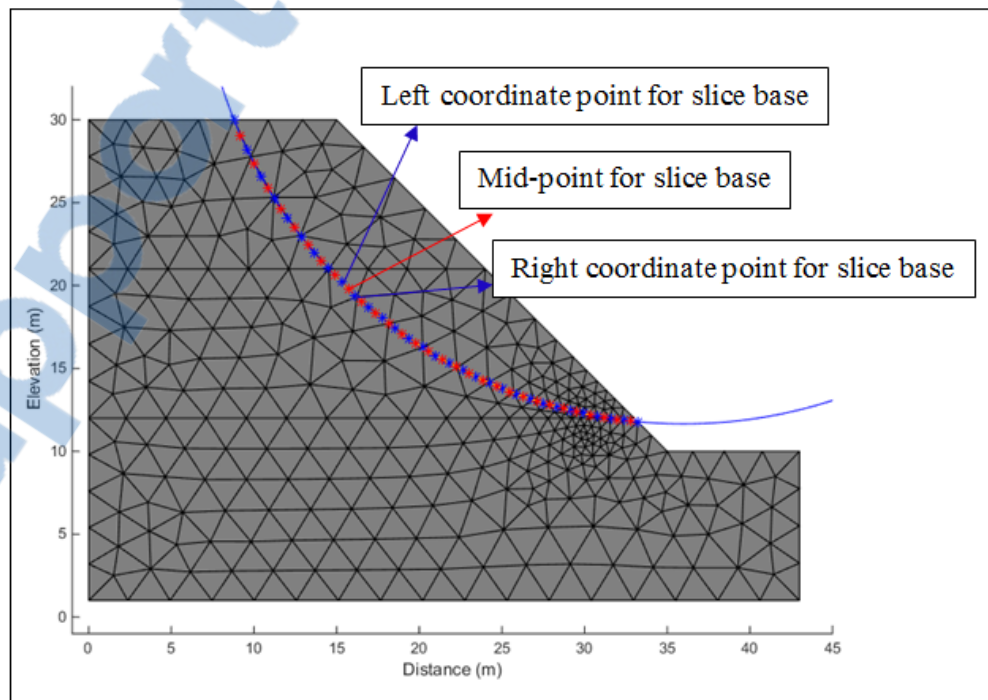
Figure 2.4 Left, center and right points coordinates of slice base

Section four of the script contains code lines to extract the stress values at the mid-point of the base of each slice from the COMSOL model. The COMSOL model interpolates σ_x, σ_y, and, τ_{xy} from the finite-element solution.

Section five applies to cases where the soil body is composed of more than one layer. The *inpolygon* function is used to find in which layer the points are located and to assign the proper c' and ϕ' values in vectors describing the Mohr-Coulomb parameters for the base of each slice.

The inclination angle α of each slice base is computed in section six and using next equation.

$$\alpha = \tan^{-1}\left[\frac{yb - ym}{xm - xb}\right] \tag{2.1}$$

The actual base length (*b*) of the slice is determined by using the inclination angle of each slice and the slice width (*w*):

$$b = \frac{w}{\cos\alpha} \tag{2.2}$$
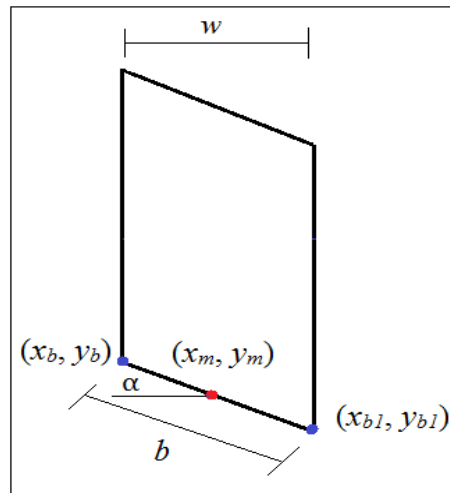
Figure 2.5 Illustrates the coordinates of slice base, horizontal slice width (w), slice base inclination (α) and actual slice base length (b)

In section seven, the stress components imported from COMSOL are rotated to calculate the normal σ_n and shear τ_n stresses at the center point of the slice base (x_m, y_m) using equation 2.3 and 2.4 respectively:

$$\sigma_n = (\sigma_x + \sigma_y)/2 + ((\sigma_x - \sigma_y)/2) \cos 2\alpha + \tau_{xy} \sin 2\alpha \tag{2.3}$$

$$\tau_n = - ((\sigma_x - \sigma_y)/2) \sin 2\alpha + \tau_{xy} \cos 2\alpha \tag{2.4}$$
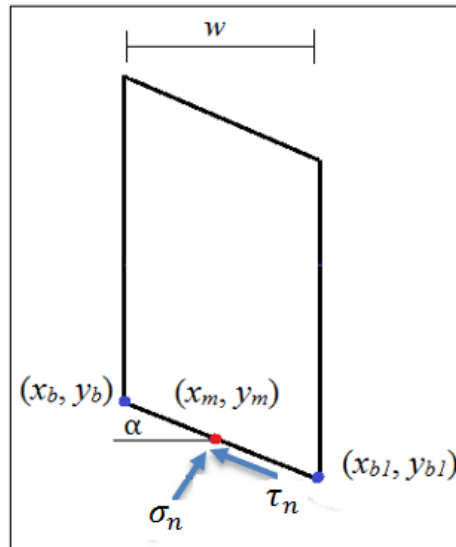
Figure 2.6 Illustrates normal and shear stresses at slice base

The normal and shear stresses are used with the soil's Mohr-Coulomb parameters to calculate the shear strength along the slice base:

$$\text{Shear strength} = c + \sigma_n \tan(\phi) \tag{2.5}$$

The mobilized shear stress corresponds to the shear stress along the slice base:

$$\text{Mobilized shear stress} = \tau_n \tag{2.6}$$

The shear strength and mobilized shear stress must be converted into forces by multiplying the stresses by the base length (b). The forces are then summed:

$$\text{Resistance shear forces} = \sum b(c + \sigma_n \tan(\phi)) \tag{2.7}$$

$$\text{Mobilized shear forces} = \sum b\,\tau_n \tag{2.8}$$

The final step consists in computing the factor of safety (F):

$$F = \frac{\text{Resistance shear forces}}{\text{Mobilized shear forces}} = \frac{\sum b(c + \sigma_n \tan(\phi))}{\sum b\,\tau_n} \tag{2.9}$$

Figure 2.4 explains schematically the main steps of the factor of safety calculations with COMSOL and the MATLAB script.

Running COMSOL multiphysics

Simulate slope models using E, v, and ρ

Solve FEA to compute σ_x, σ_y, and, τ_{xy}

Running COMSOL server

MATLAB

Defines;

x, y, R parameters for slip surface

x-y coordinates for slope model

c' and ϕ' for soil properties

COMSOL model is open in MATLAB script

for loop to test all failure surfaces and determine x_m and y_m

If: 2 layers or more

Uses in-polygon function to find x, y, c', and ϕ' [in] and x, y, c', and ϕ' [out]

Import FEA stresses

If: 1 layer

Find α, σ_n, and, τ_n

Compute resistance and mobilized forces

Calculate F

Figure 2.7 Schematic representation of the COMSOL-MATLAB script used to compute the factor of safety

2.3   GEO-SLOPE model

To verify the MATLAB script and the COMSOL model, a series of slope stability calculations were conducted with two modules from the GEO-SLOPE suite of software. The first module was SIGMA/W. It uses the FEM to compute the stress distribution in slopes based on the soil's E, v and ρ. The second tool is SLOPE/W, it uses LEM equations to calculate the factor of safety based on the soil's c' and ϕ', and the FEM stresses.

Figure 2.5 shows the distribution of vertical stresses in the first slope used for code verification (uniform slope). The geometry and soil properties were based on Krahn (2003). The second, third, and fourth slopes are respectively benches, a steep slope, and a uniform slope in a layered soil deposit. The same stress-strain and Mohr-Coulomb parameters were used for each slope, except for the layered soil deposit for which different parameters were used.

Figure 2.8 Distribution of vertical stresses in the uniform slope model using SIGMA/W

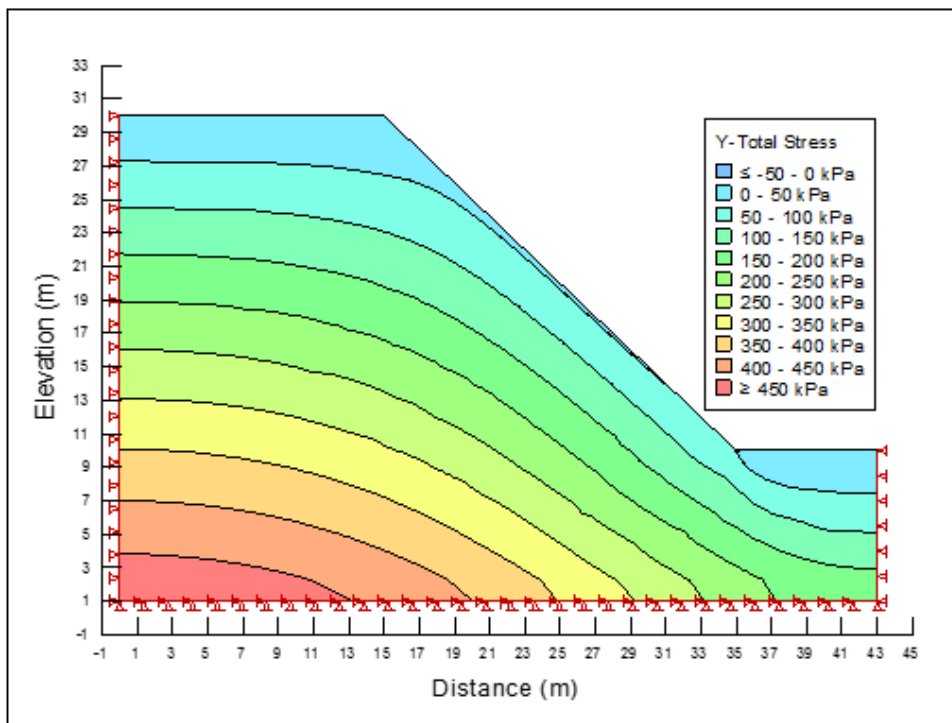The same four models were created in COMSOL and MATLAB in order to compare the results with the GEO-SLOPE models. These four models and their results will be described in detail in the following chapter.

CHAPTER 3

CODE VERIFICATION RESULTS AND DISCUSSION

The stability of slopes with different geometries and soil properties was analyzed using the COMSOL-MATLAB module introduced in the previous chapter and the stress-based method available with SLOPE/W and SIGMA/W in the GEO-SLOPE software package. Four slopes were tested: a uniform slope, a slope with benches, a steep slope, and a slope in a layered soil deposit. For each slope, the factor of safety was calculated for a series of failure surfaces. Code verification with SLOPE/W was carried out using the same slope, the same properties and the same failure surfaces. The MATLAB code programmed for this study is presented in Appendix I.

The chapter presents the results of this verification. The comparison is focused on finite element stresses and the factor of safety. A detailed comparison of finite element stresses and comparison of numerical results of finite element stresses are presented in Appendix II. The comparison of factor of safety values with graphs are presented in Appendix III.

3.1   Analysis of COMSOL-MATLAB and GEO-SLOPE models

3.1.1   Analysis of uniform slope

The uniform soil model has a height of 30 m and length of 43 m with slope height and length of 20 m (Figure 3.1). This corresponds to an inclination of 45º. The soil has a unit weight of 18 kN/m³. Linear-elastic behaviour was assumed for the finite element analysis in COMSOL and SIGMA/W with a Young's modulus of 1 GPa and a Poisson's ratio of 0.3. Cohesion and friction angle of respectively 5 kPa and 20º were assumed based on Krahn (2003). Pore pressures were not considered in the analysis.
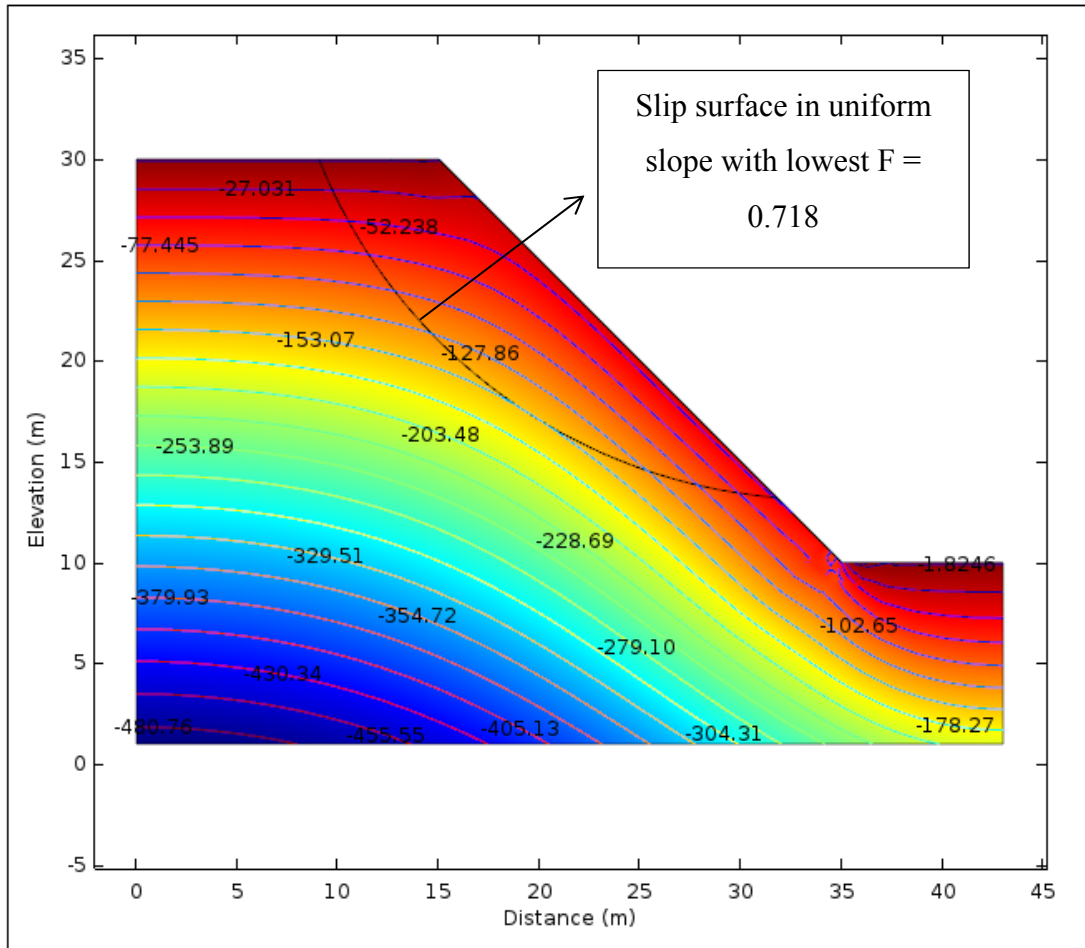
Figure 3.1 Distribution of σ_y in uniform slope computed with COMSOL with slip surface and lowest factor safety computed with MATLAB

With both MATLAB and SLOPE/W, the analysis was conducted using 30 slices. A total of 20 slip surfaces were used. The slip surfaces were specified in GEO-SLOPE using a grid for the slip surface centers and a set of slip surface radiuses. The same center coordinates and radiuses were used in the MATLAB script.

Figures 3.2 presents a comparison of the vertical finite element stresses (σ_y) obtained with COMSOL and SIGMA/W on the failure surface shown in Figure 3.1. The lowest σ_y values correspond to the top of the slope and the exit point of the failure surface at the bottom of the slope. The vertical stress reaches 157 kPa at slice 14. The results obtained with COMSOL and SIGMA/W are nearly identical with a maximum difference of 2 kPa. Horizontal σ_x and

tangent τ_{xy} stresses are also almost identical for this slope geometry with a maximum difference of 1 and 2 kPa respectively (Appendix II).

The MATLAB code presented in Appendix I divide the sliding mass in equal-width slices. This is not the case in SLOPE/W where the slope width can sometime vary slightly depending on the slope geometry. This has an impact on the location of the slice base mid-point and inclination.
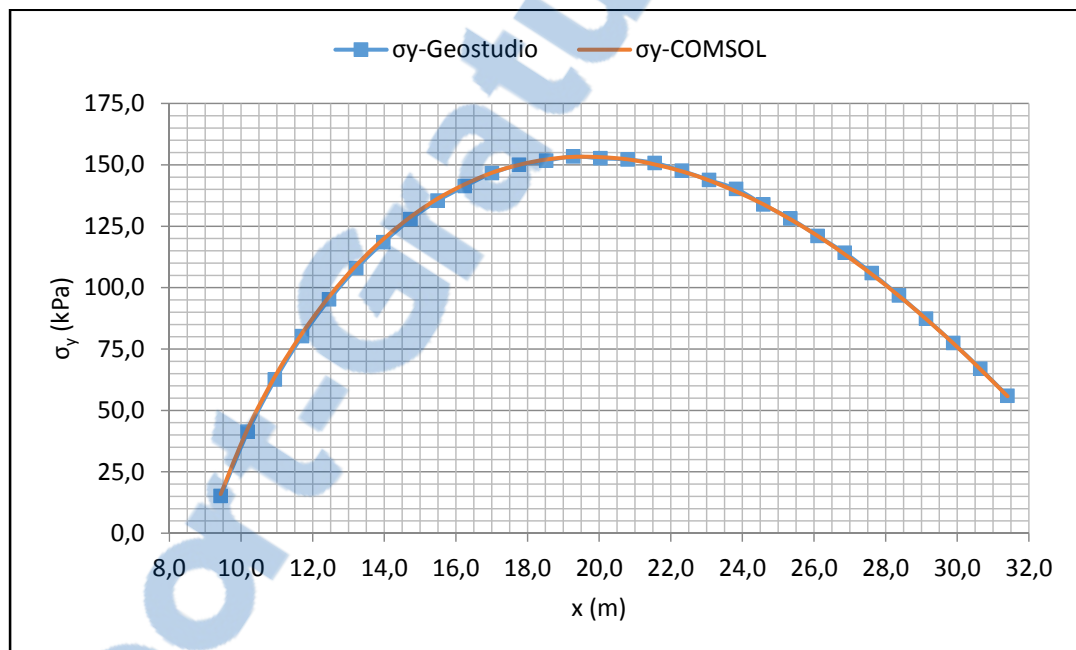
Figure 3.2 Comparison of σ_y between COMSOL and SIGMA/W
for the uniform slope

Information on the slip surface with the lowest F obtained with the MATLAB code and SLOPE/W for the uniform slope is presented in table 3.1. As shown in the table, the same surface produced the lowest F value for both MATLAB and SLOPE/W.

Figure 3.3 shows the factor of safety values that were obtained with SLOPE/W and COMSOL-MATLAB. The analysis was done for 20 slip surfaces, but only 17 slip surfaces allow computing a factor of safety. The other 3 slip surfaces did not allow a factor of safety to be calculated because they crossed the vertical boundaries of the domain. SLOPE/W also

detected these slip surfaces. In Figure 3.3, the red line shows the results of GEO-SLOPE and COMSOL-MATLAB if both are completely identical and the blue line is the obtained results. The F values vary between 0.717 (critical value) and 1.713 for COMSOL-MATLAB code and between 0.718 (critical value) and 1.696 for SLOPE/W. The linear regression has a slope of 1.0242 and an intercept of -0.0141. It indicates that SLOPE/W and COMSOL-MATLAB gave similar F values. Detailed results of factor of safety for the 20 slip surfaces are given in Appendix III.

Table 3.1 COMSOL-MATLAB and SLOPE/W results for slip surface with the lowest F for uniform slope

Tool	Slip surface with lowest F for uniform slope					
	Failure circle coordinates		Radius	Sum of resistance forces	Sum of mobilized forces	Factor of safety
	X (m)	Y (m)	R (m)	S_r (kN)	S_m (kN)	F
COMSOL-MATLAB	34	40	26.877	905.53	1260.81	0.718
GEO-SLOPE	34	40	26.877	904.85	1262.28	0.717
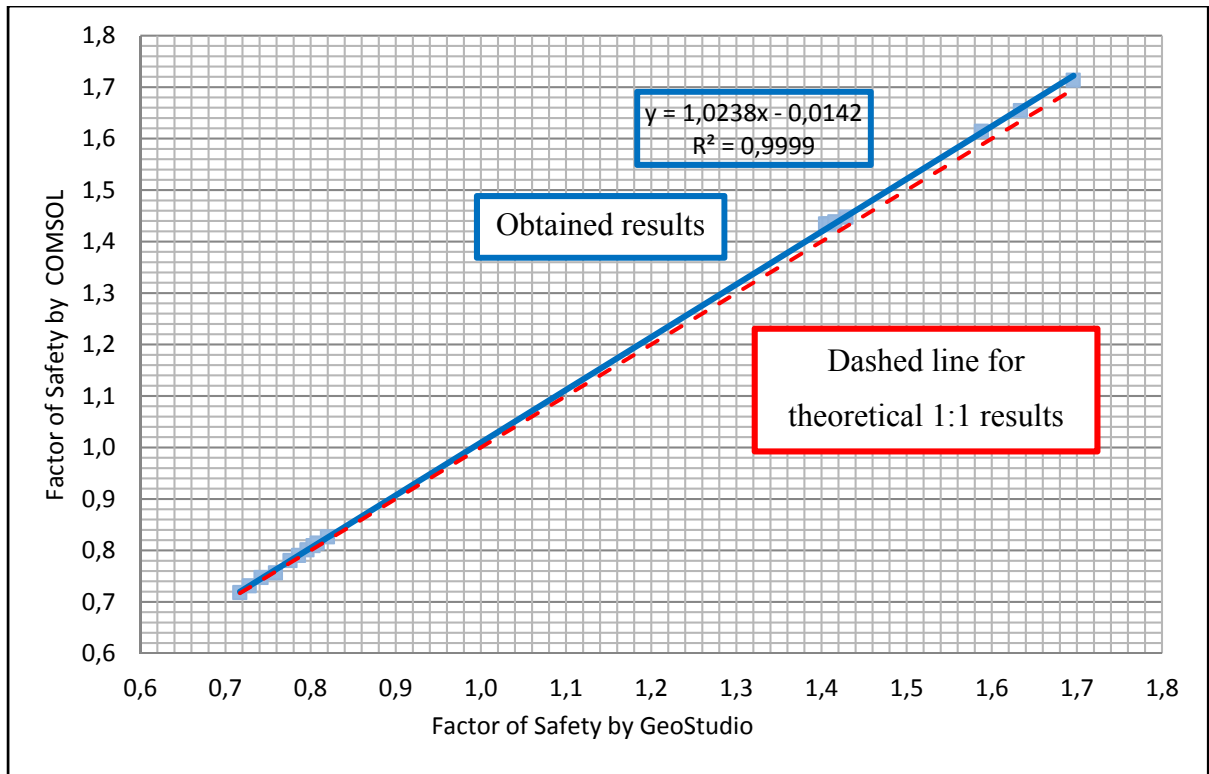
Figure 3.3 Comparison between obtained and ideal factor of safety values with SLOPE/W and COMSOL for the uniform slope

3.1.2   Analysis of slope with benches

The height and length of the slope are 30 m and 24 m respectively (Figure 3.4). The slope consists of two benches with different inclinations. The soil conditions are identical to the uniform slope. Pore pressures were also not considered in the analysis. The analysis was conducted with 30 slices. The same 20 slip surfaces were used in SLOPE/W and the MATLAB script.
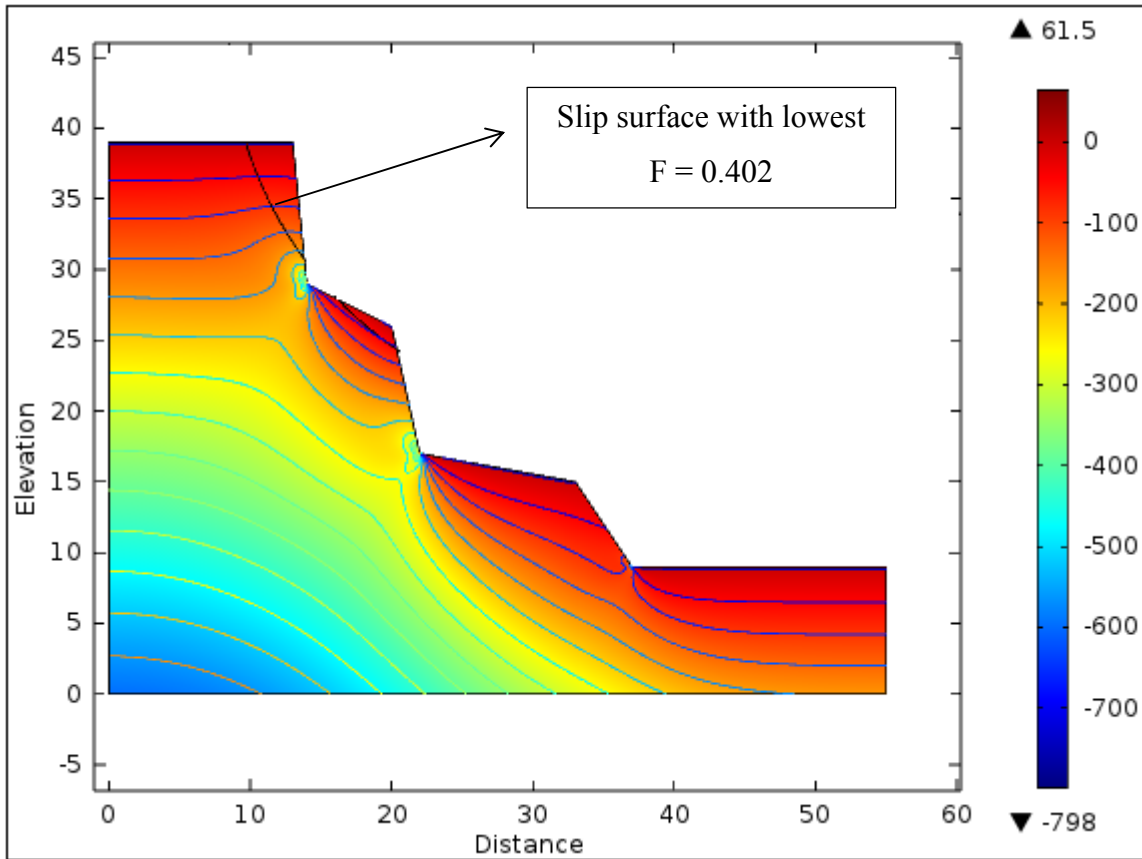
Figure 3.4 Distribution of σ_y in slope with benches computed with COMSOL with slip surface and lowest F computed with MATLAB

A comparison of the vertical stresses along the slip surface for the COMSOL and SIGMA/W finite element analyses is shown in Figure 3.5. The lowest σ_y values are concentrated at the top of the slope. The stress values for COMSOL and SLOPE/W start at x = 9.747 m to x = 13.206 m with the same values. After x = 13.206 m they began to diverge smoothly toward the exit of the slip surface at the bottom of the slope. The finite element stresses of the benches slope presented in (Appendix II).
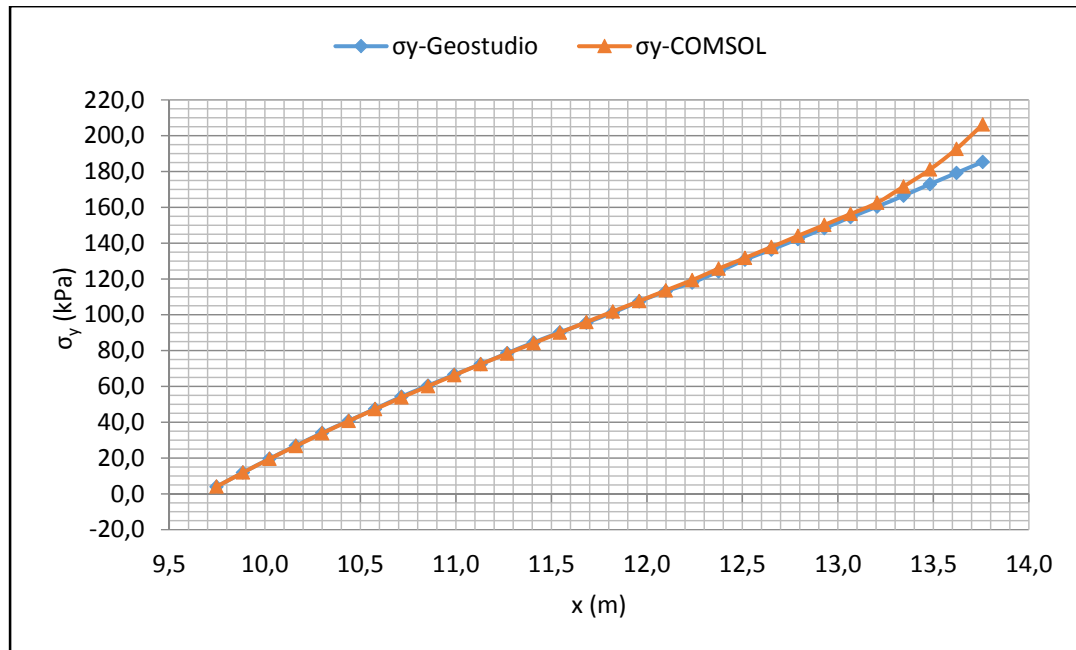
Figure 3.5 Comparison of σ_y between COMSOL and SIGMA/W for slope with benches

Table 3.2 shows the parameters of the slip surfaces with the lowest F value that were obtained with the MALTAB code and SLOPE/W for the slope with benches. Both codes identified the same slip surface with similar F values.

The part of the code where the validity of the slip surfaces is verified faces a different challenge with this slope as some slip surfaces intersect the slope at more than two points (Figure 3.4). The factor of safety is computed for the sliding mass between the first and second intersection points for both SLOPE/W and MATLAB code.

Figure 3.6 shows the factor of safety values that were obtained with SLOPE/W and COMSOL-MATLAB for 20 slip surfaces. The F values vary between 0.402 and 1.186 for the COMSOL-MATLAB code and between 0.403 and 1.216 for SLOPE/W. The linear regression shown in Figure 3.3 with a slope of 0.9605 and an intercept of 0.0201 indicates that SLOPE/W and COMSOL-MATLAB gave similar F values.

Table 3.2 COMSOL-MATLAB and SLOPE/W results for slip surface with the lowest F for
the slope with benches

Tool	Critical slip surface for benches slope					
	Failure circle coordinates		Radius	Sum of resistance forces	Sum of mobilized forces	Factor of safety
	X (m)	Y (m)	R (m)	S_r (kN)	S_m (kN)	F
COMSOL-MATLAB	36	47	27.511	100.58	250.17	0.402
GEO-SLOPE	36	47	27.511	101.485	251.627	0.403

Detailed results for the 20 slip surfaces are given in Appendix III. All slip surfaces are
passing through the slope body, so factor of safety were computed for all slip surfaces. In
Figure 3.6, the obtained results line and the ideal results line are almost identical with a very
small gap.
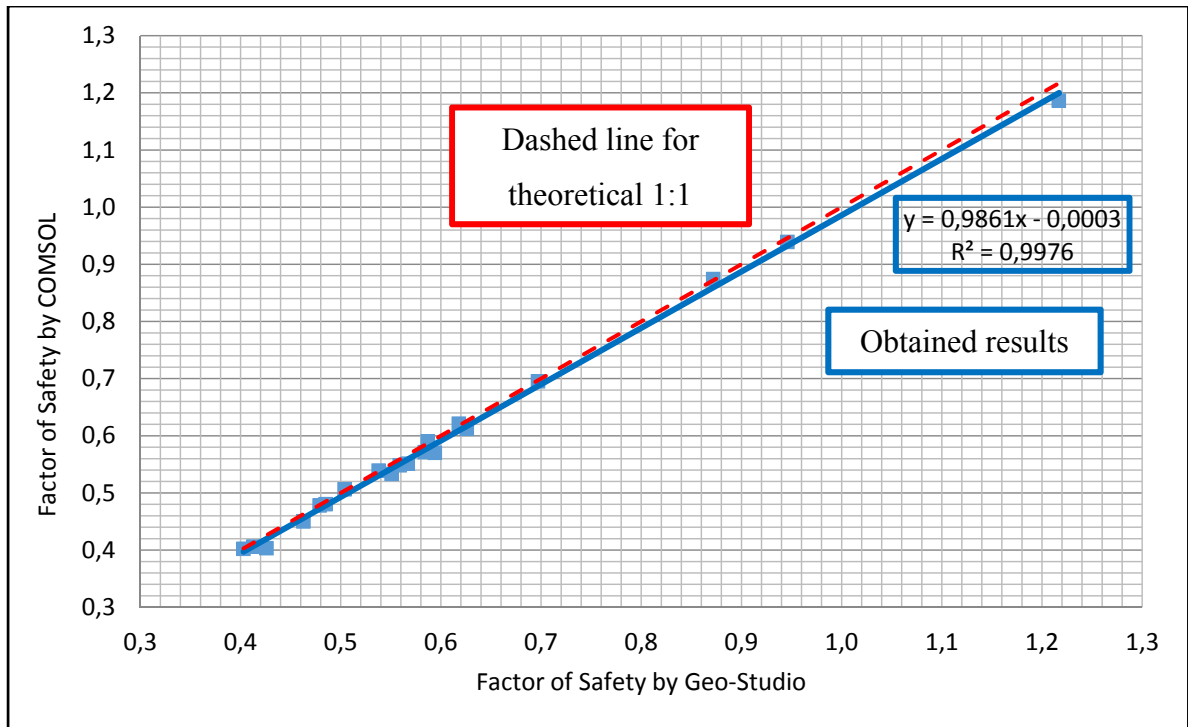
Figure 3.6 Comparison between obtained and ideal factor of safety values with SLOPE/W and COMSOL slope with benches

3.1.3   Analysis of steep slope

The steep slope has a height of 22 m and a length of 8 m (Figure 3.7). The soil properties for this example are identical to the previous examples. The analysis did not take into account pore pressures. As with the previous examples, 20 slip surfaces were compared. Each slip surface was analysed with 30 slices.
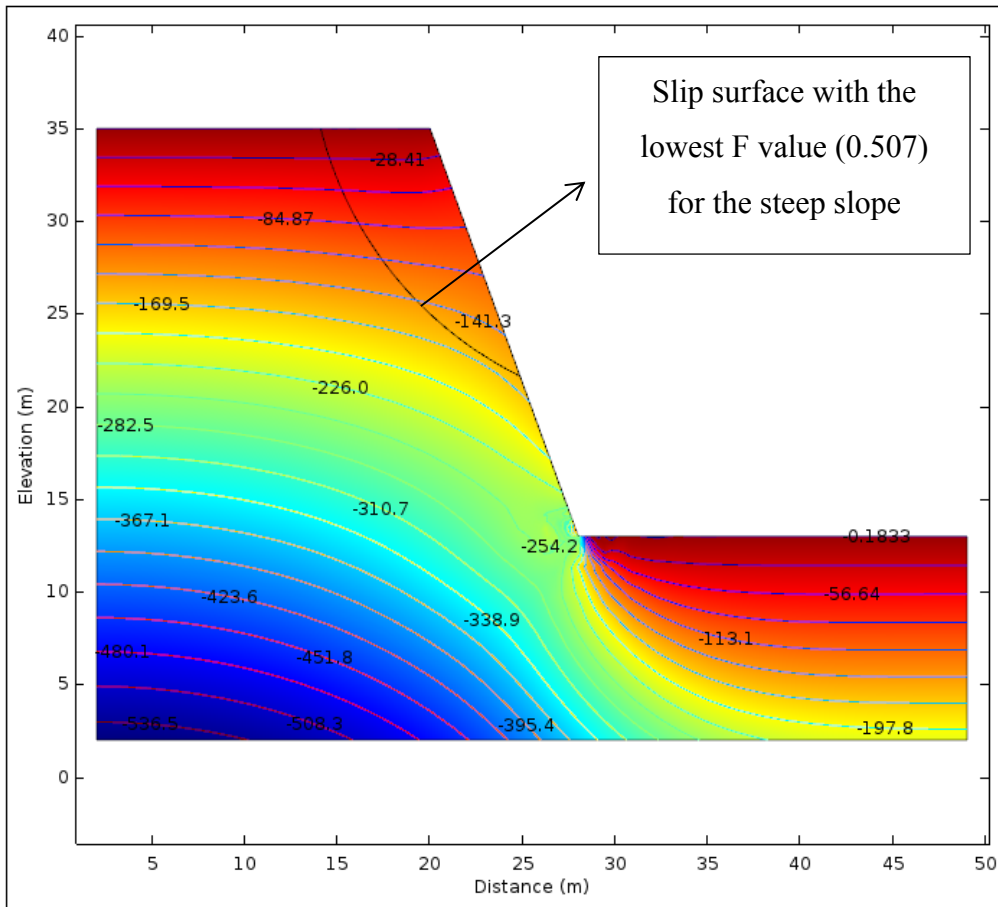
Figure 3.7 Distribution of σ_y in steep slope computed with COMSOL with slip surface and lowest F computed with MATLAB

The σ_y distributions in both models are once again similar. Figure 3.8 shows σ_y for the slip surface with the lowest F value shown in Figure 3.7. The lowest σ_y values are located at the crest and they increase toward the bottom of the slip surface. The vertical stress increase at the end of slope to around 165.4 kPa at x = 24.685 m. The difference between the σ_y values for COMSOL and SIGMA/W along the failure surface is generally small but it increases slightly at both the entry and exit points of the slip surface. The horizontal σ_x and tangent τ_{xy} stresses lead to maximum differences of 3 and 4 kPa receptively. The finite element stresses are compared in (Appendix II).
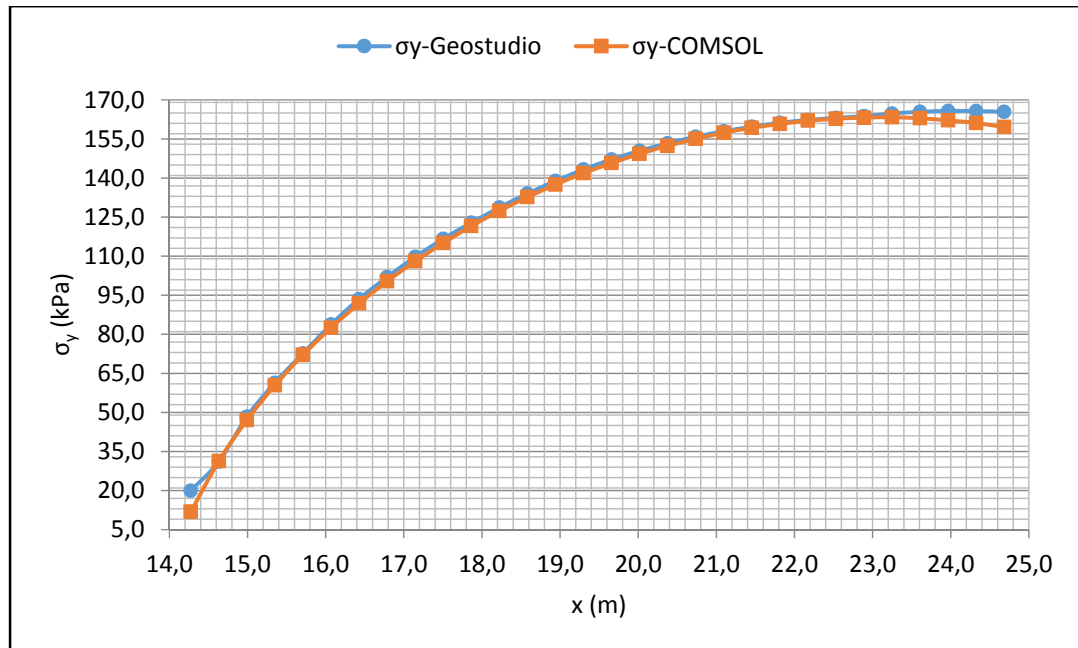
Figure 3.8 Comparison of σ_y between COMSOL and SIGMA/W in steep slope

The slip surfaces with the lowest F values in COMSOL and SLOPE/W are given in Table 3.3. Once again the same slip surfaces lead to the lowest F values in COMSOL and SLOPE/W.

Table 3.3 COMSOL-MATLAB and SLOPE/W results for slip surface with the lowest F for the steep slope

Tool	Critical slip surface results of steep slope					
	Failure circle coordinates		Radius	Sum of resistance forces	Sum of mobilized forces	Factor of safety
	X (m)	Y (m)	R (m)	S_r (kN)	S_m (kN)	F
COMSOL-MATLAB	34	40	20.524	398.48	785.53	0.507
GEO-SLOPE	34	40	20.524	399.18	785.13	0.508

Figure 3.9 shows the range of factor of safety values for SLOPE/W and COMSOL-MALTAB code for the 19 slip surfaces. The F values vary from 0.507 to 2.103 for COMSOL-MATLAB and from 0.508 to 2.105 for SLOPE/W. For slip surface number 11, the failure circle goes through the fixed vertical boundaries of the soil body slope. The failure surface was rejected by both the COMSOL-MATLAB code and SLOPE/W. The linear regression for the obtained results has a slope of 1.0009 and an intercept of 0.0049 with y = x and R^2 = 1 for the ideal results. Both lines seem to correspond for all F values. It also indicates that the COMSOL-MATLAB code gave *F* values that were similar to those of SLOPE/W for the steep slope.
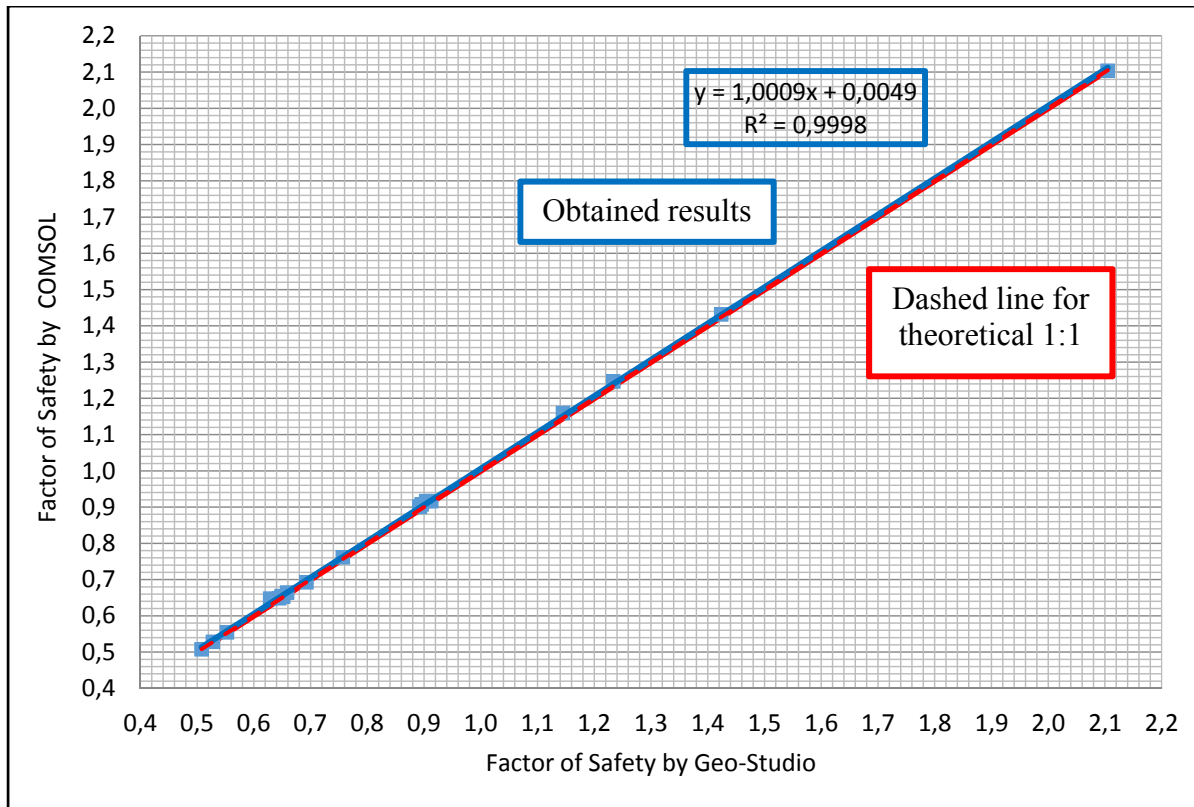
Figure 3.9 Comparison between obtained and ideal factor of safety values with SLOPE/W and COMSOL for steep slope

3.1.4 Analysis of slope in layered soil deposit

The slope body consists in three layers. The slope has a height of 20 m and a length of 20 m (Figure 3.10). The inclination of the slope is 45°. The upper and lower layers are silty to clayey sand with c' = 5 kPa, φ' = 31°, and a unit weight of 21 kN/m³. The Young's modulus and Poisson's ratio for this layer were set at 50 MPa and 0.3 respectively. The middle layer was assumed to be clay with c' = 25 kPa, φ' = 22°, and a unit weight of 17.5 kN/m³. Its Young's modulus and Poisson's ratio were set to of 20 MPa and 0.4 respectively.
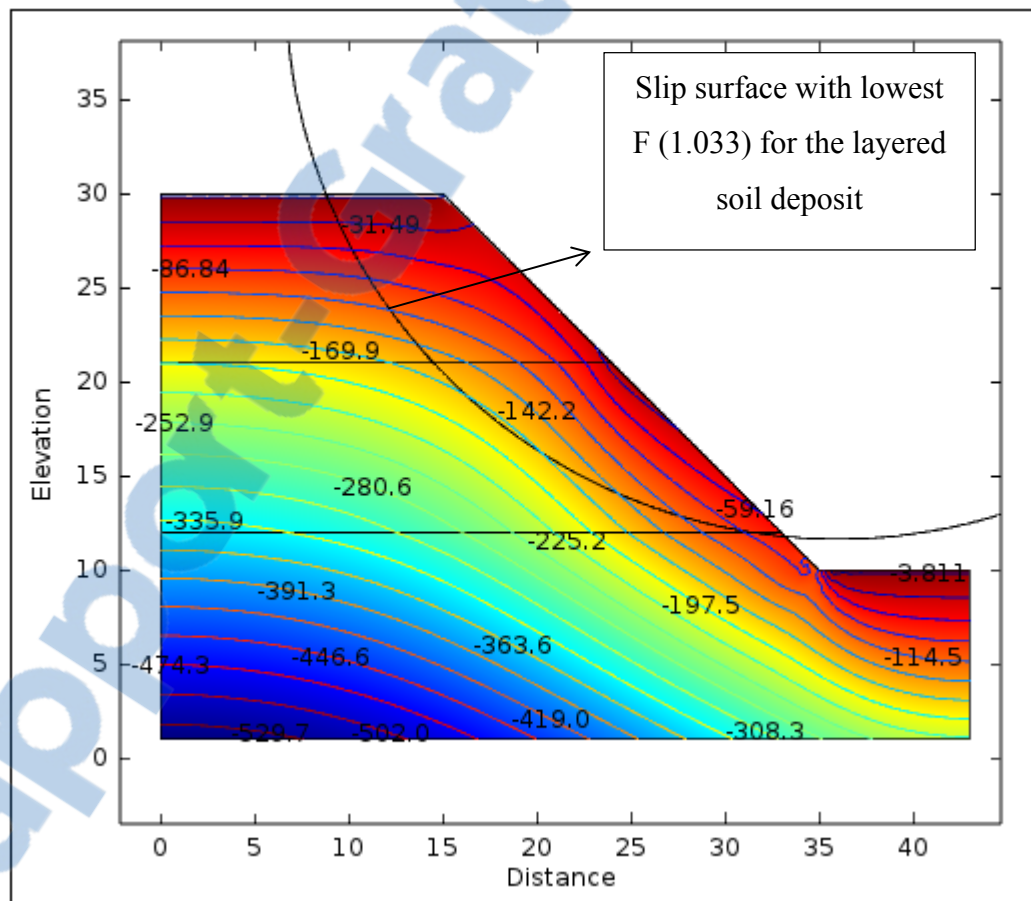
Figure 3.10 Distribution of σ_y in layered slope computed with COMSOL with slip surface and lowest F value computed with MATLAB

The analysis also was conducted using 20 slip surfaces and 30 slices for both MATLAB and SLOPE/W. The slip surfaces parameters obtained from GEO-SLOPE are used in MATLAB script following the same procedures for the previous models.

Figure 3.11 presents the distribution of vertical stresses along the lowest F failure plane in both COMSOL and SIGMA/W. The minimum values of σ_y correspond to the top of the slope and the end of the failure surface. The vertical stresses start to increase from the top of the slope until the middle at $x = 18$ m. The stresses then goes down toward the bottom of the slope until $x = 32$ m.
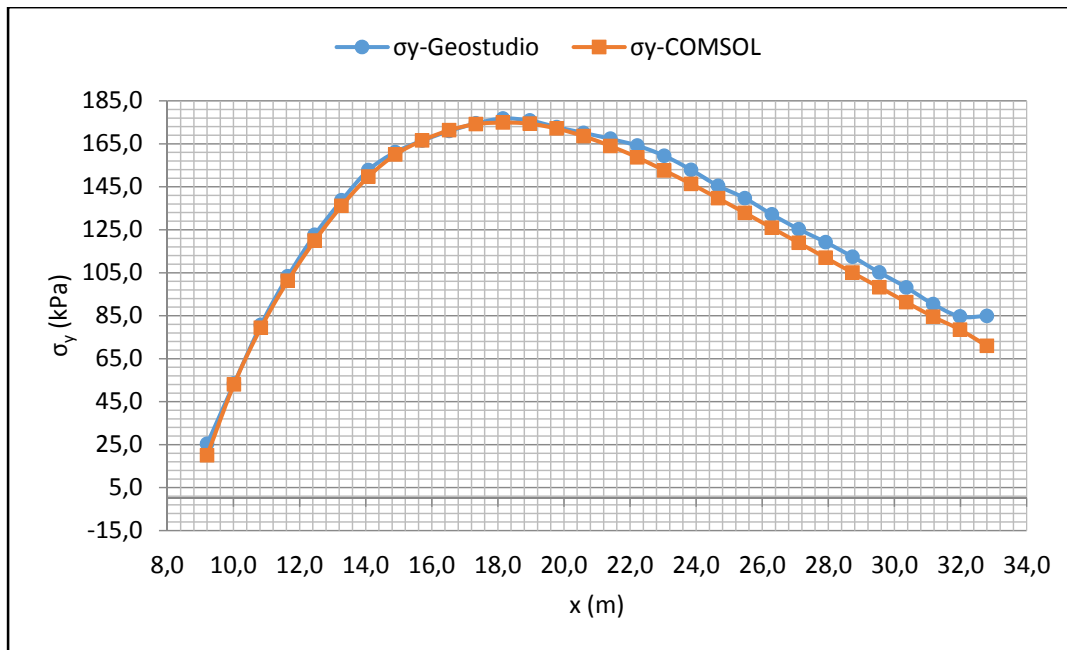
Figure 3.11 Comparison of σ_y between COMSOL and SIGMA/W
for layered soil deposit

The distribution of the horizontal σ_x is slightly complicated with a gap of stresses between x = 9.202 m and x = 14.899 m with a negative sign of two points (Figure 3.12). Also, the stresses after x = 14.899 m are not identical with each other to the end of the slope. The larger stress differences for the slip surfaces led to larger F differences.
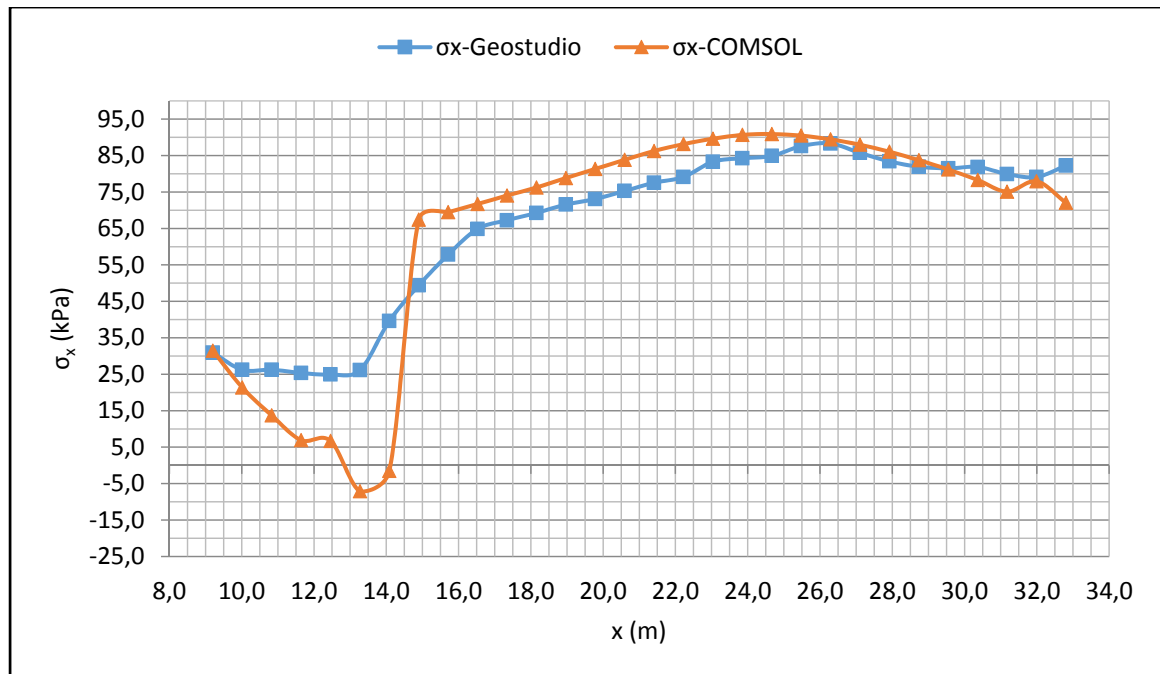
Figure 3.12 Comparison of σ_x between COMSOL and SIGMA/W
for layered soil deposit

The differences of stresses indicate that the stresses analysis of different materials in COMSOL is different than the in situ analysis (is the name of the analysis in SIGMA/W) in SIGMA/W especially in σ_x stresses. The tangent τ_{xy} are also almost identical with a small difference at the top of the slope. The τ_{xy} values tend to converge towards the bottom of slope (Appendix II).

The critical slip surface information obtained from MATLAB code and SLOPE/W for the layers slope is presented in table 3.4. The MATLAB code and SLOPE/W identified the same slip surface for the lowest F values.

Table 3.4 COMSOL-MATLAB and SLOPE/W results for slip surface with the lowest F for layered deposit soil slope

Tool	Critical slip surface results of layers slope					
	Failure circle coordinates		Radius	Sum of resistance forces	Sum of mobilized forces	Factor of safety
	X (m)	*Y (m)*	*R (m)*	*Sr (kN)*	*Sm (kN)*	*F*
COMSOL-MATLAB	36	41	29.345	1536.4	1493.4	1.033
GEO-SLOPE	36	41	29.345	1677.28	1596.36	1.051

Figure 3.13 shows the *F* values for COMSOL and GEO-SLOPE for 17 slip surfaces. Slip surfaces 5, 9, and 10 did not allow *F* to be calculated as they passed through the vertical boundary of the soil domain. The range of factor of safety for GEO-SLOPE goes from 1.051 to 1.533, and for COMSOL with MATLAB from 1.033 to 1.533. Some values are not located on the straight 1:1 line. A linear regression of the results is shown in Figure 3.13. It has a slope of 1.0061 and an intercept of − 0.0288. It indicates that the COMSOL-MALAB code gives *F* values that are reasonably close to those of SLOPE/W. The 1:1 line is parallel with the result line. This indicates that the *F* difference between SLOPE/W and COMSOL-MATLAB is approximately constant and does not depend on the slip surface.
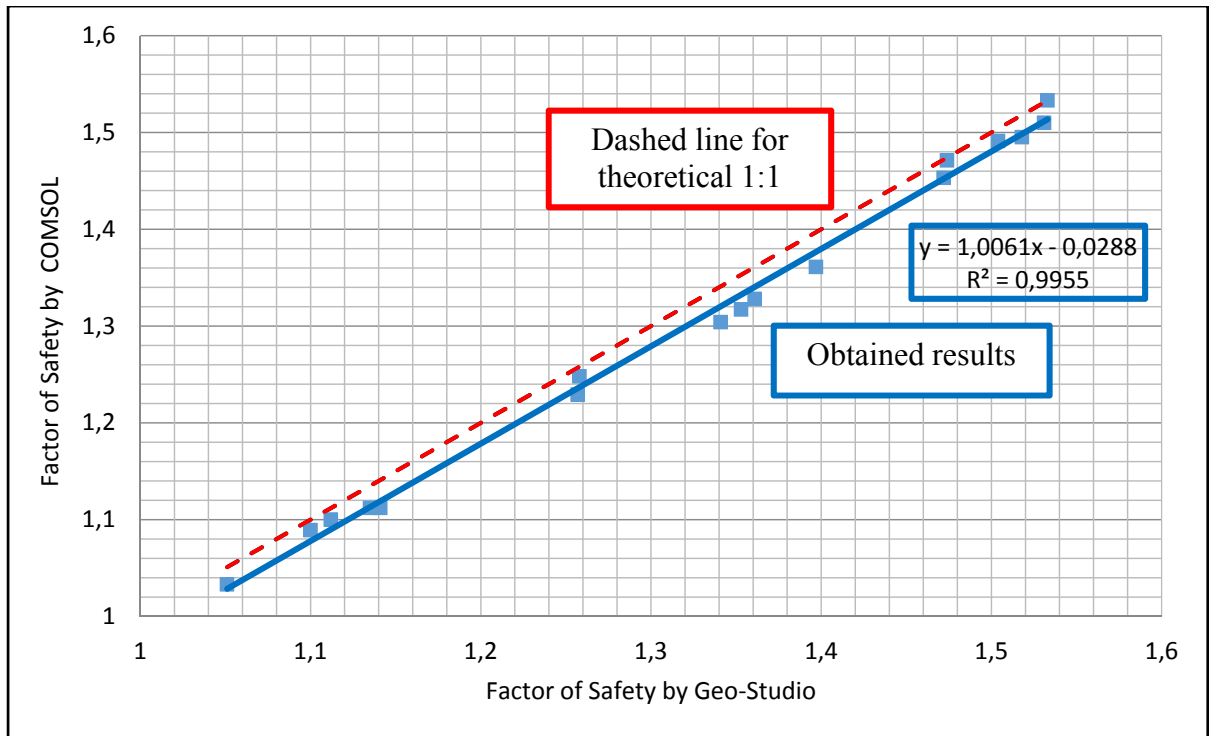
Figure 3.13 Comparison between obtained and ideal factor of safety values with SLOPE/W and COMSOL for layers slope

3.2 General discussion

During the analysis, the influence of some numerical parameters such as mesh size and number of slices was verified. The analyses were done using both very coarse meshes (1.4 m elements) and finer meshes (0.15 m size elements) for SIGMA/W and COMSOL. The results were almost the same thus demonstrating that they were mesh-independent. Analyses conducted with 30 and 60 slices were tested for all models. The results were also the same with no influence on F. The results of FOS for fine-mesh 0.15 m size with different slices numbers are presented in (Appendix IV).

All stability analyses were conducted assuming dry conditions with no effect of pore water pressure. In order to add the pore water pressure in the analysis, the solid mechanics interface shown in Fig 2.3 should be replaced by a poroelasticity interface. Poroelasticity analyses allow Darcy's law to be combined with the solid mechanics interfaces. This feature provides

an interface to define the drained elastic properties of the porous medium, porosity, permeability, and the fluid properties.

The stress distributions obtained with SIGMA/W and COMSOL-MATLAB were similar for all models. In Figures 3.14 to 3.16, the stresses for both SIGMA/W and COMSOL models are almost identical. Figure 3.15 presents a small gap for the slope with benches starting from x = 13 m for σ_y and τ_{xy}. Figure 3.16 shows similar stress distributions for the steep slope except for small differences in σ_y at near the entry and exit of the slip circle, whereas σ_x and τ_{xy} are also identical along the slip surface. It is noticeable that the identical stress distributions for the three first models (uniform, benches, and steep) lead to almost identical F values.
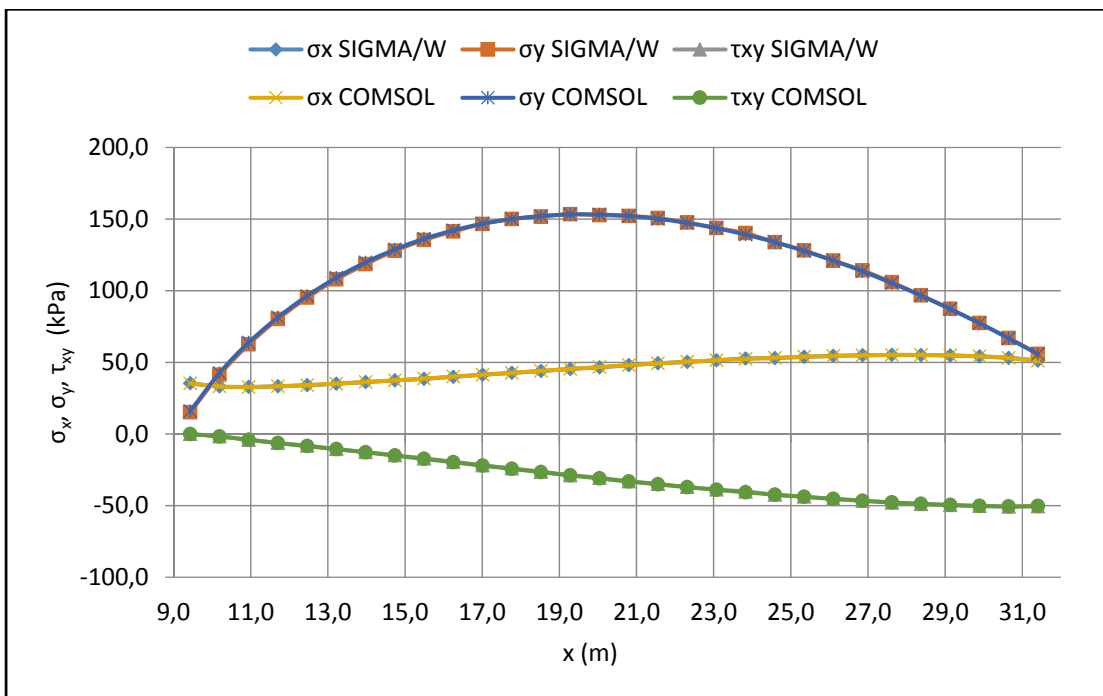
Figure 3.14 Comparisons of σ_x, σ_y, and, τ_{xy} between SIGMA/W
and COMSOL for uniform slope
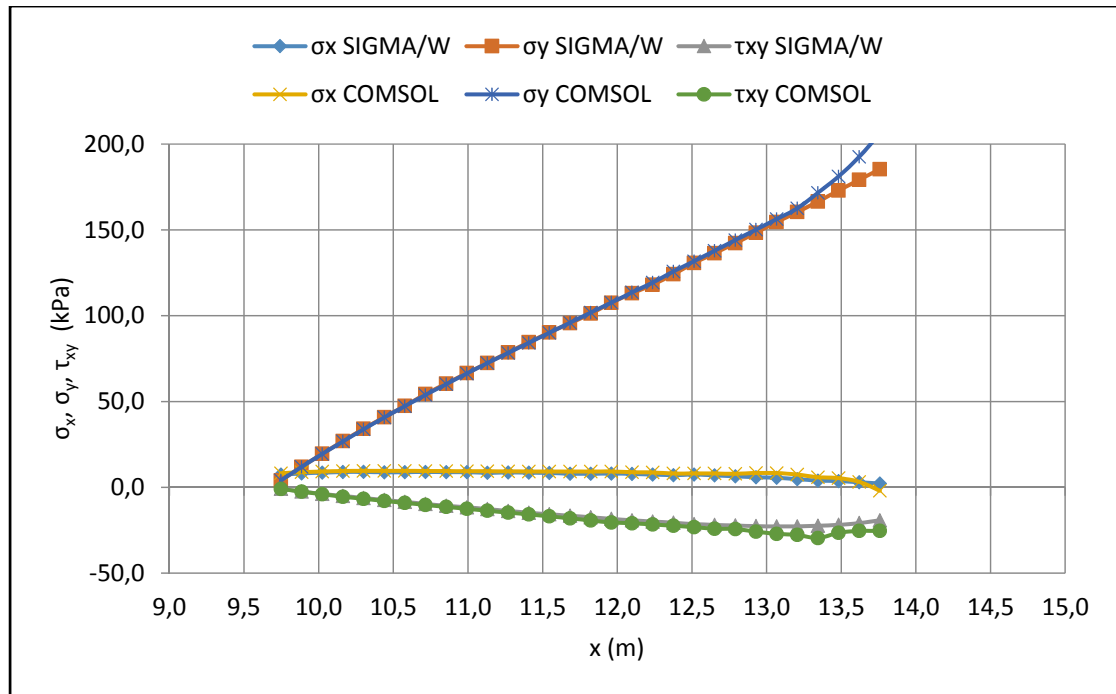
Figure 3.15 Comparisons of σ_x, σ_y, and, τ_{xy} between SIGMA/W
and COMSOL for slope with benches
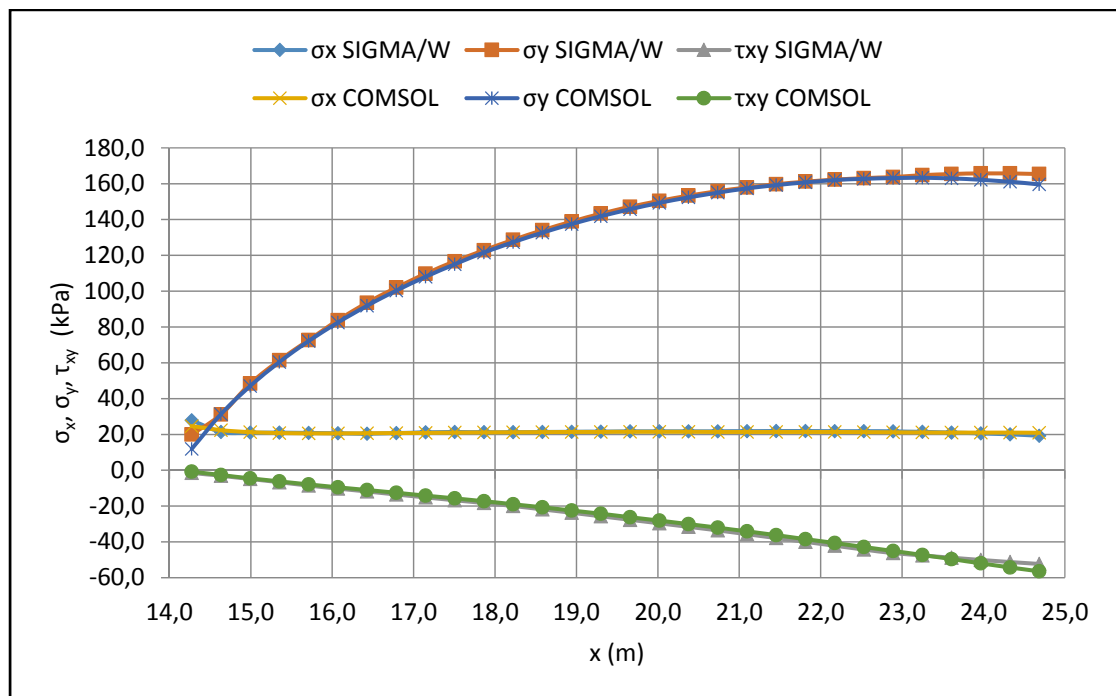
Figure 3.16 Comparisons of σ_x, σ_y, and, τ_{xy} between SIGMA/W
and COMSOL for steep slope

Figure 3.17 shows the comparisons of σ_x, σ_y, and, τ_{xy} between SIGMA/W and COMSOL for the layered soil deposit. The σ_y and τ_{xy} are identical with a small difference for the σ_y starts from the middle of the slope at x = 22 m to bottom of slope. While the differences in τ_{xy} are located between x = 11 m to x = 18 m. The stresses distributions of σ_x are significantly different at the top of the second layer. The difference is between around x = 10 m to x = 16.52 m with maximum difference about 40 kPa. This indicates that the analysis of stresses in a soil body with two materials is conducted differently by the solid mechanics interface in COMSOL and the in situ analysis in SIGMA/W.
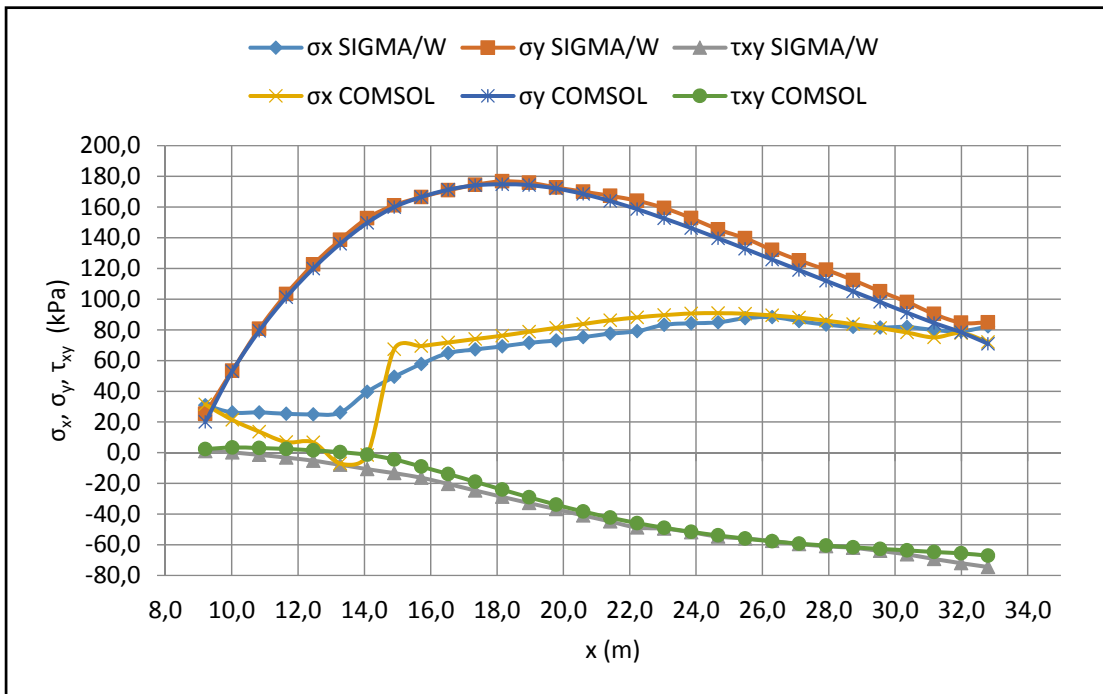
Figure 3.17 Comparisons of σ_x, σ_y, and, τ_{xy} between SIGMA/W and COMSOL for layered deposit slope

In general, the *F* values obtained for the four models with SLOPE/W and COMSOL-MATLAB were consistent. Figure 3.18 shows *F* comparisons for all models. The blue lines represent equal *F* values for SLOPE/W and the COMSOL-MATLAB script. For slopes with a homogeneous soil (a, b, and c), the factor of safety values are very close to the blue line. The difference appears greater for the layered soil deposit. The mean *F* differences between COMSOL-MATLAB and SLOPE/W are 1.1 % for the homogenous slopes and 1.7 % for the layered soil deposit. These differences are due to the gap in stress distributions between SIGMA/W and COMSOL.
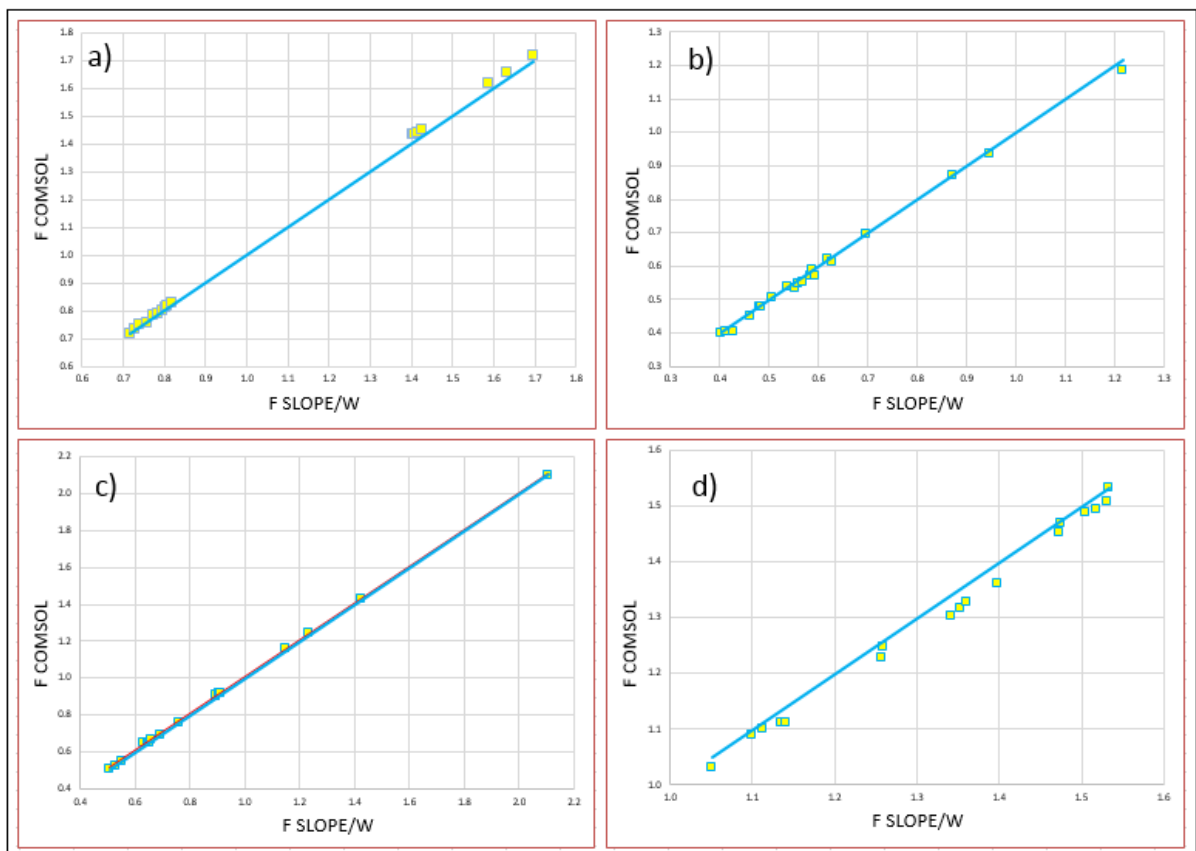
Figure 3.18 Comparisons factor of safety between SLOPE/W and COMSOL-MATLAB
script for a) Uniform slope, b) Slope with benches, c) Steep slope,
d) Layered soil deposit slope

CONCLUSION

This thesis presented a MATLAB code that allows slope stability analyses to be conducted for COMSOL model. The code was designed to use a method based on finite element stresses to analyze the stability of slopes. The code was verified based on four different slope geometries. The results were compared with the stress-based method provided by SLOPE/W and SIGMA/W. The results of factor of safety were highly satisfactory. As a consequence it is now possible to conduct slope stability analyses in COMSOL.

The code is not suitable for classical limit equilibrium methods. In order to use these methods, the code would need some modifications specific to each method. For example, to use the Swedish method, the weight and height of each slice must be computed. In Bishop's method, the horizontal forces for both sides must be considered. All limit equilibrium methods that take into account a circular failure plane can be applied in this code but some changes would have to be applied to the code.

The code currently only considers circular failure plane mechanism. The code can be improved to deal with non-circular mechanism especially in rock failure analysis. In order to do that, several wedges can be assumed (based on the length of the slope) with non-vertical interfaces affected by different forces individually. Also, other failure mechanism could be integrated into the code such as plane failure which would be easy to create and to program to define points along the plane. Such plane failures would be useful for rock slopes.

Finally, using COMSOL as a finite element tool with the ability of MATLAB to compute factor of safety values encourage future research projects on multiphysics modelling in geotechnical engineering, as this is normally the main use of COMSOL. The script will for instance be used in upcoming projects on the geotechnical engineering of Champlain clays in the context of climate change, a truly multiphysics problem.

RECOMMENDATIONS

The results of the MATLAB code proved that it can be used to evaluate the stability of soil slopes. To the author's best knowledge, this is the first code that integrates MATLAB and COMSOL to compute the factor of safety. The code could be modified to model different geotechnical applications. It could also be modified to include different slope stability methods, such as the Swedish Method, Bishop Method, and Morgenstern-Price Method.

One interesting method that could be programmed in future studies is the shear strength reduction method (SRM). The shear strength reduction technique allows the FEM to calculate factors of safety for slopes. The method predicts the stresses and deformation based on reducing the soil strength properties (cohesion and friction angle).

The code can also be modified to take into account pore water pressures. Consideration of the pore water pressure allows the stability to be verified in terms of effective stresses. To work with effective stresses, the expressions associated with the numerical features (e.g., *XStressValues*) should be changed to include the pore pressure variate (e.g., *-solid.sx-p*).

Instead of considering slices for the shear strength and shear stress integration, the integration could also be done directly in COMSOL with an integration coupling. Shear strength and shear stress can be integrated along failure planes defined by COMSOL. This can be done through a node representing an integration coupling.

In general, the code is designed as a tool to assess the stability of slope. Several features and modifications can be added to increase the capability of the code to be used for different applications and complex conditions.

APPENDIX I

MATLAB CODE

```matlab
clear variables
profile on

% Build slip circle matrix ()
CentreX = [36]'; % These values are for critical slip surface (Example)
CentreY = [41]';
Radius  = [29.345]';

% Soil properties (vector if several layers, scalar otherwise).
C_layers   = [5000 25000];
Phi_layers = [31 22];

% Number of slices based on Geo-Studio analysis.
noslice = 30;

% Slip circles matrix contains X, Y, Radius, and safety factor for slip
circle.
SlipCircles = zeros(size(CentreX,1)*size(CentreY,1)*size(Radius,1),4);
m = 1;
for i = 1:size(CentreX,1)
    for j = 1:size(CentreY,1)
        for k = 1:size(Radius,1)
            SlipCircles(m,1) = CentreX(i);
            SlipCircles(m,2) = CentreY(j);
            SlipCircles(m,3) = Radius(k);
            m=m+1;
        end
    end
end

% Variable x1 contains the entire slope body (one layer), in the slope
% with layers geometry model must be changed.
x1=[0,15,35,43,43,0,0];
y1=[30,30,10,10,1,1,30];

% Variable x2 contains the geometry of the soil with the second set of C
and Phi
% parameters in the C_layers and Phi_layers vectors. If there is only one
material,
% these lines should be preceded by "%".
x2=[0,15,24,0,0,0,33,35,43,43,0,0];
y2=[30,30,21,21,30,12,12,10,10,1,1,12];

% COMSOL file is opened. The file name can be changed based on geometry on
COMSOL model.
SlopeStabilityModel = mphload('COMSOL model4d.mph');
```

```matlab
% Create cut points in the COMSOL model where the stresses must be
calculated.
SlopeStabilityModel.result().dataset().create('Point','CutPoint2D');

% The expression to be evaluated for each cut point is defined.
SlopeStabilityModel.result().numerical().create('XStressValues','EvalPoint
');
SlopeStabilityModel.result().numerical().create('YStressValues','EvalPoint
');
SlopeStabilityModel.result().numerical().create('XYStressValues','EvalPoin
t');
SlopeStabilityModel.result().numerical('XStressValues').set('data',
'Point');
SlopeStabilityModel.result().numerical('YStressValues').set('data',
'Point');
SlopeStabilityModel.result().numerical('XYStressValues').set('data',
'Point');
SlopeStabilityModel.result().numerical('XStressValues').set('expr',
'solid.sx');
SlopeStabilityModel.result().numerical('YStressValues').set('expr',
'solid.sy');
SlopeStabilityModel.result().numerical('XYStressValues').set('expr',
'solid.sxy');

% The slope geometry is shown in a figure window.
mapshow(x1,y1)
mphmesh(SlopeStabilityModel)
% Finite element equations are solved.
SlopeStabilityModel.sol('sol1').run();

% For loop for each slip circle
for i=1:size(SlipCircles,1)

    % Define the properties of the failure circle.
    ang=0:0.01:2*pi;
    xc=SlipCircles(i,3)*cos(ang);
    yc=SlipCircles(i,3)*sin(ang);
    mapshow(SlipCircles(i,1)+xc,SlipCircles(i,2)+yc);

    % Find the intersection between geometry and circle.
    [xi,yi] = polyxpoly(x1,y1,SlipCircles(i,1)+xc,SlipCircles(i,2)+yc);

% Calculations are not done for circles that do not touch the slope or
that have more than two intersection points.
    if isempty(xi)
        disp(sprintf('Circle %d does not touch the slope',i))
    elseif size(xi,1)>2
        disp(sprintf('Circle %d has more than two intersection points',i))
    else
% If circle touches the geometry at two points - find max and min values
for x and y.
        xmax = max(xi);
        xmin = min(xi);
```

```matlab
% Slice width.
w = (xmax-xmin)/noslice;


% Determining the starting and ending points at the base of each slice.
    xb  =  xmin+(0:w:noslice*w);
    yb  = -((SlipCircles(i,3).^2-(xb-
    SlipCircles(i,1)).^2).^.5)+SlipCircles(i,2);

% Calculate the midpoint of each slice. The stress components must   be
calculated at the midpoint.
    xm = (xb(1:end-1)+xb(2:end))./2;
    ym  = -((SlipCircles(i,3).^2-(xm-
    SlipCircles(i,1)).^2).^.5)+SlipCircles(i,2);

        % Setting midpoints of each slice as a dataset in COMSOL to solve
        % the finite element analysis and to get the stresses.
        SlopeStabilityModel.result().dataset('Point').set('pointx', xm);
        SlopeStabilityModel.result().dataset('Point').set('pointy', ym);

% Calculate the x,y, and xy stresses at xm and ym points by using COMSOL
Model.
Stress = zeros(3,noslice);
        Stress(1,:)  =  -
SlopeStabilityModel.result().numerical('XStressValues').getReal()';
        Stress(2,:)  =  -
SlopeStabilityModel.result().numerical('YStressValues').getReal()';
        Stress(3,:)  =  -
SlopeStabilityModel.result().numerical('XYStressValues').getReal()';

% Merge the equations elements of normal and shear stresses to make the
calculations.
% of normal and shear stresses more suitable for calculations.
        Newstress1 =  Stress(1,:)+Stress(2,:);
        Newstress2 =  Stress(2,:)-Stress(1,:);
        Newstress3 =  Stress(3,:);

% In case, of more than one layer midpoints must be indicate separately
for each layer, in order to do that the following steps must be done.
% Using inpolygon function to find in and out points.
        if exist('x2','var')
            in = inpolygon(xm,ym,x2,y2);
            % Define C and Phi values based on the layer in which xm and
            ym points are located.
            C         = C_layers(1)*ones(1,noslice);
            Phi       = Phi_layers(1)*ones(1,noslice);
            C(~in)    = C_layers(2);
            Phi(~in) = Phi_layers(2);
        else
            C = C_layers(1)*ones(1,noslice);
            Phi = Phi_layers(1)*ones(1,noslice);
        end
```

```matlab
% The inclination of the base of each slice at am and ym points.
      Theta = atan(-(yb(2:noslice+1) -ym(1:noslice))./(xm(1:noslice)-
      xb(2:noslice+1)))*(180/pi);

% Base Length of the slice with taking into account the inclination of
each slice.
      BaseLength = abs(w./cosd(Theta));

% Calculation normal and shear stresses at xm and ym points.
      Normalstress =  0.5.*Newstress1 + 0.5.*Newstress2.*cosd(2.*Theta)-
      Newstress3.*sind(2.*Theta);
      Shearstress = -0.5.*Newstress2.*sind(2.*Theta)-
      Newstress3.*cosd(2.*Theta);

% Calculation resistance and mobilized shear forces.
      Resistancestress = (C + Normalstress.*tand(Phi));
      Resistanceforce  = sum(BaseLength.*Resistancestress);
      Mobilizedforce   = sum(BaseLength.*Shearstress);

% Calculation factor of safety based on Distribution Stresses Method.
      SlipCircles(i,4) = Resistanceforce / Mobilizedforce;
    end
end

profile viewer
```

APPENDIX II

COMPARISONS OF FINITE ELEMENT STRESSES COMPUTED FROM SIGMA/W AND COMSOL

Table-A II-1 shows comparisons of σ_x, σ_y, and τ_{xy} stresses for critical slip surface of uniform slope for SIGMA/W and COMSOL

| GEO-SLOPE stresses for coordinates X = 34 m, Y = 40 m, R =26.877 m				COMSOL stresses for coordinates X = 34 m, Y = 40 m, R =26.877 m			
x (m)	σ_x (kPa)	σ_y (kPa)	τ_{xy} (kPa)	x (m)	σ_x (kPa)	σ_y (kPa)	τ_{xy} (kPa)
9.431	35.42	15.13	-0.02	9.431	35.29	15.96	-0.1
10.189	33.15	41.30	-1.63	10.189	33.23	42.59	-1.74
10.947	32.85	62.53	-3.97	10.947	32.8	63.81	-4.11
11.705	33.27	80.21	-6.23	11.705	33.29	81.42	-6.36
12.462	34.14	95.18	-8.17	12.462	34.14	96.38	-8.48
13.22	35.06	107.9	-10.47	13.22	35.15	109.14	-10.62
13.978	36.22	118.49	-12.62	13.978	36.31	119.8	-12.85
14.736	37.39	127.87	-14.82	14.736	37.48	128.83	-15.1
15.493	38.49	135.41	-17	15.493	38.72	136.27	-17.39
16.251	39.92	141.34	-19.37	16.251	40.07	142.1	-19.72
17.009	41.32	146.59	-21.83	17.009	41.35	146.8	-22.04
17.767	42.64	149.97	-24.01	17.767	42.73	150.02	-24.34
18.524	43.91	151.7	-26.31	18.524	44.06	152.18	-26.62
19.282	45.38	153.37	-28.75	19.282	45.35	153.27	-28.86
20.04	46.49	152.67	-30.58	20.04	46.74	153.14	-31.02
20.798	48	152.17	-33.03	20.798	48	152.24	-33.16
21.555	49.34	150.71	-34.83	21.555	49.28	150.17	-35.16
22.313	50.30	147.56	-36.91	22.313	50.42	147.37	-37.11
23.071	51.38	143.81	-38.77	23.071	51.47	143.67	-38.97
23.829	52.62	140.16	-40.16	23.829	52.43	139.13	-40.71
24.586	52.95	133.82	-42.30	24.586	53.22	133.92	-42.4
25.344	53.85	128.09	-43.69	25.344	53.94	127.79	-43.91
26.102	54.55	121.03	-45.28	26.102	54.45	121.07	-45.36
26.86	55.01	114.16	-46.49	26.86	54.91	113.54	-46.64
27.617	55.15	105.87	-47.82	27.617	55.17	105.37	-47.78
28.375	55.14	96.78	-48.84	28.375	55.16	96.61	-48.79
29.133	54.76	87.31	-49.57	29.133	54.86	87.18	-49.59
29.891	54.18	77.39	-50.21	29.891	54.17	77.32	-50.24
30.648	53.12	66.94	-50.63	30.648	53.1	66.72	-50.55
31.406	51.23	55.91	-50.42	31.406	51.11	55.77	-50.24

66
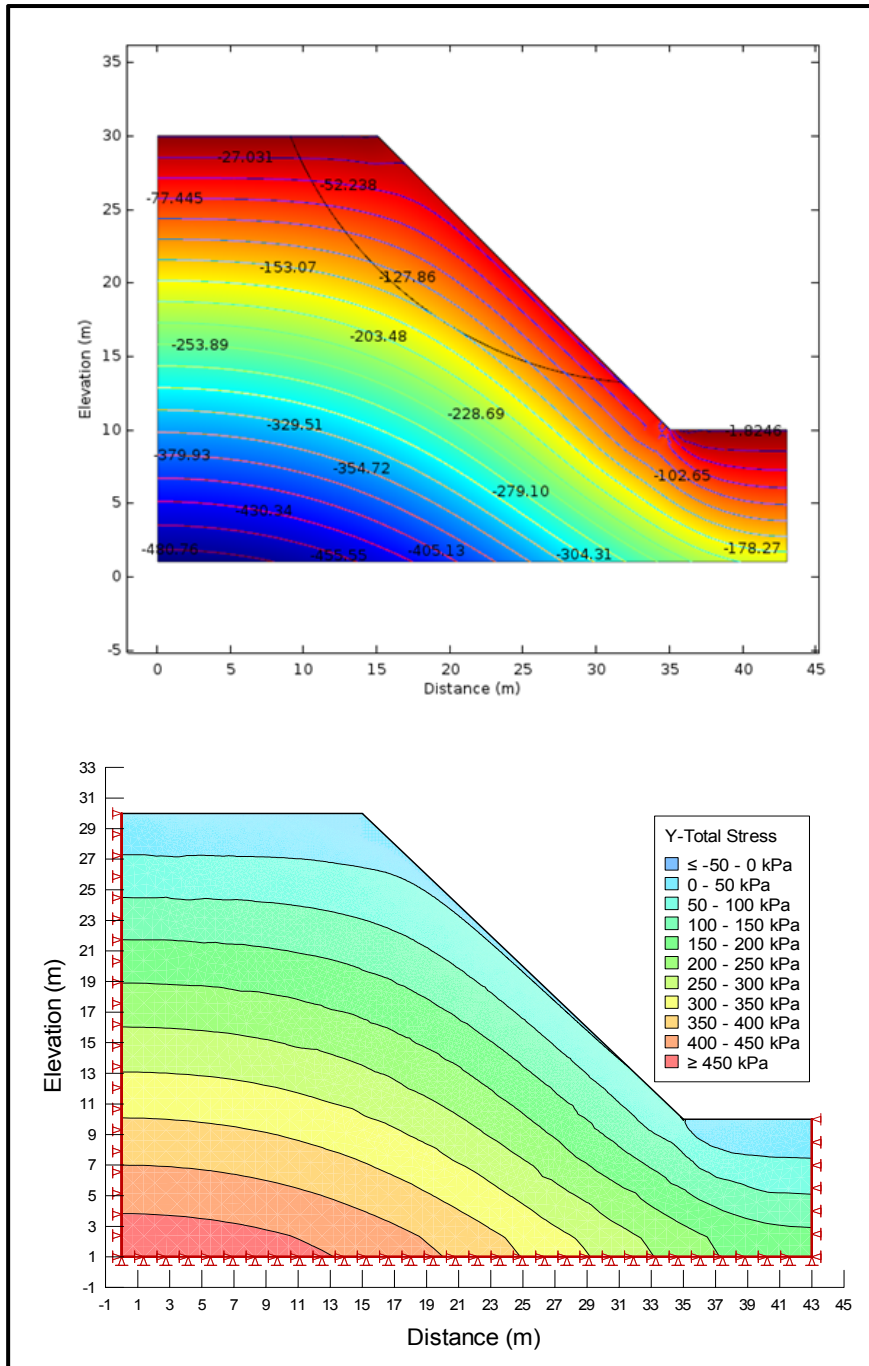
Figure-A II-1 Comparison of σ_y in uniform slope in COMSOL
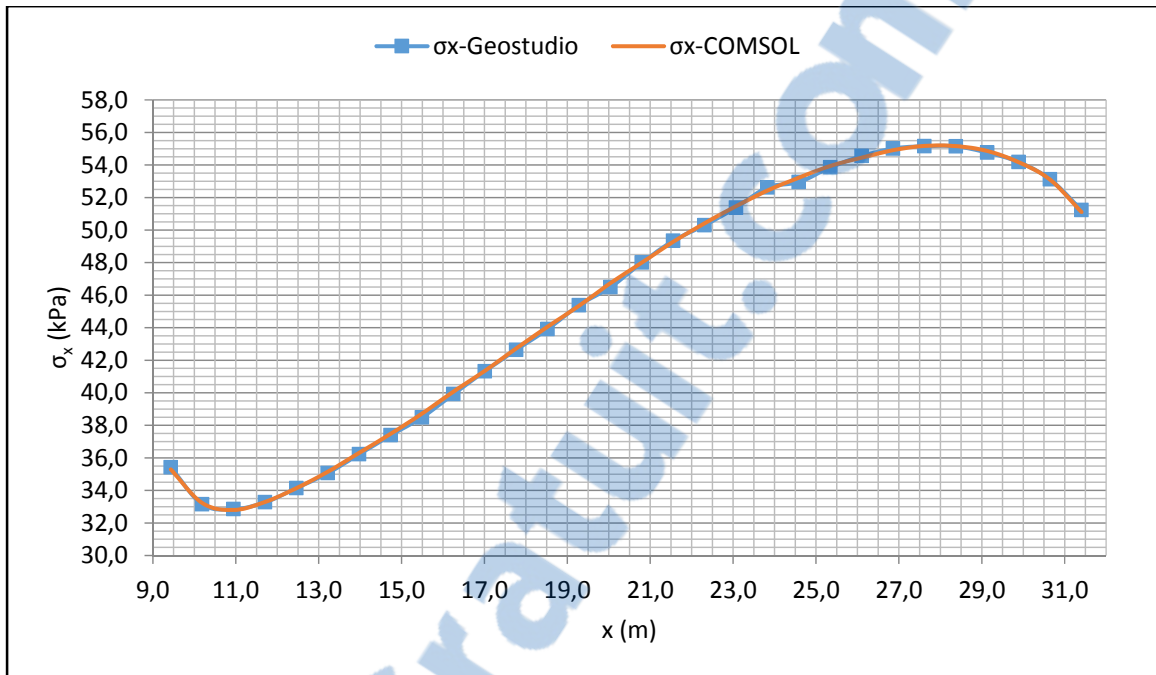and SIGMA/W via numerical models

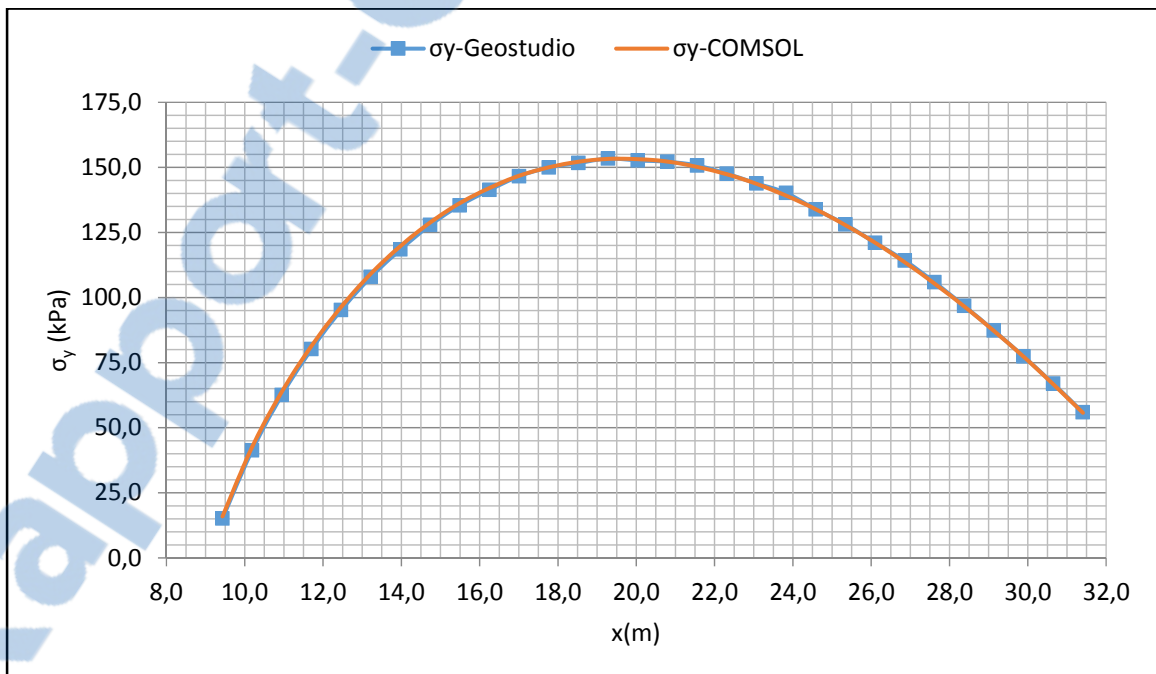Figure-A II-2 σ_x for uniform slope between COMSOL and SIGMA/W

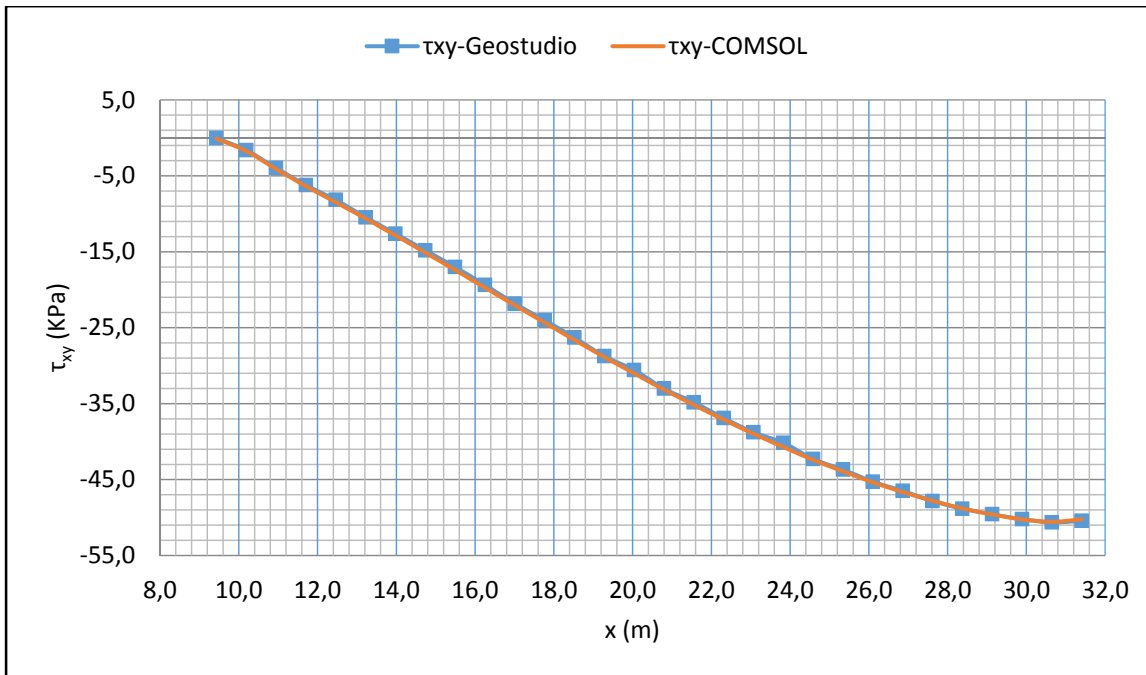Figure-A II-3 σ_y for uniform slope between COMSOL and SIGMA/W

Figure-A II-4 τ_{xy} for uniform slope between COMSOL and SIGMA/W

Table-A II-2 shows comparisons of σ_x, σ_y, and τ_{xy} stresses for critical slip surface of benches slope for SIGMA/W and COMSOL

| GEO-SLOPE stresses for coordinates X = 36 m, Y = 47 m, R =27.511 m				COMSOL stresses for coordinates X = 36 m, Y = 47 m, R =27.511 m			
x (m)	σ_x (kPa)	σ_y (kPa)	τ_{xy} (kPa)	x (m)	σ_x (kPa)	σ_y (kPa)	τ_{xy} (kPa)
9.747	7.432	4	-0.86	9.747	8.214	4.03	-0.95
9.885	8.074	11.902	-2.431	9.885	8.809	11.9	-2.52
10.024	8.579	19.575	-3.809	10.024	9.218	19.5	-4.04
10.162	8.920	26.949	-5.046	10.162	9.477	26.7	-5.52
10.3	8.98	34.067	-6.247	10.3	9.589	33.8	-6.69
10.439	8.774	40.813	-7.401	10.439	9.609	40.7	-7.91
10.577	8.795	47.434	-8.516	10.577	9.586	47.3	-9.09
10.715	8.977	54.3	-9.677	10.715	9.518	53.8	-10.24
10.854	8.882	60.443	-10.75	10.854	9.468	60.1	-11.38
10.992	8.817	66.583	-11.65	10.992	9.423	66.3	-12.52
11.13	8.487	72.429	-12.721	11.13	9.371	72.4	-13.64
11.269	8.652	78.587	-13.807	11.269	9.305	78.3	-14.73
11.407	8.556	84.532	-14.799	11.407	9.227	84.17	-15.79
11.545	8.402	90.221	-15.705	11.545	9.177	90.04	-16.91
11.684	7.92	95.611	-16.567	11.684	9.211	95.97	-18.09
11.822	7.901	101.2	-17.484	11.822	9.232	101.84	-19.28
11.96	8.028	107.45	-18.425	11.96	9.239	107.65	-20.49
12.099	7.817	113.08	-19.231	12.099	8.834	113.6	-20.96
12.237	7.443	118.03	-19.939	12.237	8.64	119.33	-21.68
12.376	7.094	124.17	-20.645	12.376	8.06	125.77	-22.35
12.514	7.477	130.74	-21.437	12.514	8.09	131.75	-23.23
12.652	7.003	136.42	-21.894	12.652	8.05	137.87	-24.16
12.791	6.381	142.28	-22.236	12.791	7.92	144.06	-24.32
12.929	5.871	148.35	-22.625	12.929	8.36	150.15	-25.82
13.067	5.574	154.54	-22.803	13.067	8.31	156.31	-27.11
13.206	4.771	160.42	-22.742	13.206	7.41	162.59	-27.74
13.344	3.929	166.5	-22.386	13.344	5.89	171.64	-29.55
13.482	3.642	172.95	-21.88	13.482	5.35	181.13	-26.49
13.621	2.933	179.22	-20.844	13.621	3.19	192.64	-25.41
13.759	2.193	185.38	-19.245	13.759	-2	206.28	-25.39
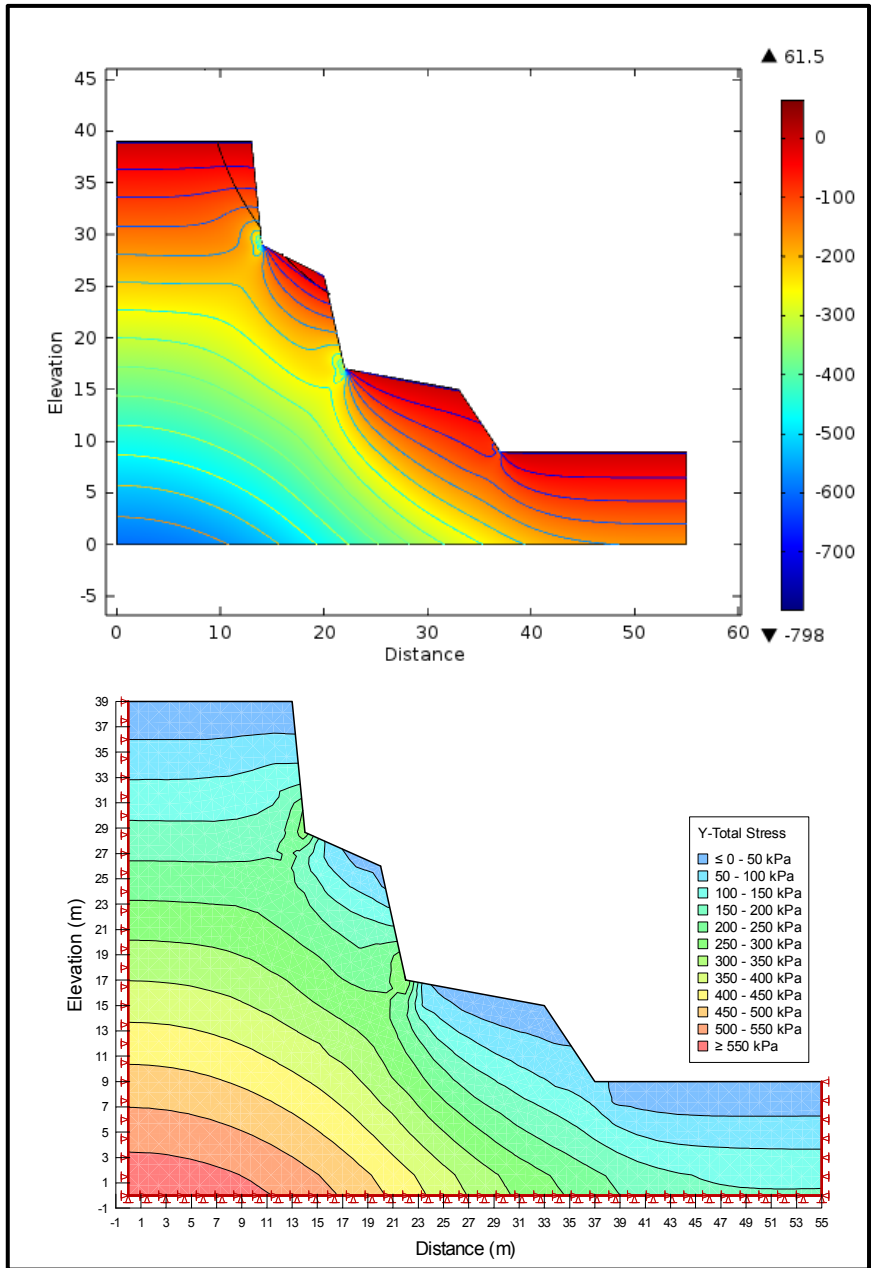
Figure-A II-5 Comparison of σ_y in benches slope in COMSOL
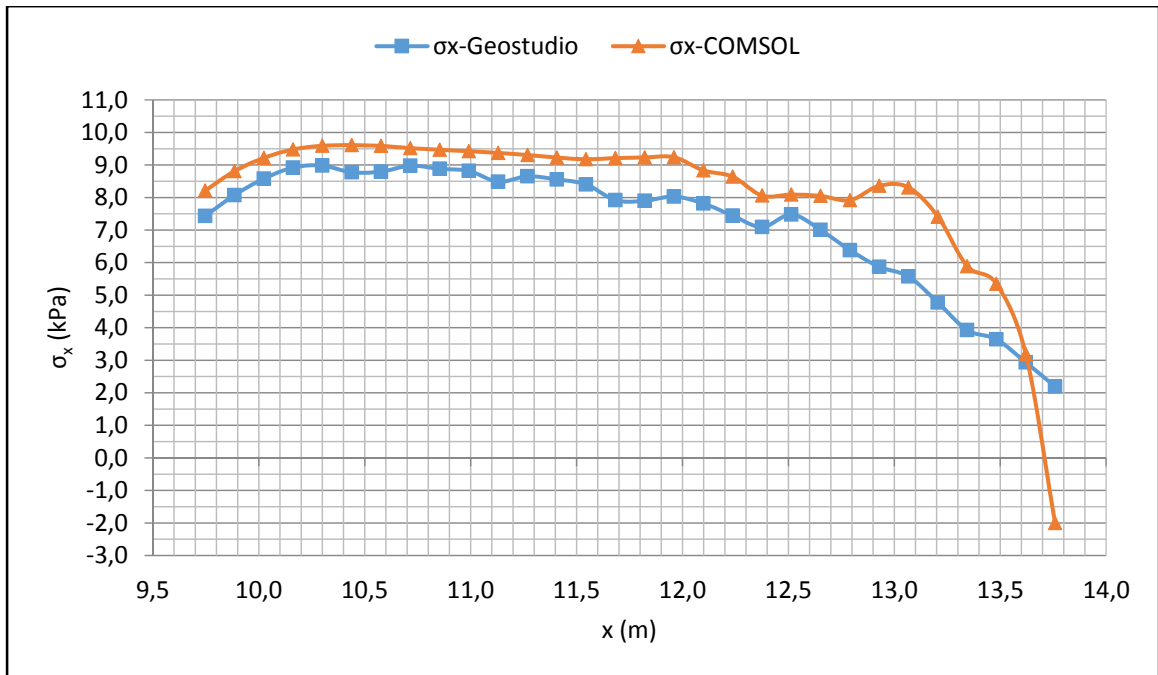and SIGMA/W via numerical models

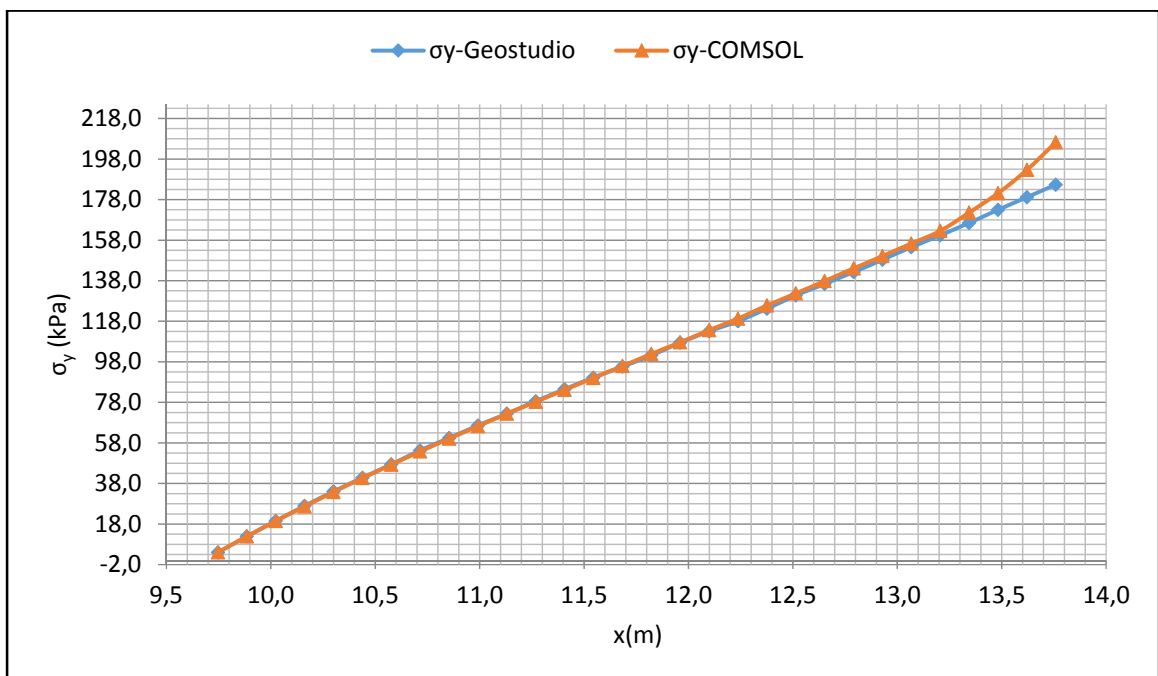Figure-A II-6 σ_x for benches slope between COMSOL and SIGMA/W

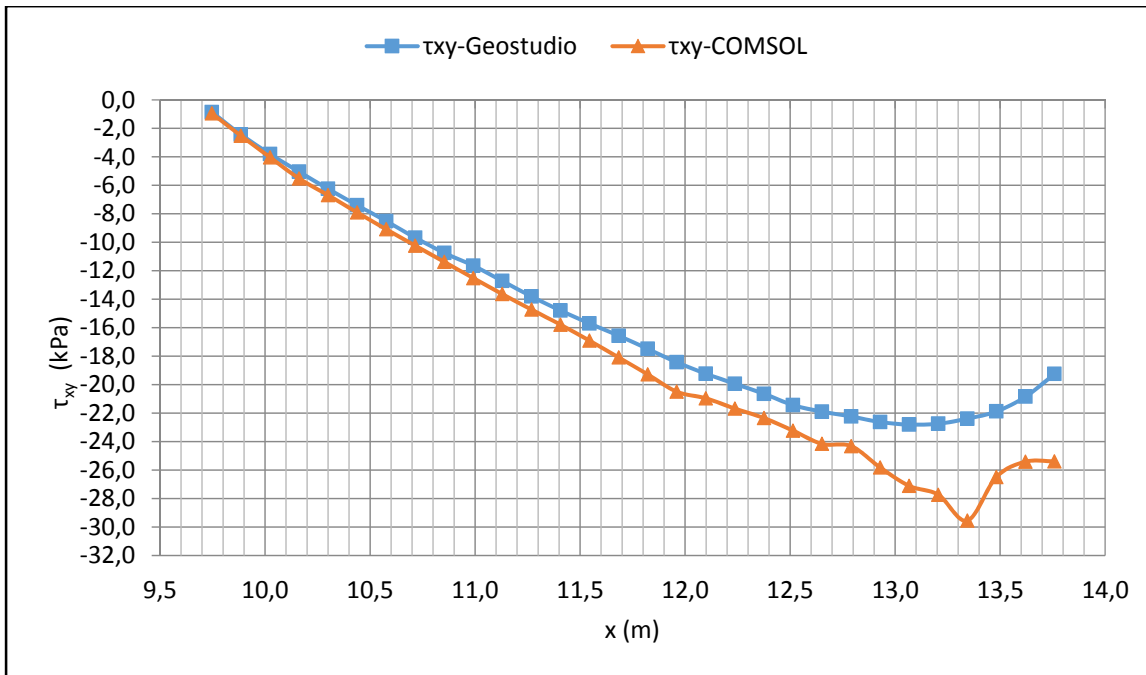Figure-A II-7 σ_y for benches slope between COMSOL and SIGMA/W

Figure-A II-8 τ_{xy} for benches slope between COMSOL and SIGMA/W

Table-A II-3 shows comparisons of σ_x, σ_y, and τ_{xy} stresses for critical slip surface of steep slope for SIGMA/W and COMSOL

| GEO-SLOPE stresses for coordinates X = 34 m, Y = 40 m, R =20.524 m				COMSOL stresses for coordinates X = 34 m, Y = 40 m, R =20.524 m			
x (m)	σ_x (kPa)	σ_y (kPa)	τ_{xy} (kPa)	x (m)	σ_x (kPa)	σ_y (kPa)	τ_{xy} (kPa)
14.274	27.91	19.98	-1.51	14.274	24.65	11.88	-0.8
14.633	21.43	31.12	-3.06	14.633	22.41	31.31	-2.65
14.992	21	48.34	-4.91	14.992	21.3	47.06	-4.51
15.351	21.02	61.38	-6.71	15.351	20.79	60.44	-6.25
15.71	20.86	72.68	-8.58	15.71	20.58	72.14	-7.91
16.069	20.64	83.77	-10.27	16.069	20.56	82.51	-9.5
16.428	20.44	93.51	-11.88	16.428	20.64	91.86	-11.05
16.787	20.77	101.97	-13.54	16.787	20.76	100.34	-12.58
17.146	21.19	109.71	-15.18	17.146	20.88	108.03	-14.13
17.505	21.35	116.66	-16.74	17.505	20.99	115.05	-15.71
17.864	21.27	122.82	-18.31	17.864	21.08	121.58	-17.3
18.223	21.26	128.67	-19.96	18.223	21.2	127.35	-18.99
18.582	21.39	134.01	-21.84	18.582	21.29	132.67	-20.69
18.941	21.51	138.86	-23.76	18.941	21.36	137.48	-22.47
19.3	21.58	143.31	-25.69	19.3	21.41	141.87	-24.3
19.659	21.71	147.11	-27.71	19.659	21.49	145.75	-26.2
20.018	21.77	150.43	-29.66	20.018	21.47	149.3	-28.09
20.377	21.78	153.33	-31.56	20.377	21.46	152.35	-30.05
20.736	21.79	155.85	-33.55	20.736	21.43	155.01	-32.06
21.095	21.87	157.92	-35.73	21.095	21.38	157.4	-34.09
21.454	21.91	159.69	-37.88	21.454	21.41	159.26	-36.26
21.813	21.89	161.17	-40.01	21.813	21.42	160.76	-38.45
22.172	21.88	162.29	-42.151	22.172	21.35	162.02	-40.64
22.531	21.85	163.1	-44.28	22.531	21.32	162.75	-42.86
22.89	21.74	163.76	-46.26	22.89	21.24	163.17	-45.09
23.249	21.45	164.76	-47.59	23.249	21.08	163.34	-47.29
23.608	21.06	165.44	-48.85	23.608	21.06	162.96	-49.6
23.967	20.61	165.75	-50.09	23.967	21.07	162.19	-51.97
24.326	20.01	165.73	-51.25	24.326	21	161.1	-54.26
24.685	19.27	165.4	-52.33	24.685	20.92	159.6	-56.45
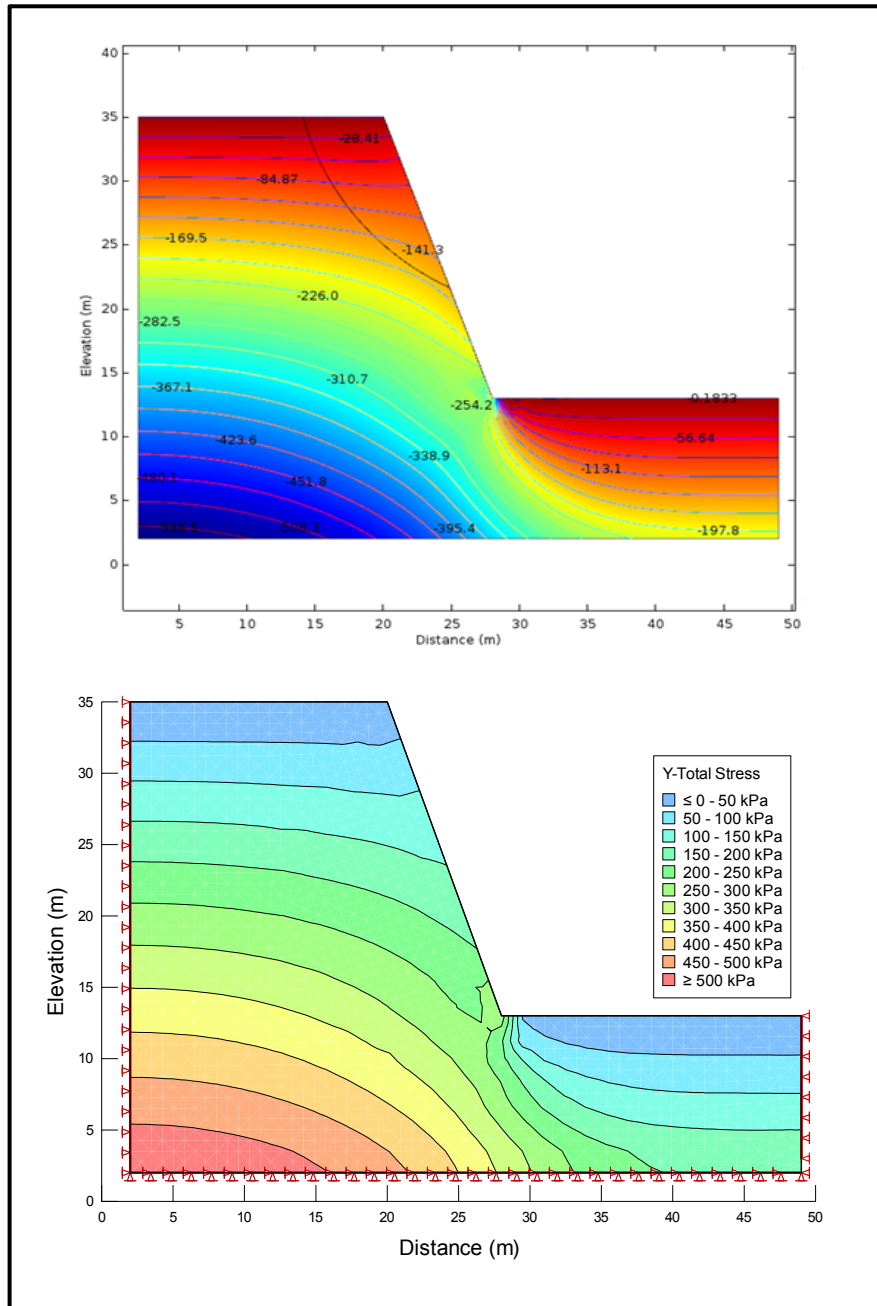
Figure-A II-9 Comparison of σ_y in steep slope in COMSOL
and SIGMA/W via numerical models
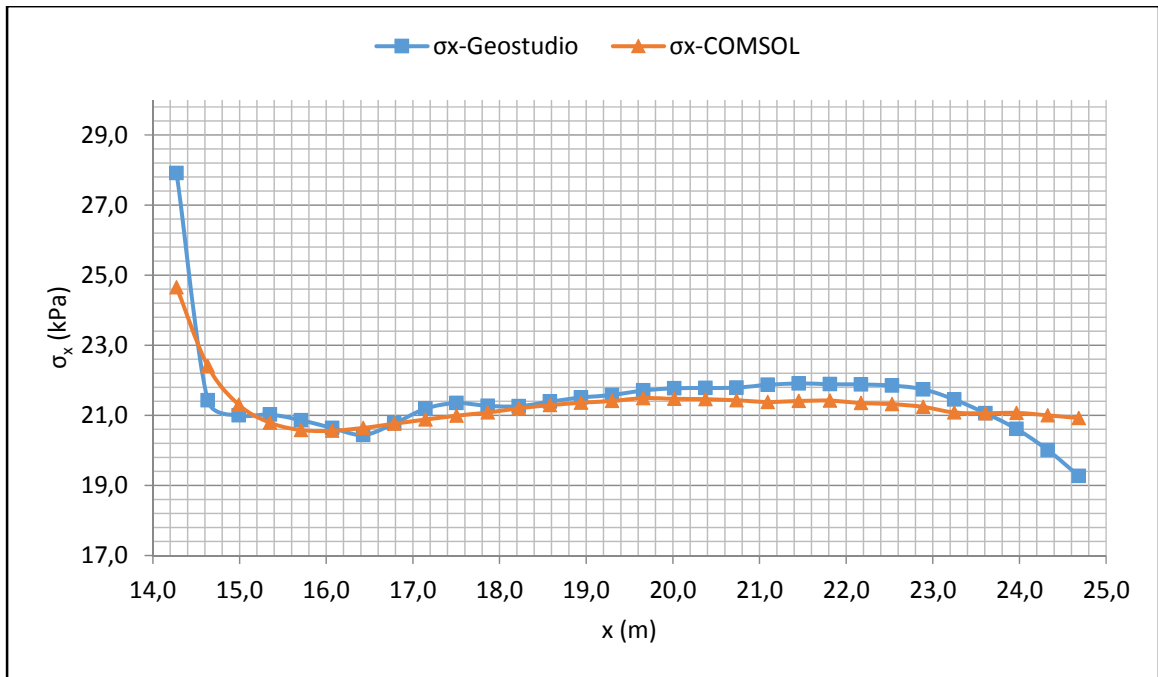
Figure-A II-10 σ_x for steep slope between COMSOL and SIGMA/W
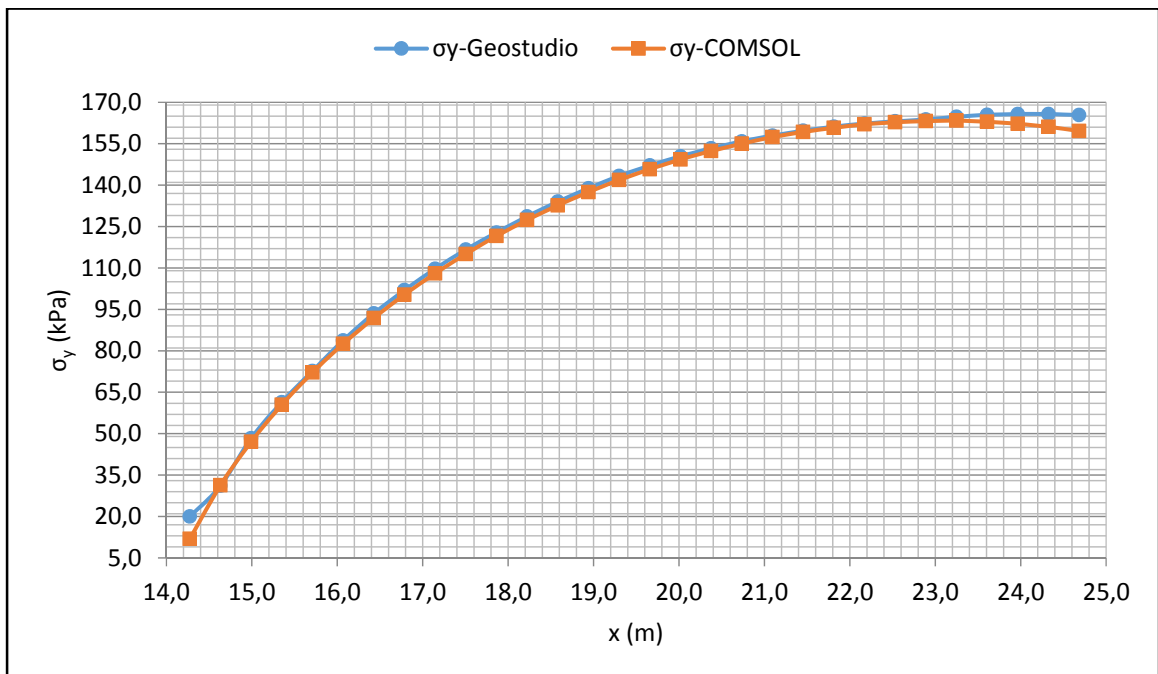
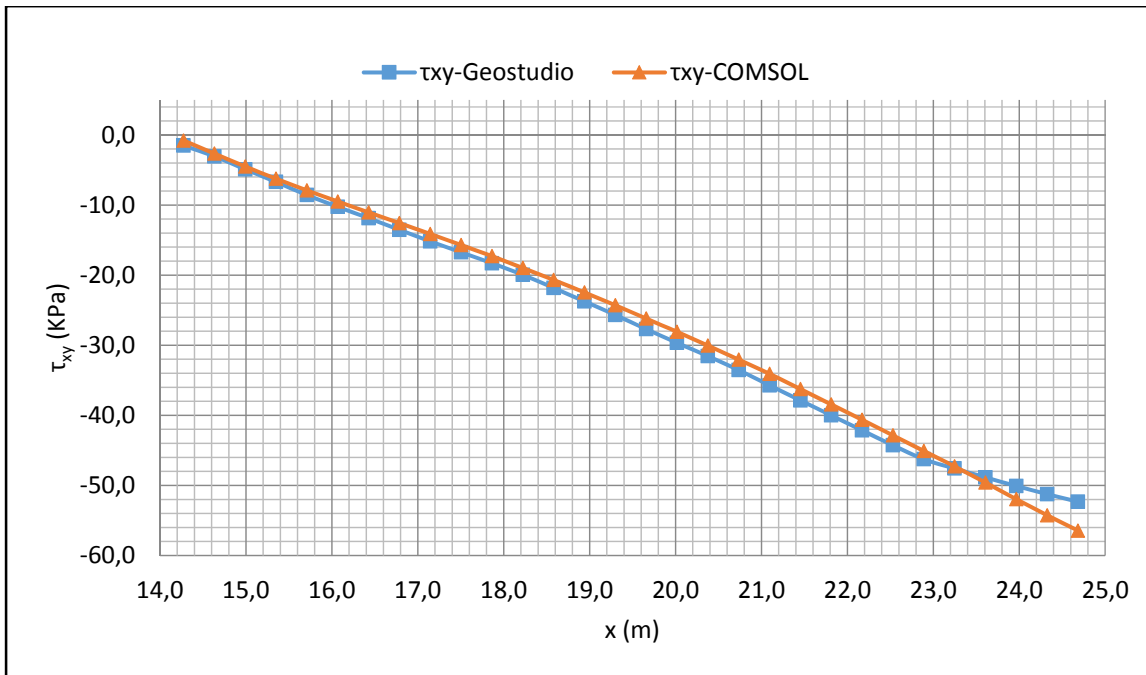Figure-A II-11 σ_y for steep slope between COMSOL and SIGMA/W

Figure-A II-12 τ_{xy} for steep slope between COMSOL and SIGMA/W

Table-A II-4 shows comparisons of σ_x, σ_y, and τ_{xy} stresses for critical slip surface of layers slope for SIGMA/W and COMSOL

| GEO-SLOPE stresses for coordinates X = 36 m, Y = 41 m, R =29.345 m				COMSOL stresses for coordinates X = 36 m, Y = 41 m, R =29.345 m			
x (m)	σ_x (kPa)	σ_y (kPa)	τ_{xy} (kPa)	x (m)	σ_x (kPa)	σ_y (kPa)	τ_{xy} (kPa)
9.202	30.93	25.36	0.93	9.202	31.45	20.04	2.36
10.015	26.22	53.43	0.18	10.015	21.37	53.01	3.39
10.829	26.23	80.68	-1.43	10.829	13.71	79.34	3.03
11.643	25.34	103.35	-3.19	11.643	6.92	101.25	2.39
12.457	24.93	122.61	-5.24	12.457	6.71	119.92	1.53
13.271	26.14	138.67	-7.87	13.271	-7.08	136.06	0.33
14.085	39.61	152.78	-10.74	14.085	-1.52	149.75	-1.3
14.899	49.39	161.11	-13.32	14.899	67.4	159.96	-4.42
15.713	57.82	166.47	-16.31	15.713	69.46	166.53	-9.07
16.527	64.87	170.93	-20.36	16.527	71.72	171.32	-13.92
17.34	67.23	174.51	-24.63	17.34	74.03	174.16	-18.95
18.154	69.26	176.77	-28.78	18.154	76.23	174.86	-24.08
18.968	71.55	175.82	-32.84	18.968	78.82	174.34	-29.08
19.782	73.08	172.76	-36.81	19.782	81.33	172.1	-33.88
20.596	75.28	170.07	-40.92	20.596	83.82	168.56	-38.34
21.41	77.54	167.33	-44.84	21.41	86.24	163.95	-42.32
22.224	79.13	164.13	-48.78	22.224	88.14	158.64	-45.89
23.038	83.29	159.38	-49.49	23.038	89.62	152.58	-48.97
23.852	84.27	152.84	-51.86	23.852	90.66	146.3	-51.58
24.666	84.91	145.41	-54.68	24.666	90.9	139.65	-53.91
25.479	87.58	139.66	-55.94	25.479	90.47	132.82	-55.94
26.293	88.31	132.11	-57.535	26.293	89.44	125.86	-57.73
27.107	85.73	125.24	-59.62	27.107	87.97	118.92	-59.24
27.921	83.41	119.18	-60.97	27.921	86.05	112	-60.54
28.735	81.93	112.44	-62	28.735	83.73	105.04	-61.67
29.549	81.50	105.09	-63.99	29.549	81.18	98.17	-62.69
30.363	81.86	98.15	-66.29	30.363	78.28	91.26	-63.65
31.177	79.91	90.35	-69.26	31.177	75.1	84.49	-64.66
31.991	79.13	84.65	-71.98	31.991	77.93	78.45	-65.58
32.805	82.23	84.88	-74.49	32.805	72.06	70.92	-67.06
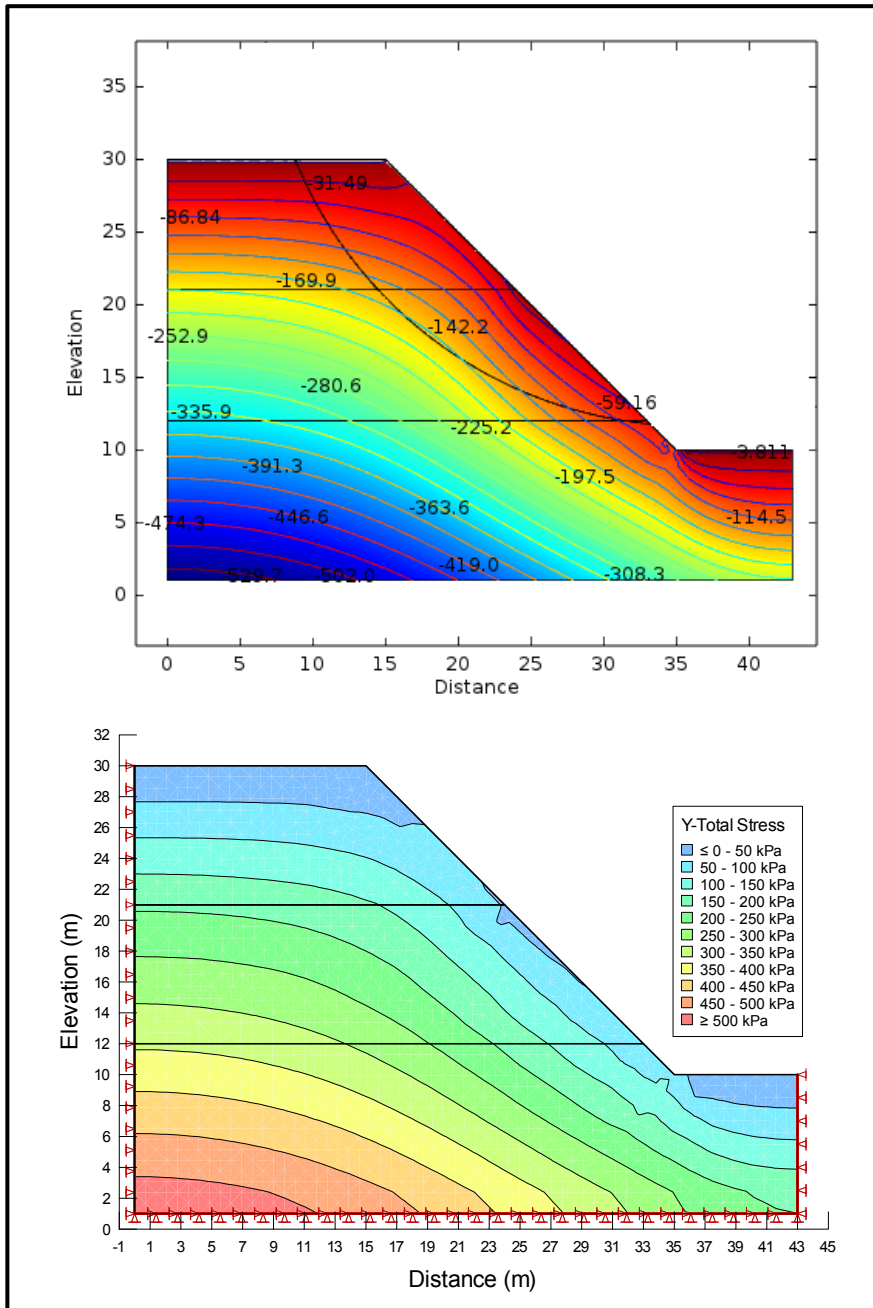
Figure-A II-13 Comparison of σ_y in layers slope in COMSOL
and SIGMA/W via numerical models
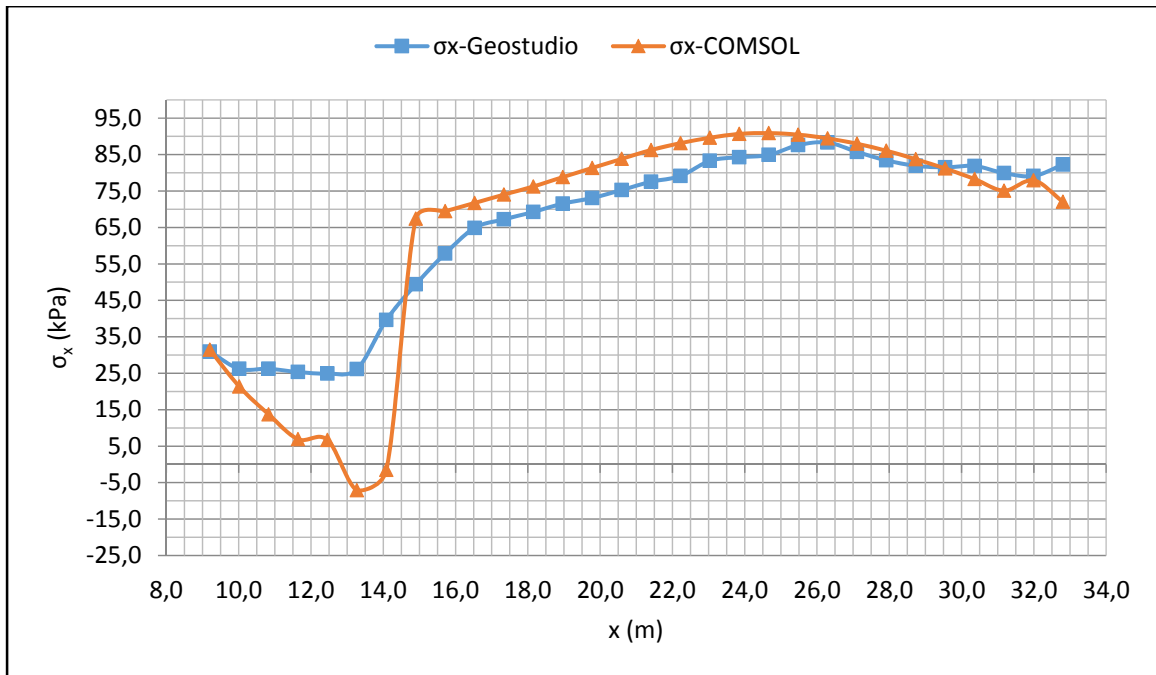
Figure-A II-14 σ_x for layers slope between COMSOL and SIGMA/W
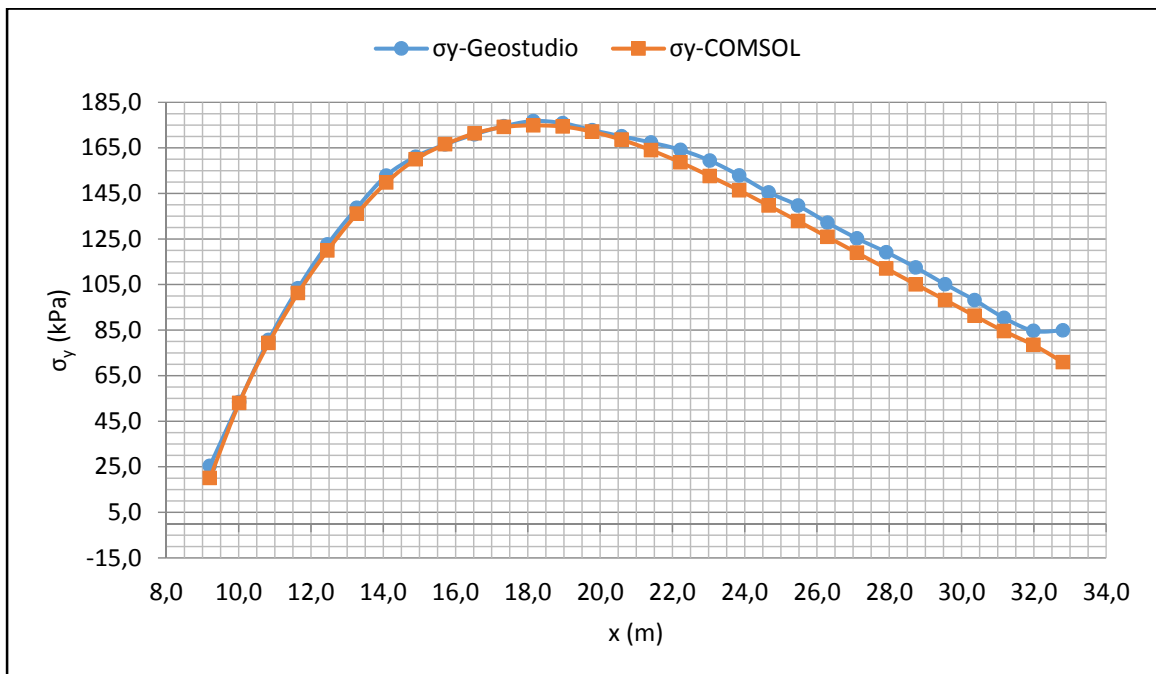
Figure-A II-15 σ_y for layers slope between COMSOL and SIGMA/W
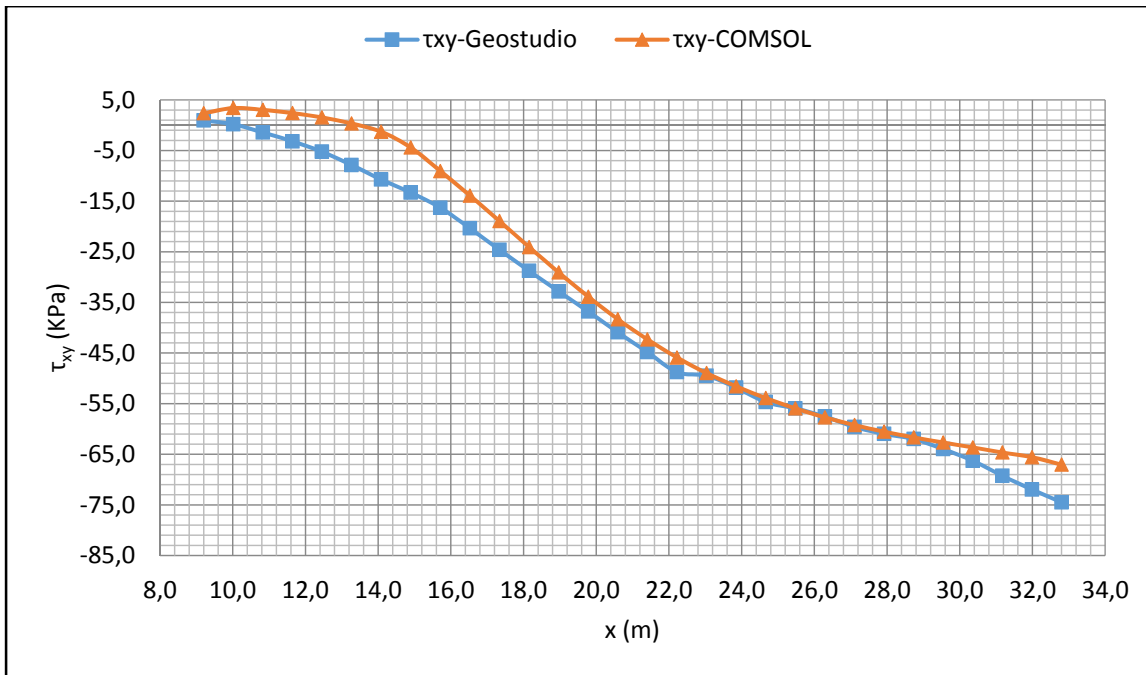
Figure-A II-16 τ_{xy} for layers slope between COMSOL and SIGMA/W

APPENDIX III

COMPARISONS OF FACTOR OF SAFETY BETWEEN SLOPE/W AND COMSOL

Table-A III-1 factors of safety values by SLOPE/W and COMSOL in uniform slope

Slip #	F by SLOPE/W	F by COMSOL
6	0.717	0.718
7	0.728	0.731
8	0.742	0.747
9	0.759	0.756
1	0.776	0.780
2	0.786	0.790
3	0.796	0.801
10	0.803	0.809
4	0.808	0.814
5	0.82	0.826
19	1.405	1.434
18	1.409	1.434
17	1.416	1.438
16	1.429	1.447
13	1.588	1.614
12	1.634	1.654
11	1.696	1.713
14	Passing the slope limits	N/A
15	Passing the slope limits	N/A
20	Passing the slope limits	N/A

Figure-A III-1 Comparisons of factor of safety between SLOPE/W and
COMSOL-MATLAB script for uniform slope

Table-A III-2 factors of safety values by SLOPE/W and COMSOL in benches slope

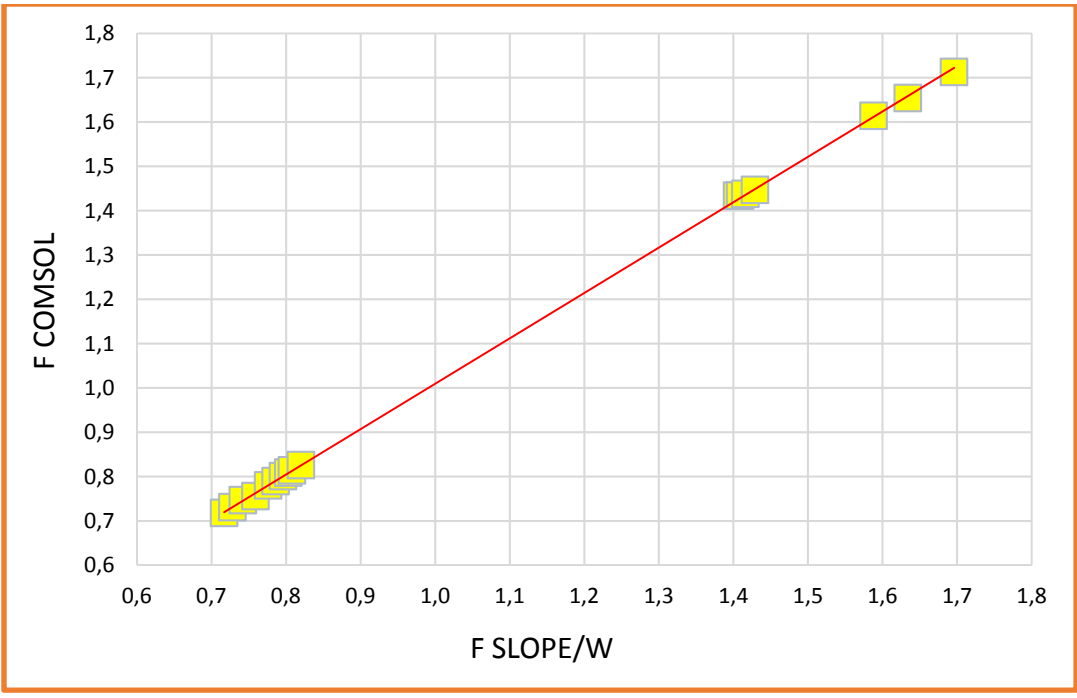| Slip #	F by SLOPE/W	F by COMSOL
2	0.403	0.402
7	0.407	0.478
17	0.413	0.403
8	0.461	0.450
4	0.479	0.478
3	0.485	0.480
13	0.505	0.506
12	0.538	0.539
18	0.551	0.533
5	0.561	0.548
19	0.566	0.551
20	0.583	0.571
14	0.586	0.590
9	0.595	0.570
15	0.617	0.621
10	0.625	0.612
1	0.697	0.695
11	0.873	0.874
6	0.951	0.939
16	1.216	1.186

Figure-A III-2 Comparisons of factor of safety between SLOPE/W and
COMSOL-MATLAB script for benches slope

Table-A III-3 factors of safety values by SLOPE/W and COMSOL in steep slope

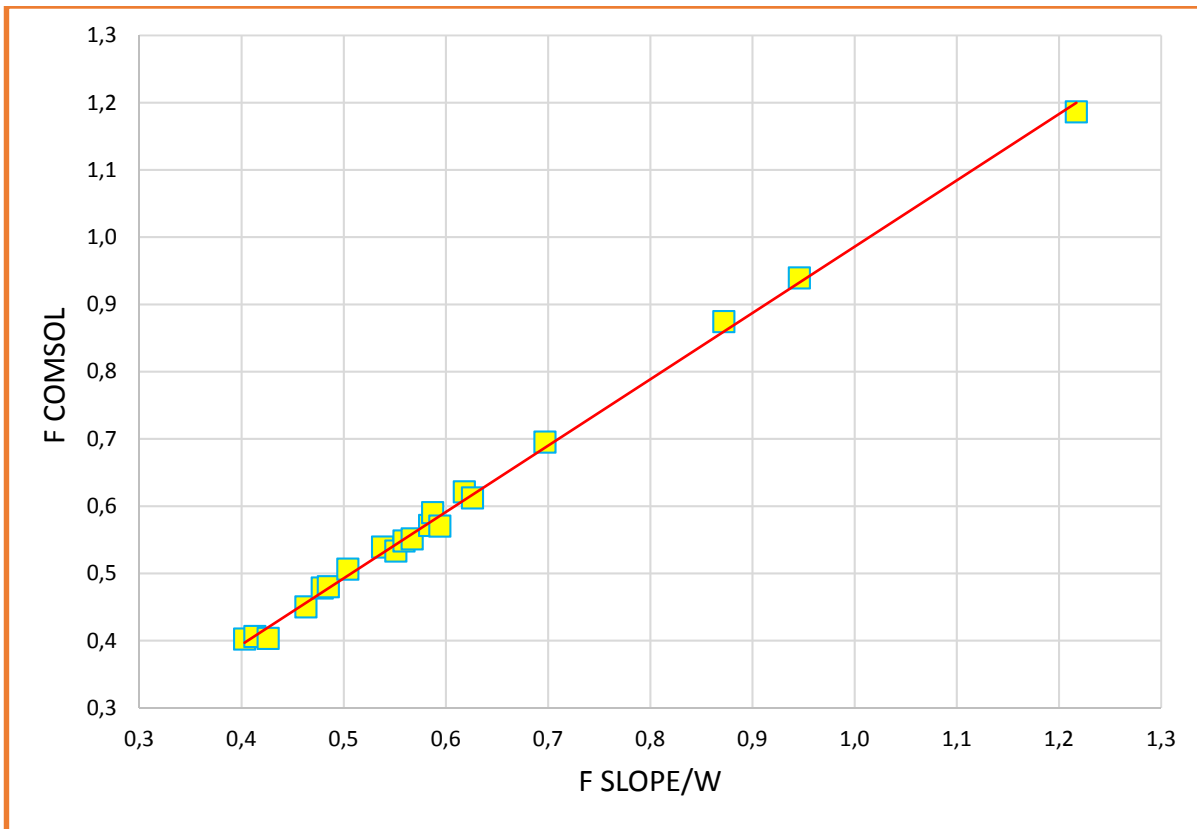| Slip #	F by SLOPE/W	F by COMSOL
6	0.508	0.507
7	0.531	0.528
8	0.556	0.554
9	0.634	0.629
3	0.646	0.648
4	0.66	0.664
2	0.653	0.653
5	0.659	0.554
1	0.693	0.692
10	0.757	0.760
18	0.895	0.9
17	0.893	0.901
19	0.896	0.907
20	0.904	0.916
16	0.917	0.916
15	1.142	1.159
14	1.234	1.24
13	1.424	1.431
12	2.105	2.101
11	Circle does not touch slope	Circle does not touch slope
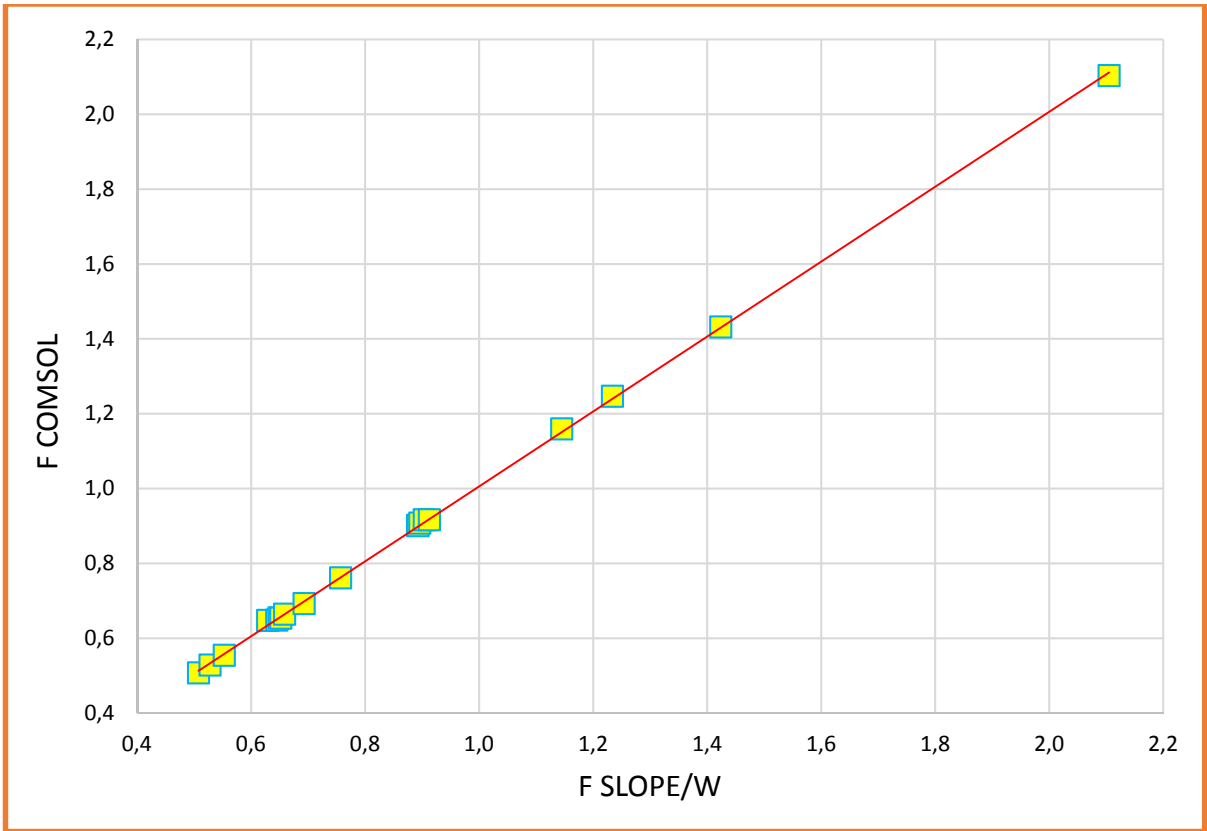
Figure-A III-3 Comparisons of factor of safety between SLOPE/W and
COMSOL-MATLAB script for steep slope

Table-A III-4 factors of safety values by SLOPE/W and COMSOL in layers slope

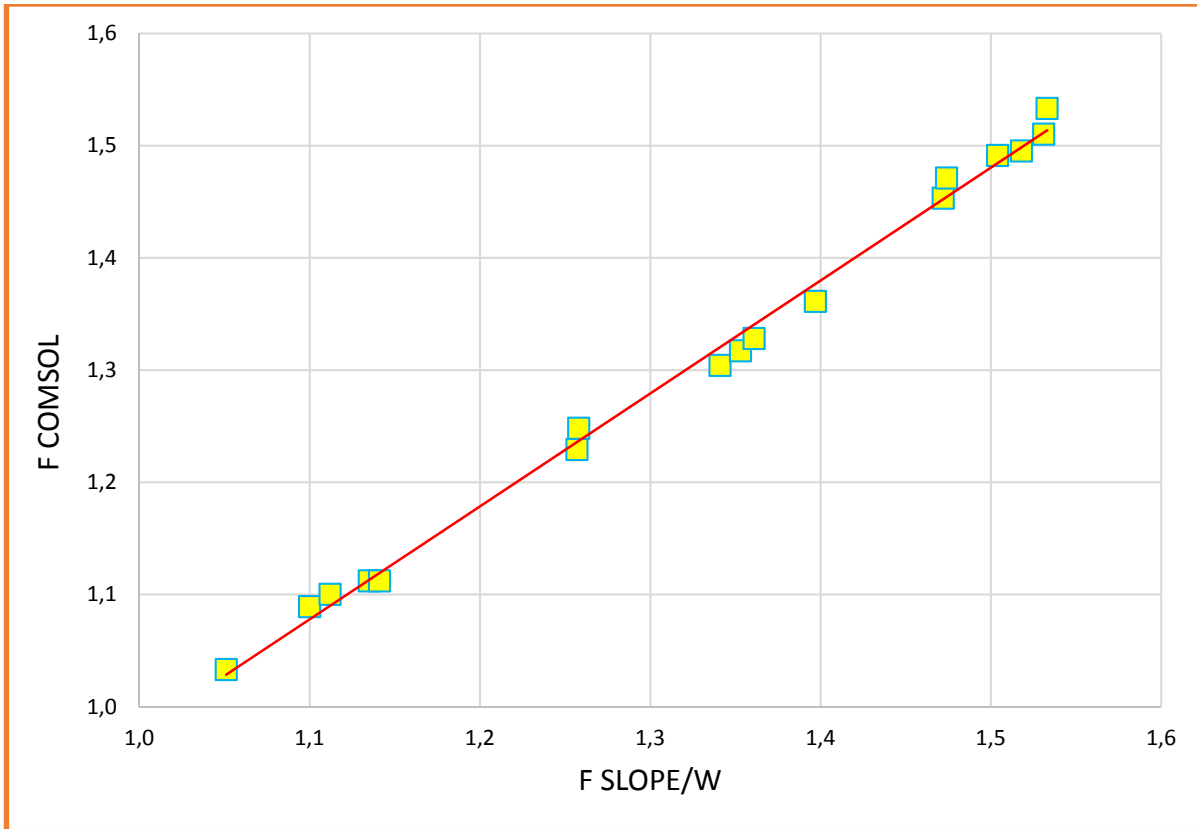| Slip #	F by SLOPE/W	F by COMSOL
1	1.258	1.258
2	1.112	1.089
3	1.051	1.033
4	1.135	1.112
5	Passing the slope limits	N/A
6	1.533	1.533
7	1.141	1.134
8	1.11	1.112
9	Passing the slope limits	N/A
10	Passing the slope limits	N/A
11	1.518	1.495
12	1.472	1.453
13	1.531	1.51
14	1.504	1.491
15	1.474	1.471
16	1.257	1.229
17	1.341	1.304
18	1.353	1.317
19	1.361	1.328
20	1.397	1.361

Figure-A III-4 Comparisons of factor of safety between SLOPE/W and
COMSOL-MATLAB script for layered soil deposit slope

APPENDIX IV

COMPARISONS OF FACTOR OF SAFETY BASED ON THE INFLUENCE OF FINE MESH SIZE FOR 30 AND 60 SLICES

Table-A IV-1 shows comparisons of FOS in uniform slope for fine size mesh with 0.15 m for 30 and 60 slices for the same slip surface

Uniform model with 0.15 m mesh size for 30 slices					Uniform model with 0.15 m mesh size for 60 slices				
Slip #	FOS	X Center	Y Center	Radius	Details	Slip #	FOS	X Center	Y Center	Radius	Details
1	0.777	34	47	32.295		1	0.777	34	47	32.295	
2	0.785	34	47	33.351		2	0.785	34	47	33.351	
3	0.796	34	47	34.406		3	0.796	34	47	34.406	
4	0.808	34	47	35.461		4	0.808	34	47	35.461	
5	0.82	34	47	36.517		5	0.82	34	47	36.517	
6	0.717	34	40	26.877	Critical	6	0.717	34	40	26.877	Critical
7	0.729	34	40	27.933		7	0.729	34	40	27.933	
8	0.743	34	40	28.988		8	0.743	34	40	28.988	
9	0.758	34	40	30.044		9	0.758	34	40	30.044	
10	0.804	34	40	31.099		10	0.804	34	40	31.099	
11	1.698	19	47	22.797		11	1.698	19	47	22.797	
12	1.634	19	47	23.852		12	1.634	19	47	23.852	
13	1.59	19	47	24.907		13	1.59	19	47	24.907	
14	E998	19	47	25.963	N/A	14	E998	19	47	25.963	N/A
15	E998	19	47	27.018	N/A	15	E998	19	47	27.018	N/A
16	1.429	19	40	17.379		16	1.429	19	40	17.379	
17	1.415	19	40	18.434		17	1.415	19	40	18.434	
18	1.408	19	40	19.49		18	1.408	19	40	19.49	
19	1.405	19	40	20.545		19	1.405	19	40	20.545	
20	E998	19	40	21.6	N/A	20	E998	19	40	21.6	N/A

Table-A IV-2 shows comparisons of FOS in slope with benches for fine size mesh with 0.15 m for 30 and 60 slices for the same slip surface

Benches model with 0.15 m mesh size for 30 slices					Benches model with 0.15 m mesh size for 60 slices				
Slip #	FOS	X Center	Y Center	Radius	Details	Slip #	FOS	X Center	Y Center	Radius	Details
1	0.697	36	47	25.423		1	0.697	36	47	25.423	
2	0.403	36	47	27.511	Critical	2	0.403	36	47	27.511	Critical
3	0.484	36	47	29.595		3	0.484	36	47	29.595	
4	0.48	36	47	31.673		4	0.48	36	47	31.673	
5	0.559	36	47	33.744		5	0.556	36	47	33.744	
6	0.946	36	40	22.489		6	0.946	36	40	22.489	
7	0.426	36	40	24.679		7	0.425	36	40	24.679	
8	0.463	36	40	26.867		8	0.462	36	40	26.867	
9	0.594	36	40	29.052		9	0.593	36	40	29.052	
10	0.626	36	40	31.231		10	0.624	36	40	31.231	
11	0.872	26	47	16.343		11	0.872	26	47	16.343	
12	0.538	26	47	18.365		12	0.538	26	47	18.365	
13	0.504	26	47	20.385		13	0.504	26	47	20.385	
14	0.587	26	47	22.401		14	0.586	26	47	22.401	
15	0.618	26	47	24.411		15	0.618	26	47	24.411	
16	1.217	26	40	13.41		16	1.218	26	40	13.41	
17	0.413	26	40	15.534		17	0.413	26	40	15.534	
18	0.551	26	40	17.658		18	0.55	26	40	17.658	
19	0.567	26	40	19.78		19	0.566	26	40	19.78	
20	0.584	26	40	21.898		20	0.583	26	40	21.898	

Table-A IV-3 shows comparisons of FOS in steep slope for fine size mesh with 0.15 m for 30 and 60 slices for the same slip surface

Steep model with 0.15 m mesh size for 30 slices					Steep model with 0.15 m mesh size for 60 slices				
Slip #	FOS	X Center	Y Center	Radius	Details	Slip #	FOS	X Center	Y Center	Radius	Details
1	0.693	34	49	23.519		1	0.693	34	49	23.519	
2	0.652	34	49	25.69		2	0.652	34	49	25.69	
3	0.645	34	49	27.884		3	0.645	34	49	27.884	
4	0.65	34	49	30.097		4	0.65	34	49	30.097	
5	0.659	34	49	32.323		5	0.659	34	49	32.323	
6	0.508	34	40	20.524	Critical	6	0.509	34	40	20.524	Critical
7	0.528	34	40	22.956		7	0.528	34	40	22.956	
8	0.553	34	40	25.412		8	0.553	34	40	25.412	
9	0.629	34	40	27.885		9	0.628	34	40	27.885	
10	0.757	34	40	30.37		10	0.756	34	40	30.37	
11	E990	24	49	14.089	N/A	11	E990	24	49	14.089	N/A
12	2.105	24	49	16.162		12	2.105	24	49	16.162	
13	1.424	24	49	18.269		13	1.425	24	49	18.269	
14	1.234	24	49	20.404		14	1.234	24	49	20.404	
15	1.145	24	49	22.561		15	1.145	24	49	22.561	
16	0.913	24	40	11.094		16	0.913	24	40	11.094	
17	0.893	24	40	13.428		17	0.893	24	40	13.428	
18	0.892	24	40	15.796		18	0.892	24	40	15.796	
19	0.896	24	40	18.192		19	0.896	24	40	18.192	
20	0.904	24	40	20.608		20	0.903	24	40	20.608	

Table-A IV-4 shows comparisons of FOS in layered slope for fine size mesh with 0.15 m for 30 and 60 slices for the same slip surface

Layered model with 0.15 m mesh size for 30 slices					Layered model with 0.15 m mesh size for 60 slices					
Slip #	FOS	X Center	Y Center	Radius	Details	Slip #	FOS	X Center	Y Center	Radius	Details
1	1.256	36	41	24.749		1	1.257	36	41	24.749	
2	1.101	36	41	27.047		2	1.101	36	41	27.047	
3	1.051	36	41	29.345	Critical	3	1.051	36	41	29.345	Critical
4	1.111	36	41	31.643		4	1.112	36	41	31.643	
5	E998	36	41	33.941	N/A	5	E998	36	41	33.941	N/A
6	1.546	36	34	19.799		6	1.544	36	34	19.799	
7	1.141	36	34	22.097		7	1.137	36	34	22.097	
8	1.078	36	34	24.395		8	1.079	36	34	24.395	
9	E998	36	34	26.693	N/A	9	E998	36	34	26.693	N/A
10	E998	36	34	28.991	N/A	10	E998	36	34	28.991	N/A
11	1.497	24	41	16.263		11	1.497	24	41	16.263	
12	1.459	24	41	18.562		12	1.46	24	41	18.562	
13	1.535	24	41	20.86		13	1.535	24	41	20.86	
14	1.495	24	41	23.158		14	1.494	24	41	23.158	
15	1.478	24	41	25.456		15	1.478	24	41	25.456	
16	1.226	24	34	11.314		16	1.227	24	34	11.314	
17	1.326	24	34	13.612		17	1.326	24	34	13.612	
18	1.339	24	34	15.91		18	1.34	24	34	15.91	
19	1.36	24	34	18.208		19	1.36	24	34	18.208	
20	1.392	24	34	20.506		20	1.391	24	34	20.506	

LIST OF REFERENCES

Abramson, L.W., Lee, T.S., Sharma, S., and Boyce, G.M. 2002. Slope stability and stabilization methods. 2nd ed., John Wiley & Sons, New York.

Bishop, A. W. (1952). The stability of earth dams. Ph. D. Thesis, Imperial College, London.

Bishop, A. W. (1955). The use of the Slip Circle in the Stability Analysis of Slopes. Géotechnique, 5(1), 7-17.

Cheng, Y., Lansivaara, T., & Wei, W. (2007). Two-dimensional slope stability analysis by limit equilibrium and strength reduction methods. Computers and Geotechnics, 34(3), 137-150.

Cheng, Y., & Lau, C. (2014). Slope Stability Analysis and Stabilization: New Methods and Insight. Taylor & Francis, New York.

COMSOL AB. (2011). COMSOL Multiphysics User's Guide - Version 5. COMSOL AB: Stockholm, Sweden.

COMSOL AB. (2013). COMSOL Multiphysics - LiveLink for Matlab User's Guide – Version 5. COMSOL AB: Stockholm, Sweden.

Donald, I. B., & Giam, S. K. (1988). Application of the nodal displacement method to slope stability analysis. In Proceedings of the fifth Australia–New Zealand conference on geomechanics, Sydney, Australia, p.456-460.

Duncan, J. M. (1996). State of the art: limit equilibrium and finite-element analysis of slopes. Journal of Geotechnical engineering, 122(7), 577-596.

Duncan, J. M., & Wright, S. G. (2005). Soil Strength and Slope Stability. Mechanics of Limit Equilibrium Procedures. John Wiley & Sons, New York.

Fellenius, W. (1936). Calculation of the stability of earth dams. In proceedings of the 2nd congress on large dams, Washington, DC.

Fredlund, D., & Krahn, J. (1977). Comparison of slope stability methods of analysis. Canadian Geotechnical Journal, 14(3), 429-439.

Fredlund, D., Krahn, J., & Pufahl, D. (1981). The relationship between limit equilibrium slope stability methods. In Proceedings of the 10th Conference of the International Society for Soil Mechanics and Foundation Engineering (ISSMFE), Stockholm, Sweden, Vol. 3, pp. 409–416.

Fredlund, D. G., Scoular, R.,& Zakerzadeh, N. (1999). Using a finite element stress analysis to compute the factor of safety. In proceedings of the 52nd Canadian Geotechnical Conference, Regina, Saskatchewan.

GEO-SLOPE International Ltd (2007). Stress-Deformation Modeling with SIGMA/W. GEO-SLOPE International Ltd. Calgary, Alberta, Canada.

GEO-SLOPE International Ltd (2012). Stability Modeling with SLOPE/W. GEO-SLOPE International Ltd. Calgary, Alberta, Canada.

Griffiths, D. V., & Lane, P. A. (1999). Slope stability analysis by finite elements. Geotechnique, 49(3), 387-403.

Janbu, N. (1954). Application of composite slip surfaces for stability analysis. In Proceedings of the European Conference on Stability of Earth Slopes, Stockholm, Sweden.

Janbu, N. (1973). Slope Stability Computions. John Wiley and Sons, New York.

Kondner, R. L. (1963). Hyperbolic stress-strain response: cohesive soils. Journal of the Soil Mechanics and Foundations Division, 89(1), 115-144.

Krahn, J. (2003). The 2001 RM Hardy Lecture: The limits of limit equilibrium analyses. Canadian Geotechnical Journal, 40(3), 643-660.

Li, L. C., Tang, C. A., Zhu, W. C., & Liang, Z. Z. (2009). Numerical analysis of slope stability based on the gravity increase method. Computers and Geotechnics, 36(7), 1246-1258.

Lu, N., Şener-Kaya, B., Wayllace, A., & Godt, J. W. (2012). Analysis of rainfall-induced slope instability using a field of local factor of safety. Water Resources Research, 48, (Paper W09524).

Matsui, T., & San, K.-C. (1992). Finite element slope stability analysis by shear strength reduction technique. Soils and foundations, 32(1), 59-70.

Morgenstern, N., & Price, V. E. (1965). The analysis of the stability of general slip surfaces. Geotechnique, London, 15(1), 79-93.

Nash, D. (1987). Comparative review of limit equilibrium methods of stability analysis. Slope Stability: Geotechnical Engineering and Geomorphology. John Wiley and Sons New York. p. 11-75.

Ozana, S., Pies, M., Docekal, T., Simos, T., & Tsitouras, C. (2016). Case studies on optimization problems in MATLAB and COMSOL multiphysics by means of the livelink. AIP Conference Proceedings, 1738, paper 370006.

Pirnia, P., Duhaime, F., Ethier, Y., & Dubé, J. S. (2016). Development of a multiscale numerical modelling tool for granular materials. GeoVancouver 2016. Vancouver, Canada.

Shao, W., Bogaard, T., & Bakker, M. (2014). How to Use COMSOL Multiphysics for coupled dual-permeability hydrological and slope stability modeling. Procedia Earth and Planetary Science, 9, 83-90.

Shao, W., Bogaard, T. A., Bakker, M., & Greco, R. (2015). Quantification of the influence of preferential flow on slope stability using a numerical modelling approach. Hydrology and Earth System Sciences, 19(5), 2197-2212.

Swan, C. C., & Seo, Y. K. (1999). Limit state analysis of earthen slopes using dual continuum/FEM approaches. International Journal for Numerical and Analytical Methods in Geomechanics, 23(12), 1359-1371.

Ugai, K., & Leshchinsky, D. O. V. (1995). Three-dimensional limit equilibrium and finite element analyses: a comparison of results. Soils and Foundations, 35(4), 1-7.

Zaruba, Q., & Mencl, V. (1982). Landslides and their control. 2nd ed. Developments in Geotechnical Engineering, 31. Amsterdam: Elsevier Scientific Publishing Company.

Zeng, S., Sun, B., Yang, S., & Tan, K. (2009). Search for critical slip surface and reliability analysis of soil slope stability based on MATLAB. In proceedings of the 2009 GeoHunan International Conference, Changsha, Hunan, China.

Zienkiewicz, O., Humpheson, C., & Lewis, R. (1977). Discussion: Associated and non-associated visco-plasticity and plasticity in soil mechanics. Géotechnique, 27(1), 101-102.

Zúñiga, E. H., Fernández, P. O., & Frez, F. R. (2007). Some applications to mine geotechnical design using MATLAB. In proceedings of the 6th Congreso Chileno de Geotechnia. Valparaiso, Chile.